

SYNTHESIS OF THIOPHENE, SELENOPHENE AND
THIOPHENE-S-DIOXIDE BASED ORGANIC
SEMICONDUCTORS FOR ORGANIC ELECTRONICS

By

DEVANG P. KHAMBHATI

Bachelor of Science in Chemistry
B. K. M. Science College
Valsad, India
2005

Master of Science in Organic Chemistry
Veer Narmad South Gujarat Univesity
Surat, India
2007

Submitted to the Faculty of the
Graduate College of the
Oklahoma State University
in partial fulfillment of
the requirements for
the Degree of
DOCTOR OF PHILOSOPHY
May, 2017

SYNTHESIS OF THIOPHENE, SELENOPHENE AND
THIOPHENE-S-DIOXIDE BASED ORGANIC
SEMICONDUCTORS FOR ORGANIC ELECTRONICS

Dissertation Approved:

Dr. Toby L. Nelson

Dissertation Adviser

Dr. Kenneth D. Berlin

Dr. Richard A. Bunce

Dr. Jeffery L. White

Dr. Mario Borunda

ACKNOWLEDGEMENTS

My journey was nothing less than a roller coaster ride. There were many ups and downs. I had many vertical free falls, too! But nonetheless, finally with God's grace, I was able to finish it. I could not have gone through this without the immense support of God, my adviser, my first family, group members, and the whole chemistry department and my relatives.

I dedicate my entire dissertation to Dr. Toby Nelson. I want to thank him for his constant support and faith in me. During my Ph.D., I was going through some problems in my personal and professional life. I might not be alive today, if you did not support me at that time. I cannot imagine my career if you were not my advisor. You are an incredible, helpful and humble person. You are not only my adviser but also my friend, philosopher and guide for me. I appreciate all your help from bottom of my heart.

I appreciate my parents and sisters. I am grateful to them for providing me everything. You have helped me so much. You were very selfless. You constantly supported me throughout my life for all my decision, even if you did not like some of them. I thank my sisters, Sejal and Hemali, for always thinking of my well-Being and all the favors. I am so lucky to have such great relatives. My aunt, Sushilaben, my cousins, Nimishaben and Nipulbhai) for helping me and supporting in everything. I am very happy to have such lovely nephews and nieces. You made my life extremely vibrant.

I am grateful to my beloved group members: Daniel, Paula, Subha, Niradha, Santosh, Fatima, Seth and Susan. Every one of you is very close to my heart. We were like a family. We fought over small things, nevertheless supported one another from personal life to professional career. Your cooperation was great. Because of you, I never had stress about work environment in my lab. You made our lab a happy and alive place. I wish that we could just work together for the rest of our lives.

I would also like to thank my advisory committee members, Dr. K. Darrell Berlin, Dr. Richard A. Bunce, Dr. Jeffery L. White, and Dr. Mario Borunda. Even though you have busy schedules, you read and attended my defenses. Your advices were extremely helpful. I specially thank Dr. K. Darrell Berlin, for your immense support throughout my Ph.D. Thank you Dr. Kenneth D. Berlin and Dr. Richard A. Bunce for writing reference letters. I am also grateful to all the professors who taught me courses. And lab coordinators, with whom I worked. I convey my gratitude to all the OSU chemistry department Staff members past and present. Thank you for all your kind help and bearing all my questions and requests. Bob, Dana, Cheryl, Karen, Pam, Joe and Kelly, I will miss all the conversations and laughter with you.

And last, but not least, I express gratitude to my beloved Oklahoma State University from bottom of my heart. You gave me an outstanding opportunity to pursue my Ph.D. My blood is now orange and I will always be hardcore Cowboys fan wherever I go, GO POKES! This is where my story began, I wish that one day I can visit Stillwater for homecoming celebration.

Name: DEVANG P. KHAMBHATI

Date of Degree: MAY, 2017

Title of Study: SYNTHESIS OF THIOPHENE, SELENOPHENE AND THIOPHENE-S-DIOXIDE BASED ORGANIC SEMICONDUCTORS FOR ORGANIC ELECTRONICS

Major Field: ORGANIC CHEMISTRY

Abstract:

Solid materials having electrical conductivity greater than insulators but less than metals are semiconductors. Carbon-based materials that exhibit semiconductor properties are known as organic semiconductors (OSCs). These materials hold promise for flexible, lightweight, inexpensive and easy to fabricate devices. Due to these advantages, OSCs have gained tremendous interest in recent decades for their use in solar cells, thin film transistors and light emitting diodes. OSCs can be broadly classified in two categories: conjugated polymers (CPs) and small molecules.

(1) CPs: Organic macromolecules which have a backbone chain of alternating double/triple- and single-Bonds are known as CP. Application and device fabrication is dictated by the Energy gap between highest occupied molecular orbital (HOMO) and lowest unoccupied molecular orbital (LUMO). Therefore it is a vital parameter for CPs. Here, the synthesis a narrow bandgap conjugated polymer- Poly(3- alkoxy selenophene), inspired from poly(3-alkoxythiophene), will be discussed.

Li ion batteries may catch fire due to the conventionally used cathode material, LiCoO₂. We have formed a mixture, comprised of poly(3-alkoxy thiophene) and Li salt, as an alternative material for the cathode in Li ion batteries.

(2) Small molecules: Small molecules were synthesized based on the electron deficient moiety of Benzodithiophene-S,S-tetraoxide (BDTT) via Cu catalyzed C-H activated direct arylation. Reaction conditions were optimized for various parameters like catalysts, ligands and base. Also, the optoelectronic properties of these molecules were studied.

TABLE OF CONTENTS

Chapter	Page
I. INTRODUCTION	1
1.1 Organic Semiconductors	1
1.1.1 Band theory of solids	3
1.2 Classification of OSCs:.....	5
1.2.1 Small molecules	5
1.2.2 Conjugated polymer.....	6
1.3 N-type OSCs	7
1.4 Poly(3-hexylthiophene).....	9
1.5 Effect of side chains on OSCs Properties	10
1.6 Direct arylation via C-H activation.....	11
1.6 References.....	14
II. ATTEMPTED SYNTHESIS OF POLY-(3-ALKOXY SELENOPHENE) AND POLYTHIAZOLE	17
2.1 Poly(3-alkoxyselenophene).....	17
2.1.1 Introduction.....	17
2.1.2 Design	18
2.1.3 Synthesis and discussion.....	19
2.2 Polythiazoles	20
2.2.1 Introduction.....	20
2.2.2 Design	20
2.2.3 Attempted reactions	21
2.3 Experimental section.....	23
2.4 References.....	27
III. POLYTHIOPHENE BASED MATERIAL FOR Li-ION BATTERY ELECTRODE	29
3.1 Introduction.....	29
3.2 Design	31
3.3 Synthesis	32
3.4 Polymer/salt mixture preparation and initial testing.....	33
3.5 Experimental section.....	34
3.6 References.....	37

IV. SYNTHESIS OF BENZODITHIOPHENE- <i>S,S</i> -TETRAOXIDE (BDTT) BASED SMALL MOLECULES VIA COPPER CATALYZED DIRECT ARYLATION	43
4.1 Introduction	43
4.2 Design	44
4.3 Copper-catalyzed direct arylation	46
4.4 Synthesis of benzodithiophene- <i>S,S</i> -tetraoxide (BDTT)	46
4.5 Results and discussion	47
4.5.1 Reaction optimization	47
4.5.2 Scope study	52
4.6 Plausible mechanism	53
4.7 Other projects in progress work with BDTT	54
4.7.1 Synthesis of 4,8-dihexylbenzo[1,2-B:4,5-B']dithiophene- <i>S,S</i> -tetraoxide	54
4.7.2 Synthesis of 2,6-diiodo-4,8-didodecyloxybenzo[1,2-B:3,4-B]dithiophene- <i>S,S</i> -tetraoxide	54
4.7.3 Synthesis of 2,6-dibromo-4,8-didodecyloxybenzo[1,2-B:3,4-B]dithiophene- <i>S,S</i> -tetraoxide	55
4.7.4 4,8-Bis(dodecyloxy)-2,6-Bis(trimethylstannyl)benzo[1,2-B:4,5-B']dithiophene- <i>S,S</i> -tetraoxide:	56
4.7.5 Synthesis of benzo[1,2-B:3,4-B]dithiophene- <i>S,S</i> -tetraoxide containing CPs via Stille coupling reactions	56
4.8 Optical properties	57
4.9 Crystal structure	59
4.10 Experimental section	60
4.11 References	92
V. CONCLUSIONS AND FUTURE OUTLOOK	97
5.1 Introduction	97
5.2 Conclusions	97
5.3 Future outlook	98
5.4 References	99

LIST OF TABLES

Table	Page
4.1: Oxidation and reduction potential of BDT and BDTT	46
4.2: Various parameters for reaction optimization.....	49
4.3: Various parameters for reaction optimization.....	49
4.4: Various parameters for reaction optimization.....	50
4.5: Various parameters for reaction optimization.....	50
4.6: Various parameters for reaction optimization.....	51
4.7: Optimization of benzodithiophene- <i>S,S</i> -tetraoxide cross-coupling reaction with iodobenzene	52
4.8: Optical properties (in chloroform solution)	60
4.9: Crystal data and structure refinement for Ph-BDTT-Ph	84
4.10: Atomic coordinates and equivalent isotropic displacement parameters	85

LIST OF FIGURES

Figure	Page
1.1: OSCs: (a) organic solar cell (b) radio frequency identification (c) organic light emitting diode (d) biomedical device (e) sensor	2
1.2: Carbon: atomic orbitals and sp^2 molecular orbitals	2
1.3: Conjugation: (a) localized (b) delocalized orbitals	3
1.4: Bandgap formation	3
1.5: VB and CB of conductors, semiconductors and insulators	4
1.6: Small molecules used for various application	6
1.7: Conjugated polymers used for various application.....	7
1.8: Poly(benzobisimidazobenzophenanthroline), BBL	8
1.9: C_{60} (left) and Phenyl C_{61} butyric acid methyl ester (right).....	8
1.10: Naphthalene diimides (NDIs) and perylene diimides (PDIs)	9
1.11: 3-Alkyl thiophene, regioregular and regioirregular P3AT	10
1.12: Polythiophene with alkyl chain, poly(3-alkylthiophene) (left), and alkoxy-chain poly(alkoxythiophene)	11
1.13: Poly(2,3-bis(4-octylthiophen-2-yl)-5-(thiophen-2-yl)quinoxaline) (left) and 1,1'-((5-(thiophen-2-yl)quinoxaline-2,3-diyl)bis(thiophene-5,3-diyl))bis(octan-1-one) (right).....	11
1.14: Conventional coupling reaction and direct arylation coupling	12
1.15: C-H activated arylation reaction	12
1.16: Direct arylation of thiazole	13

1.17: Cu-catalyzed direct arylation	13
2.1: (a) poly(3-alkoxy thiophene) (b) poly(3-hexyl selenophene) and (c) proposed polymer: poly(3-alkoxy selenophene)	18
2.2: Poly(4-alkylthiazole)	20
2.3: Proposed polymerization	21
2.4: Alkylation of 4-Bromothiazole	21
2.5: Debromination of thiazole	21
2.6: Synthesis of 4-hexylthiazole	21
2.7: Bromination of 4-Bromothiazole	22
2.8: Cyanation of 2-Bromothiazole	22
3.1: Li-ion battery charging and discharging	30
3.2: Block co-polymer for Li ion and electron conductivity	31
3.3: Proposed polymer, poly(3-alkoxythiophene)	32
4.1: Widely used heterocyclic blocks for OSCs	44
4.2: Oxidation of benzodithiophene	45
4.3: Conventional coupling reaction and direct arylation	46
4.4: Thin layer chromatography for the reactions in Table 4.7	48
4.5: Substrate scope of Cu-catalyzed cross-coupling of aryl iodides with benzadithiophene- <i>S,S</i> -tetraoxide (BDTT)	52
4.6: Plausible mechanism for Cu-catalyzed direct arylation	54
4.7: Absorption spectra of BDTT derivatives (in chloroform solution)	58
4.8: Emission spectra BDTT derivatives (in chloroform solution)	58
4.9: Crystal structure of 4,8-Didodecyloxy-2,6-diphenylbenzo[1,2- <i>b</i> :4,5- <i>b'</i>]dithiophene- <i>S,S</i> -tetraoxide	59

LIST OF REACTIONS SCHEMES

Scheme	Page
2.1: Synthesis of monomer and attempted polymerization	20
3.1: Synthesis of poly(3-alkoxythiophene).....	32
4.1: Synthesis of BDTT	47
4.2: Cu-catalyzed direct arylation of BDTT	51
4.3: Utilization of the Cu-catalyzed direct arylation	53
4.4: Synthesis of BDTT with alkyl chain.....	55
4.5: Synthetic routes for 2,6-diiodobenzo[1,2-b:4,5-b']dithiophene- <i>S,S</i> -tetraoxide (DiIBDTT)	55
4.6: Synthetic routes for 2,6-dibromoobenzo[1,2-b:4,5-b']dithiophene- <i>S,S</i> -tetraoxide (DiBrBDTT).....	56
4.7: Proposed synthetic routes for BDTT derivative for Stille coupling	56
4.8: Proposed synthetic route to make BDTT containing Conjugated polymers	57

CHAPTER I

INTRODUCTION

1.1 ORGANIC SEMICONDUCTORS (OSCs):

Carbon based material which has semiconductor properties are known as organic semiconductors (OSCs). OSCs hold promise for lightweight, inexpensive flexible material. Due to these advantages, OSCs have gained tremendous interest in recent decades for their use in organic photovoltaics (OPVs), organic film transistors (OFTs), sensors, radio frequency infrared detection (RFIDs) tags and organic light emitting diodes (OLEDs). Samsung, Sony, LG, and Nokia have used OLED technology for display screens in smart phones, tablets and televisions. Heliatek, a German company, has made an OPV with 12.0 % efficiency. OFET based flexible displays have also been fabricated. Here are some organic devices in real life application. **(Figure. 1.1)**.¹

The essential feature of the OSCs is conjugation throughout the structure. A series of alternate series of π bonds and σ bonds is known as “conjugation”. In **Figure 1.2**, the atomic orbitals of carbon are shown. Here, $s + p_x + p_y$ atomic orbitals hybridise to give three sp^2 molecular orbitals. These three orbitals form triangular planar structure. The unhybridized p_z orbital is perpendicular to the plane of the sp^2 orbitals. The sp^2 molecular orbitals form σ bonds with other carbon, hydrogen or other heteroatoms. The p_z atomic orbitals are half filled. These p_z orbitals form a π bond with p_z orbital of a neighboring atom [**Figure 1.3(a)**]. These π bonds can delocalise

due to conjugation [Figure 1.3(b)].²

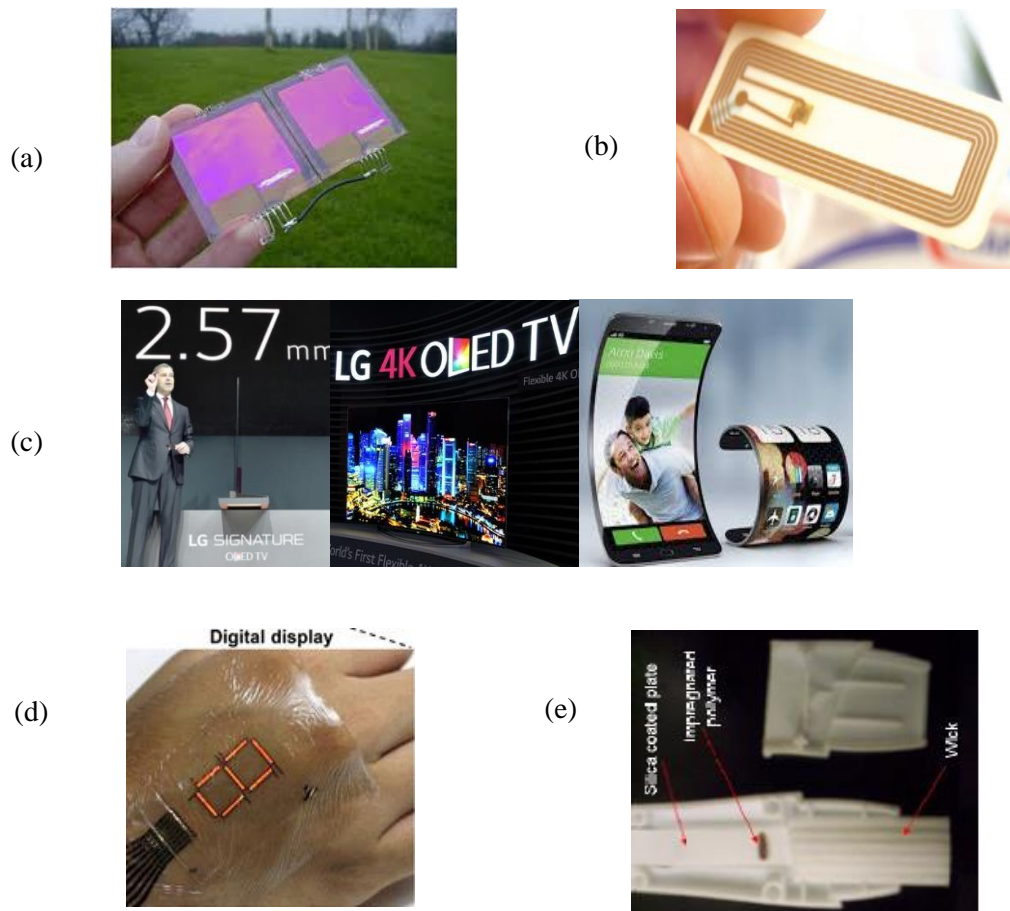


Figure 1.1: OSCs: (a) organic solar cell (b) RFID (c) OLED (d) biomedical device (e) sensor devices.

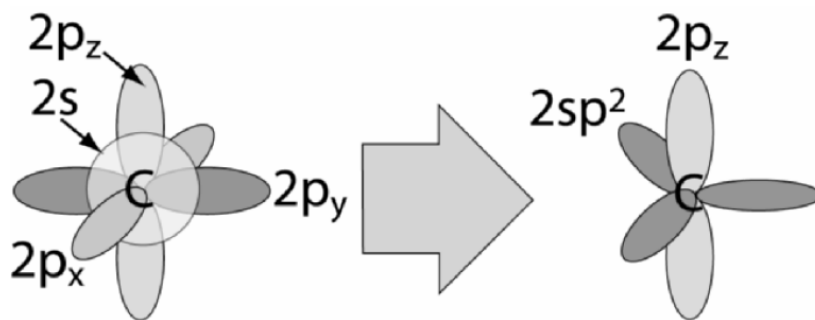


Figure 1.2 : Carbon: atomic orbitals (left) and sp² molecular orbitals (right)²

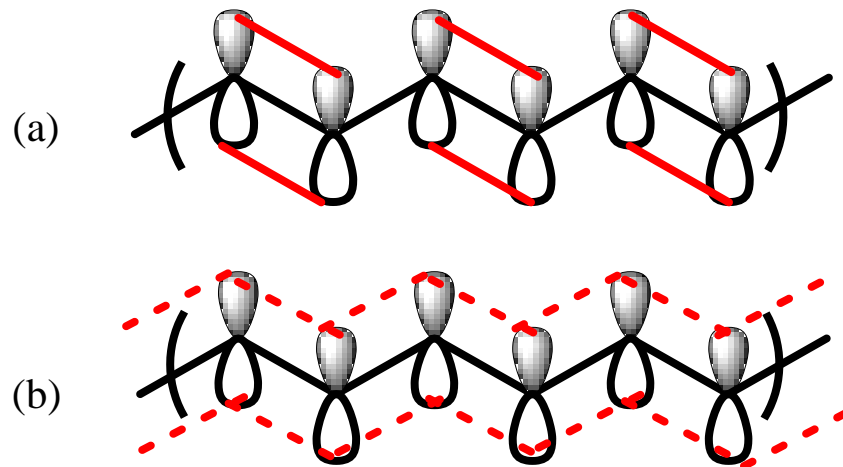


Figure 1.3: Conjugation: (a) localized (b) delocalized orbitals

1.1.1 Band theory of solids:

In **Figure 1.4** (on the left side), two p_z atomic orbitals of carbon atoms are shown. Both of

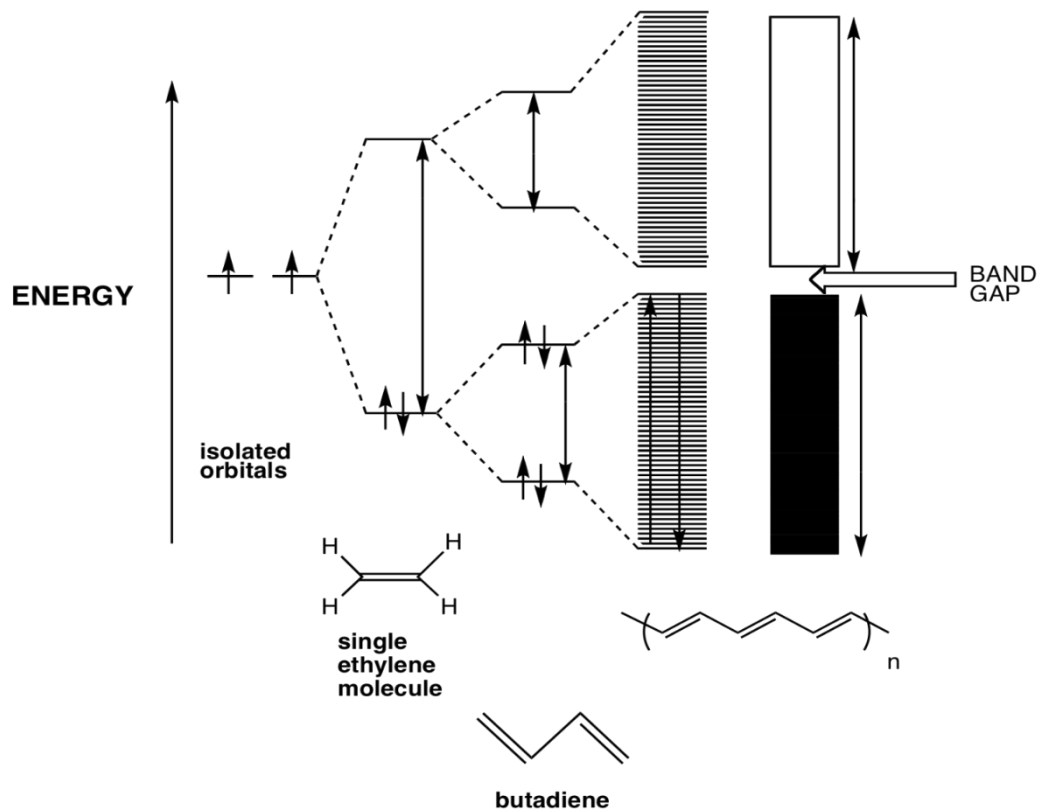


Figure 1.4: Bandgap formation

these orbitals have one electron. When these atoms form an ethylene molecule, π and π^* molecular orbitals are generated. The bonding π orbital is occupied with two electrons from C atoms. In case of butadiene, four molecular orbitals will be generated. Two bonding orbitals are occupied with electrons, while two antibonding orbitals are empty. One noticeable difference is that energy difference between highest bonding orbital and lowest antibonding orbital is decreased compared to ethylene. When the conjugation is extended, the bandgap reduces significantly. And also many bonding orbitals and antibonding orbitals will be formed. These new bonding orbitals are very close to one another in terms of energy. So, these bonding orbitals form a band, which is filled with electrons. This band is called the valence band (VB). Similarly,

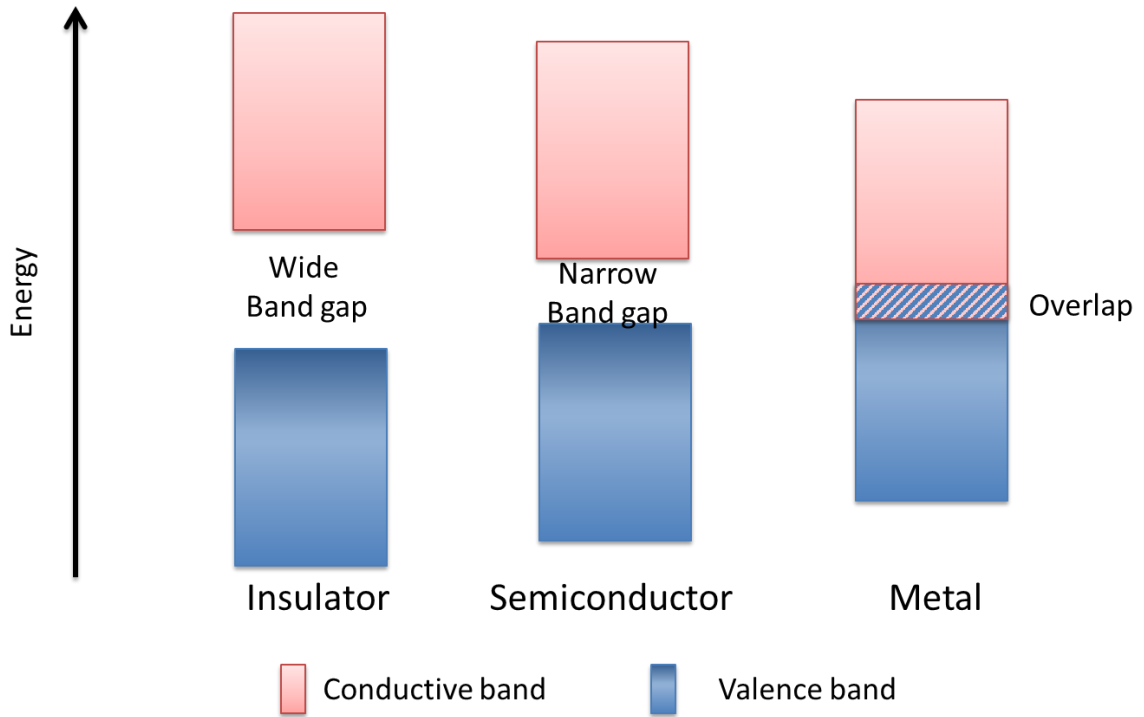


Figure 1.5: VB and CB of conductors, semiconductors and insulators

antibonding orbitals form a band, which is called the conduction band (CB). The energy difference between them is called the bandgap. VB and CB of conductors, semiconductors and insulators are shown in **Figure 1.5**.³

In conductors, the VB and the CB overlap with each other. Due to this overlap, electrons can move freely from the VB to the CB and makes the material electronically conductive. In insulators, there is wide gap between VB and CB. Consequently, electrons cannot jump from the VB to CB. While in semiconductors, the bandgap is narrow such that electrons can excite from the VB to the CB if enough energy is provided.⁴

The bandgap is an important properties of any OSC. This bandgap is a crucial factor in determining an OSC's application. For example, to make a blue light emitting OLED, a relatively large bandgap OSC is needed, while to make a red light emitting OLED, relatively a short bandgap OSC is needed. For OPVs, ideally an OSC should absorb a broad range of electromagnetic radiation. Large bandgap OSCs cannot absorb in the higher wavelength part of the visible region/ near IR part of the electromagnetic spectra. Therefore, lot of energy of the sun is wasted. Narrow bandgap OSCs can absorb in this region, which makes OPVs more efficient.⁵⁻⁶ They can be used in tandem solar cell to maximize the absorption of sunlight, which results in highly efficient OPVs. Many wide bandgap OSCs can conduct either *via* electrons or holes. It has been observed that narrow bandgap OSCs possess ambipolar (electrons and holes) conductivity. This quality makes them ideal for Field effect transistors.⁶⁻⁷ The near-IR light sensing is essential for many scientific, military and industrial applications. It is used for night vision technology, remote control and optical communications. OSCs which have a narrow bandgap, can provide a viable alternative.⁷ Hence, it is very important to synthesize new narrow bandgap OSCs.

1.2 Classification of OSCs: small molecules (SMs) and conjugated polymers (CPs).

1.2.1 Small molecules:

These OSCs are made of conjugated polycyclic rings i.e. linear and/or two-dimensional and/or

fused non heterocyclic/heterocyclic aromatic rings. These molecules can be packed into well-organized polycrystalline films, which enhances mobility of charge carriers. Highly crystalline SMs have limited solubility in common organic solvents. Therefore, in order to use them in device, they must be vapor deposited. However, in recent years, novel approaches have been explored to improve their processability from solutions i.e. the use of spin coating, slot coating and blade coating, since solution processing can be used for large scale production. It is also less expensive compared to vacuum deposition.²

Compared to CPs, SMs offer various inherent advantages in organic electronic applications. SMs are monodisperse with well-defined chemical structures. Their syntheses are reproducible. Therefore, SMs can have very specific properties, e.g. they can produce very sharp and narrow emissions, which makes them ideal for OLEDs. Perylene, C47 and bathocuprione are some SMs which are used for OLEDs. SMs such as, sexithienyl, pentacene and pentathienoacene have been utilized in OTFTs (**Figure 1.6**).⁸

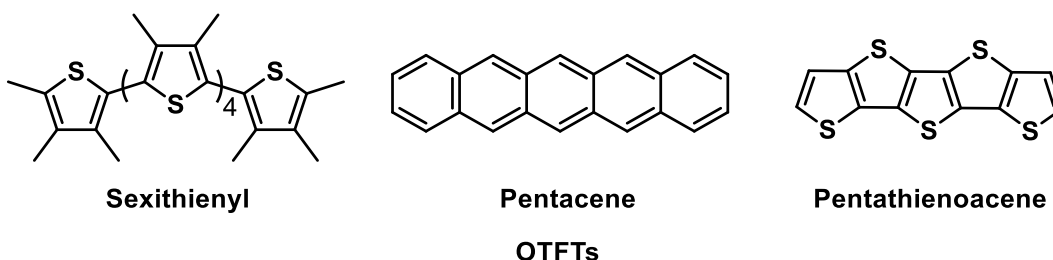


Figure 1.6: SMs used for various application

1.2.2 Conjugated polymers (CPs):

As the name suggest, CPs are polymers with conjugation throughout the entire backbone. One of the main advantages of CPs is that, generally they are soluble in common solvents such as chloroform and tetrahydrofuran. Due to their solubility, they can be processed with spin-coating, stamp printing, and ink-jet printing. These low-cost techniques will make the devices more affordable. CPs can be modified to a great extent to obtain desired properties. The advancement

in synthetic methodology allowed the synthesis of CPs with reproducible specific number average molecular weight (M_n) ranges and very low polydispersity. M_n is the total weight of all the polymer chains in a sample, divided by the number of polymer chains. Morphology of the CP is also very important. Development of device fabrication, with optimum morphology can greatly enhance their performance.² Polyphenylene vinylenes (PPVs) are used in OLEDs. They could be used from green to red color light. Polyfluorenes are also a very important class of CPs. They are mainly blue light emitters for the OLEDs as they provide strong emissions in the 380-420 nm wavelength range. Poly(3-hexylthiophene) (P3HT) is one of the most widely used CPs. It is used

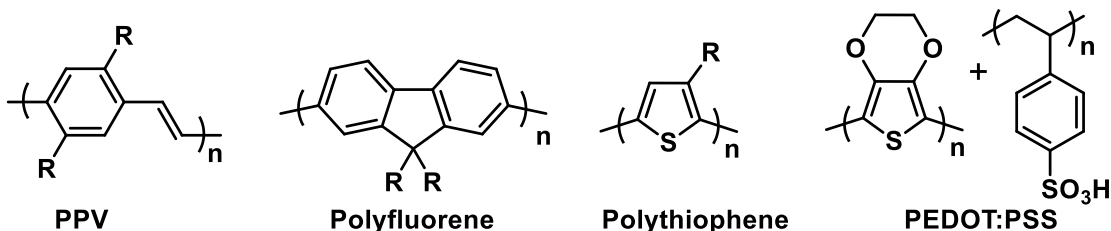


Figure 1.7: CPs used for various application

as a standard to determine the efficiency of other materials for OPVs. They are also used in OFTs as well as in many other applications. Poly(3,4-ethylenedioxythiophene) (PEDOT) and poly(4-styrenesulphonic acid) (PSS), polymer blend is used in many devices as a hole transport layer. Their use reduces the device operating voltage, increases lifetime, and results in better device performance overall (**Figure 1.7**).⁸

1.3 N-type OSCs:

There are two types of OSCs, p-type (which conducts electron holes) and n-type (which conducts electrons). Both kinds of OSCs are very important. For example, OFTs are either PNP or NPN junctions. As their name suggest, these junctions are made of p-type and n-type semiconductors. P-type and n-type OSCs are also required for fabrication of OPVs, OLED as well as other devices. Although there have been many p-type OSCs reported, air stable and soluble n-type CPs are very limited.⁹ This remains a main hurdle to the advancement of organic electronics.

There is a critical need to develop novel n-type CPs which have good solubility, facile synthesis and air stability.¹⁰

Poly(benzobisimidazobenzophenanthroline), BBL (**Figure 1.8**), is one the earliest reported n-channel polymers with air stability. However it is not soluble in common organic solvents. For solubilization, it requires harsh Lewis acid solutions (GaCl_3 or methanesulfonic acid), which is undesirable for large scale production.¹¹

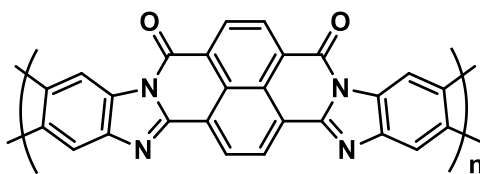


Figure 1.8: BBL

Fullerene C_{60} (**Figure 1.9**) is mainly used in OPVs. Since C_{60} is insoluble, its soluble derivative phenyl C_{61} butyric acid methyl ester (PCBM) (**Figure 1.9**) is used. Fullerenes have low LUMO and good electron conductivity, however PCBM is sensitive to O_2 . Phase separation also occurs when they are used with polymer and they have low light absorption.¹²

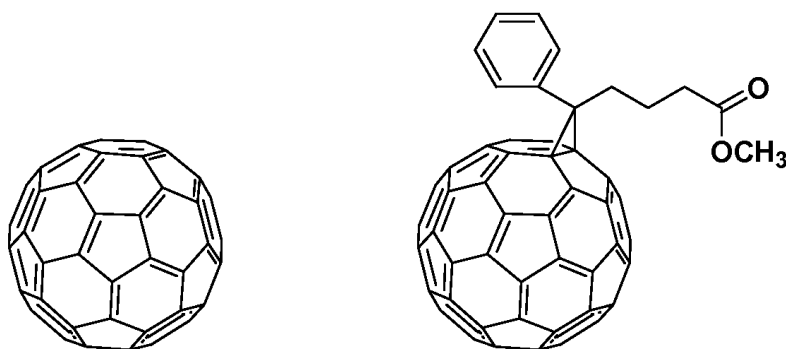


Figure 1.9: C_{60} (left) and PCBM (right)

Naphthalene diimides (NDIs) and perylene diimides (PDIs) (**Figure 1.10**) are used for OPVs and OFETs. They have good electron affinity. But instability in air is the major issue. Their electron mobility is also less compared to Fullerene.¹⁰

There are many strategies to make n-type OSCs. Typical electron-withdrawing groups (EWGs) are exemplified by carbonyls, cyano, perfluoroalkyl, imide, amide and their analogues.

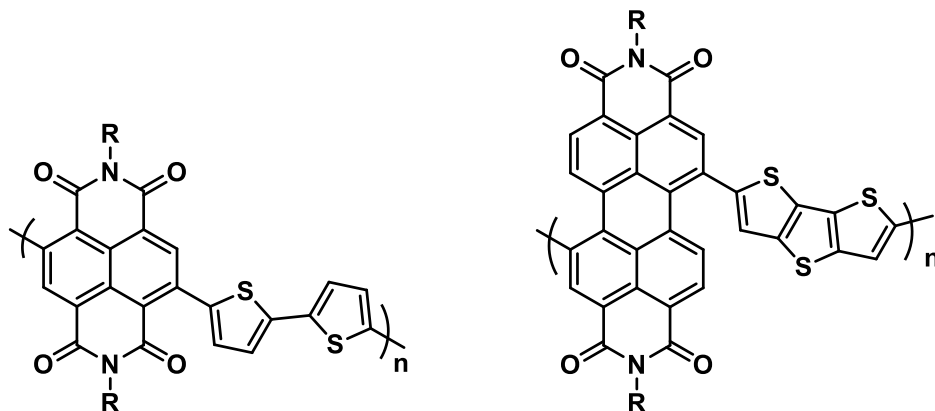


Figure 1.10: NDIs (left) and PDIs (right)

Connecting the EWGs to the π -conjugated systems can lower the LUMO energy levels.

Connecting perfluoroalkyl groups or their analogues with π -systems, instead of alkyl groups, effectively reduces the electron density at the nuclei of the atoms in the π -systems and therefore tend to lower the HOMO and LUMO. The use of electron poor moieties would also tend to lower the HOMO and LUMO energy levels.

1.4 Poly(3-hexylthiophene) (P3HT):

Polythiophene (PT) was first synthesized in the 1980s. However, this unsubstituted PT was insoluble in organic solvents and possessed low electron conductivity. To overcome this issue, researchers attached an alkyl chain to thiophene. Poly(3-alkyl thiophene) (P3AT) were soluble in chloroform and tetrahydrofuran. But first, P3AT were regioregular (**Figure 1.11**), which had very low conductivity. In 1992, McCullough and Rieke came up with their different methodology to synthesize regioregular P3AT (**Figure 1.11**).¹³ This regioregular P3AT had far superior properties compared to the regioregular one. Regioregularity is described here.

Second and fifth position of 3-alkyl thiophene can be named head and tail, respectively. The P3AT which has random connection of head and tail is referred as regioregular. Due to steric bulk, thiophene units are not in the same plane. So effective conjugation decreases and hence the

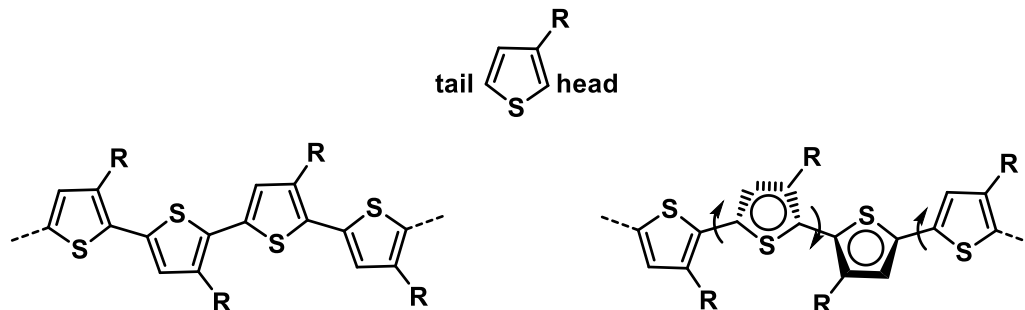


Figure 1.11: 3-alkylthiophene (top), regioregular (bottom left) and regioregular P3AT (bottom right)

conductivity is reduced. The P3AT, which has 99% thiophene units connected as head to tail are called regioregular. In this polymer, thiophene units are in the same plane, which leads to higher conductivity.¹⁴ The synthesis of regioregular polythiophene was a milestone in the field of CPs. Due to easy synthesis, high solubility, very good conductivity and other properties, they are widely used in the field of OSCs. PTs have been used in a variety of applications such as, OPVs, OFETs, OLEDs and sensors.

1.5 Effect of side chains on OSCs properties:

Initially side chains were introduced to solubilize OSCs. But, the side chains' role is above and beyond just to solubilize. A side chain directly effects the electron density in the OSC backbone. Side chains are important tools to manipulate different properties such as absorption, emission, energy level, molecular packing, and charge transport as well as solubility.¹⁵

Alkoxy groups are the most frequently used as electron donating side chains (**Figure 1.12**).¹⁵

Here, Poly(3-alkoxythiophene) (P3AoT) has higher a HOMO level (due to the electron donating alkoxy chain) than P3AT. Their LUMO levels however are similar. Hence, alkoxy chains have decreased the bandgap.

This strategy could be useful particularly for the synthesis of p-type OSCs. EWG generally decreases the LUMO level but does not significantly affect the HOMO level and thus reduces the bandgap. The EWG stabilizes the LUMO level, which is necessary to make n-type materials.

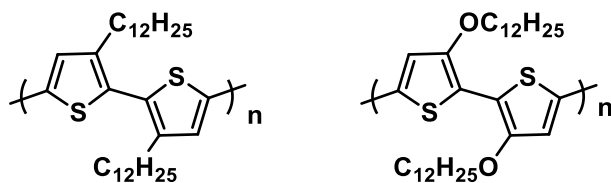


Figure 1.12: PT with alkyl chain, P3AT (left) and alkoxy chain, P3AoT (right)

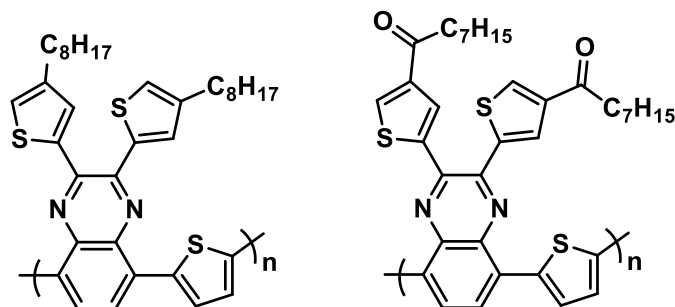


Figure 1.13: Poly(2,3-bis(4-octylthiophen-2-yl)-5-(thiophen-2-yl)quinoxaline) (left) and 1,1'-((5-(thiophen-2-yl)quinoxaline-2,3-diyl)bis(thiophene-5,3-diyl))bis(octan-1-one) (right)

Here, when the methylene bonded to thiophene was changed to electron withdrawing carbonyl group (**Fig 1.13**), the LUMO stabilized and since there was very little change in the HOMO level, the bandgap gets reduced.¹⁵

1.6 C-H bond activated direct arylation:

Many OSCs synthesis involves aryl C-C coupling reactions. Suzuki,¹⁶ Stille,¹⁷ Heck,¹⁸ Negishi,¹⁹ Kumada²⁰ and Sonogashira²¹ couplings, have been widely used cross coupling reactions for aryl C-C bond formation.²²⁻²⁴ In these reactions, an aryl halide reacts with an organometallic compound to form a desired C-C bond (**Figure 1.14**). The organometallic reagents are often not commercially available or are very expensive. Their syntheses from aromatic compounds require number of steps. By-products are also formed during these syntheses. Organometallic reagents are typically unstable and difficult to handle and store. They may also cause other safety concerns such as fire hazards and toxicities. Furthermore, organometallic compounds used in stoichiometric amount give more byproducts, which may be toxic.

To overcome these concerns, scientists have searched for alternative routes. One alternative is C-H bond activation (**Figure 1.14**), for C-C bond formation. There are many examples of such reactions in the literature during the last 15 years. This is a facile approach for an aryl C-C bond formation, since there is no need for an organometallic precursor. This route is also atom economical, which makes it even more attractive with respect to green chemistry. The C-H bond

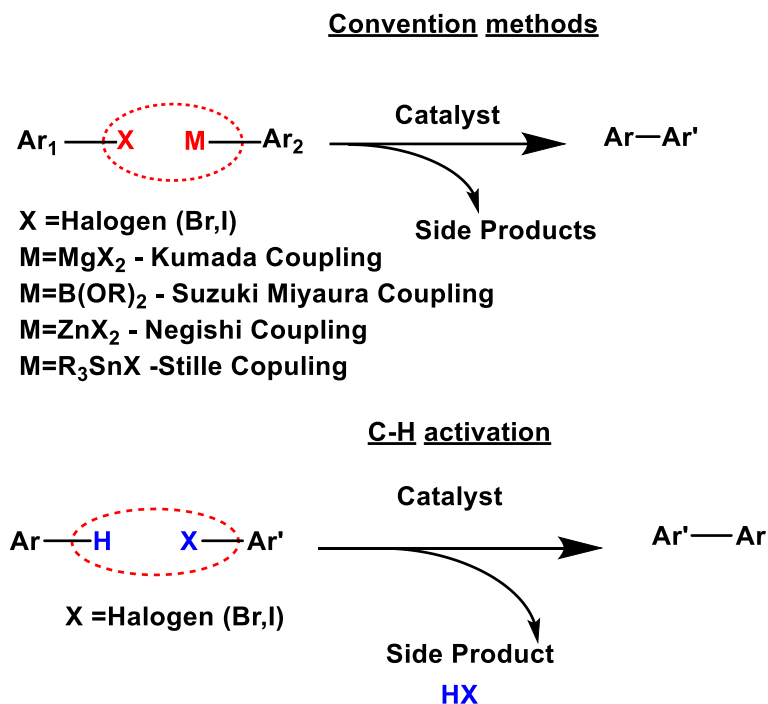


Figure 1.14: Conventional coupling reaction (above) and direct arylation coupling (below) activation approach enables previously unachievable C-C disconnections. Glorious *et al.* have suggested that this approach could be used for late stage diversification of compounds to generate a large library of derivatives.²⁵

A typical C-H activated direct arylation reaction may be envisioned as in **Figure 1.15**:

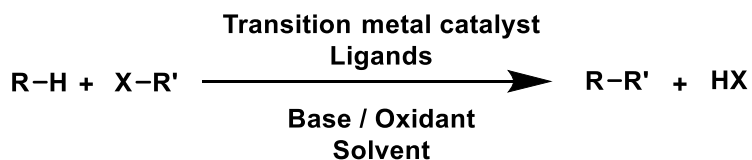


Figure 1.15: C-H activated direct arylation reaction

Generally Pd, Ru and Rh based catalysts are extensively used for direct arylation, such as Pd(OAc)₂, PdCl₂(dppf), Pd(PPh₃)₄, Pd(OH)₂/C, Pd(PPh₃)Cl₂, [RhCl(coe)₂]₂, and [RhCl(CO)₂]₂.²⁶ These catalysts can be expensive and toxic. Thus, Cu, Fe or other catalysts, which are inexpensive as well as environment friendly needed to be explored for such reactions. In the mid 2000s, Daugulis et al. noticed the effect of Cu salts on regioselective direct arylation of thiazole (**Figure 1.6**). They postulated that there must be some kind of organocopper species responsible for regioselective arylation in above reactions. They wondered if an organocopper intermediate could be generated without a palladium co-catalyst, a cheap and efficient method for

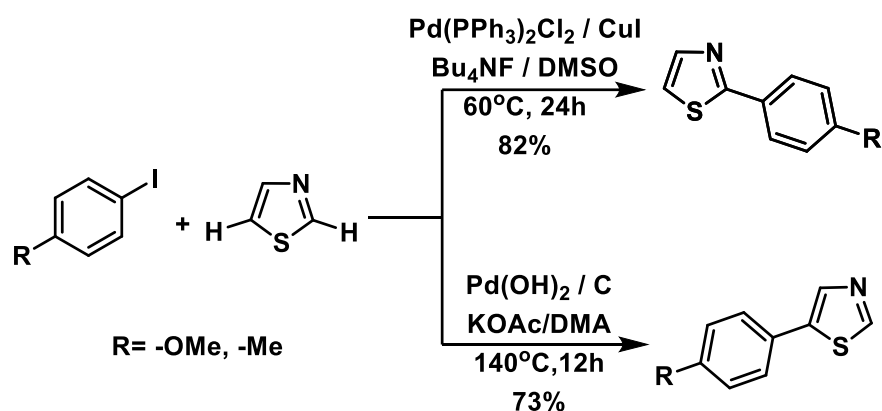


Figure 1.16: direct arylation of thiazole

the direct arylation might be achieved. Based on this idea, they came up with Cu-catalyzed direct arylation of heterocycle C-H bonds (**Figure 1.17**).²⁷ After this paper, there were many examples of Cu-catalyzed direct arylation.²⁸

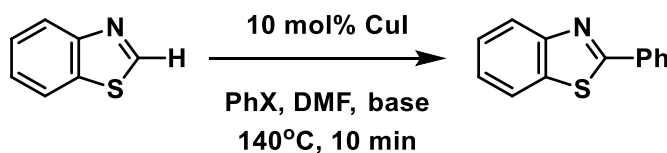


Figure 1.17: Cu-catalyzed direct arylation

1.7 References:

1. Skotheim, T. A.; Reynolds, J., *Conjugated polymers: processing and applications*. Taylor & Francis: 2006.
2. Rockett, A., *The Materials science of semiconductors*. Springer US: 2007.
3. Capek, I., *Advances In Polymer Science VI45.: Radical polymerisation polyelectrolytes*. Springer Berlin Heidelberg: 1999.
4. Sirdeshmukh, D.; Sirdeshmukh, L.; Subhadra, K. G.; Sunandana, C. S., *Electrical, electronic and magnetic properties of solids*. Springer international publishing: 2014.
5. Bundgaard, E.; Krebs, F. C., Narrow bandgap polymers for organic photovoltaics. *Solar Energy Materials and Solar Cells* **2007**, *91* (11), 954-985.
6. Dou, L.; Liu, Y.; Hong, Z.; Li, G.; Yang, Y., Low-Bandgap near-ir conjugated polymers/molecules for organic electronics. *Chemical Reviews* **2015**, *115* (23), 12633-12665.
7. Sirringhaus, H., Organic semiconductors: An equal-opportunity conductor. *Nat Mater* **2003**, *2* (10), 641-642.
8. Organic Semiconductors. In *The materials science of semiconductors*, Springer US: Boston, MA, 2008; pp 395-453.
9. Lei, T.; Dou, J.-H.; Cao, X.-Y.; Wang, J.-Y.; Pei, J., Electron-deficient poly(p-phenylene vinylene) provides electron mobility over $1 \text{ cm}^2 \text{ v}^{-1} \text{ s}^{-1}$ under ambient conditions. *Journal of the American Chemical Society* **2013**, *135* (33), 12168-12171.
10. Anthony, J. E.; Facchetti, A.; Heeney, M.; Marder, S. R.; Zhan, X., n-Type organic semiconductors in organic electronics. *Advanced Materials* **2010**, *22* (34), 3876-3892.
11. Usta, H.; Risko, C.; Wang, Z.; Huang, H.; Deliomeroğlu, M. K.; Zhukhovitskiy, A.; Facchetti, A.; Marks, T. J., Design, synthesis, and characterization of ladder-type molecules and polymers. air-stable, solution-processable n-channel and ambipolar

- semiconductors for thin-film transistors via experiment and theory. *Journal of the American Chemical Society* **2009**, *131* (15), 5586-5608.
12. Facchetti, A., π -Conjugated polymers for organic electronics and photovoltaic cell applications†. *Chemistry of Materials* **2010**, *23* (3), 733-758.
 13. Osaka, I.; McCullough, R. D., Advances in molecular design and synthesis of regioregular polythiophenes. *Accounts of Chemical Research* **2008**, *41* (9), 1202-1214.
 14. McCullough, R. D.; Lowe, R. D.; Jayaraman, M.; Anderson, D. L., Design, synthesis, and control of conducting polymer architectures: structurally homogeneous poly(3-alkylthiophenes). *The Journal of Organic Chemistry* **1993**, *58* (4), 904-912.
 15. Mei, J.; Bao, Z., Side chain engineering in solution-processable conjugated polymers. *Chemistry of Materials* **2014**, *26* (1), 604-615.
 16. Miyaura, N.; Suzuki, A., Palladium-catalyzed cross-coupling reactions of organoboron compounds. *Chemical Reviews* **1995**, *95* (7), 2457-2483.
 17. Milstein, D.; Stille, J. K., A general, selective, and facile method for ketone synthesis from acid chlorides and organotin compounds catalyzed by palladium. *Journal of the American Chemical Society* **1978**, *100* (11), 3636-3638.
 18. Beletskaya, I. P.; Cheprakov, A. V., The Heck reaction as a sharpening stone of palladium catalysis. *Chemical Reviews* **2000**, *100* (8), 3009-3066.
 19. King, A. O.; Okukado, N.; Negishi, E.-i., Highly general stereo-, regio-, and chemo-selective synthesis of terminal and internal conjugated enynes by the Pd-catalysed reaction of alkynylzinc reagents with alkenyl halides. *Journal of the Chemical Society, Chemical Communications* **1977**, (19), 683-684.
 20. Tamao, K.; Sumitani, K.; Kumada, M., Selective carbon-carbon bond formation by cross-coupling of Grignard reagents with organic halides. Catalysis by nickel-phosphine complexes. *Journal of the American Chemical Society* **1972**, *94* (12), 4374-4376.

21. Sonogashira, K.; Tohda, Y.; Hagihara, N., A convenient synthesis of acetylenes: catalytic substitutions of acetylenic hydrogen with bromoalkenes, iodoarenes and bromopyridines. *Tetrahedron Letters* **1975**, *16* (50), 4467-4470.
22. Bates, R., *Organic synthesis using transition metals*. Wiley: 2000.
23. Jana, R.; Pathak, T. P.; Sigman, M. S., Advances in transition metal (pd,ni,fe)-catalyzed cross-coupling reactions using alkyl-organometallics as reaction partners. *Chemical Reviews* **2011**, *111* (3), 1417-1492.
24. Yin; Liebscher, J., Carbon-carbon coupling reactions catalyzed by heterogeneous palladium catalysts. *Chemical Reviews* **2006**, *107* (1), 133-173.
25. Delord Joanna, G. F., C-H bond activation enables the rapid construction and late-stage diversification of functional molecules. *Nature Chemistry* **2013**, *5* (5), 369-375.
26. Ackermann, L., *Modern arylation methods*. Wiley: 2009.
27. Do, H.-Q.; Daugulis, O., Cu-catalyzed arylation of heterocycle C-H bonds. *Journal of the American Chemical Society* **2007**, *129* (41), 12404-12405.
28. Yu, J.-Q., Lutz. Ackermann, Zhangjie. Shi, *C-H activation (topics in current chemistry, 292)*. SpringerLink: 2010; Vol. 292.

CHAPTER II

ATTEMPTED SYNTHESIS OF POLY-(3-ALKOXY SELENOPHENE) AND POLYTHIAZOLE

2.1 POLY(3-ALKOXYSELENOPHENE) (PAoSe):

2.1.1 Introduction:

OSCs have gained a lot of attention in past decades. They are particularly useful for OPVs, OLEDs, photodetectors (sensors) and FETs. Among them, polythiophene is one of the most important OSCs. They are easy to make, environmentally stable, highly processable, and exhibit high electrical conductivity. As mentioned in Chapter 1, regioregular polythiophenes exhibit far superior properties when compared to regioirregular one. One of the reason is that regioregular P3HT can self-assemble in highly crystalline fiber called fibrils.¹³ Various properties of OSCs can be modified by attaching different side chains. For example, unsubstituted polythiophene is insoluble in organic solvents, but an alkyl chain substituted at the 3-position on thiophene rings, the resulting polymer is soluble in many solvents. In poly(3-hexylthiophene), electron density in the backbone can be increased by attaching a more electron rich chain, such as alkoxy, instead of an alkyl chain. This alkoxy chain raises the HOMO level but have minimal affect the LUMO level, which results in a narrow bandgap. These polythiophenes with alkoxy have been synthesized McCullough et al.²⁹ As described in Chapter 1, narrow bandgap OSCs are needed for many specific applications.

In this Chapter, Our attempt to synthesize alkoxy functionalized polyselenophenes will be

presented. I will first discuss, why these particular polymers were chosen to be synthesized. This will be followed by the monomer preparation. In the second part of the Chapter, I will discuss our initial efforts to synthesize polythiazoles.

2.1.2 Design:

The energy difference between the HOMO and LUMO energy level, in an OSC, is called the bandgap. It is a crucial parameter for determining an application of any OSC. To reduce the bandgap, many strategies have been used. Out of these, the following two approaches caught our attention. First, attaching an electron rich side chain will increase the electron density in the aromatic backbone (**Figure 2.1 a**). Second, replacing the sulfur atom, of the thiophene unit, with a less electronegative atom like selenium will also increase electron density (**Figure 2.1 b**).

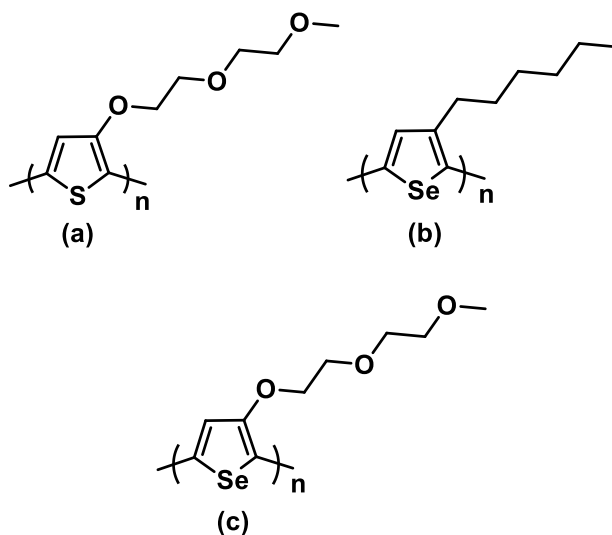


Figure 2.1: (a) poly(3-alkoxythiophene) (b) poly(3-hexylselenophene)

(c) proposed polymer: poly(3-alkoxyselenophene)

When the alkoxy chain is attached to thiophene, the ether oxygen (connected to thiophene) donates its electron density to the thiophene ring, this increases the HOMO level of the polymer, but only slightly affects the LUMO. Thus the bandgap is reduced. There is an added benefit with alkoxy chains. Due to such chains, polymer chains can pack tightly in the solid state. This leads

to better interaction between two polymer chains and increases the charge carrier mobility. Thus, alkoxy-substitution leads to desirable properties, such as reduced bandgap, and lower oxidation potential.²⁹

In selenophene, Se atom lowers the LUMO level significantly and increases the HOMO level slightly compared to thiophene.³⁰ Thus, selenophene has a narrow bandgap than thiophene.

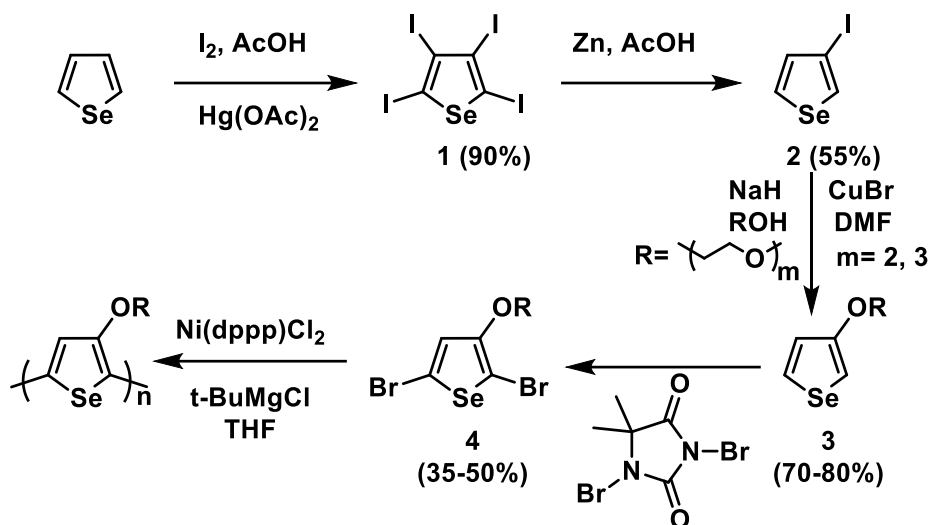
Thus, polyselenophene is more stable in the oxidized state. In this oxidized state, polymer chains are more planar because of restricted inter-ring rotation. Selenium-containing compounds experience increased intermolecular interactions from a partial Se-Se bonding interaction. These interactions are weak or not present in sulfur-containing analogues. The Se-Se interactions lead to tight packing of chains in films. All such factors result in a narrow bandgap and a higher charge carrier mobility in polyselenophene.³⁰⁻³⁶

Consequently, we hypothesized that, when both of these strategies were utilized together, a CP (**Figure 2.1 c**) with a very narrow bandgap (< 2.0 eV) could be obtained. Such a system could also have lower oxidation potential and enhanced charge carrier mobility. For this project, our specific goal was to synthesize a narrow bandgap polymer poly(3-alkoxyselenophene) (Fig 2.1 c).

2.1.3 Synthesis and Discussion

The proposed synthesis of poly(3-alkoxyselenophene) is shown in **Scheme 2.1**. Iodination of selenophene with iodine and mercury (II) acetate produced tetraiodoselenophene **1** with 90% yield. The later was reduced with zinc to afford 3-iodoselenophene **2** (yield 55%).³⁶⁻³⁷ The alokoxylation of **2** was achieved, by reaction of **2** with R (glycol ethers), NaH and CuBr as catalyst. This reaction gave 70-80% yield. **3** was readily brominated with 1,3-Dibromo-5,5-dimethylhydantoin to give 2,5-dibromo-3-alkoxyselenophene (yield 35-50%).²⁹ It was planned to perform polymerization of the monomer **4**, but unfortunately, it was very unstable. This is most likely due to high electron density in **4**, which could lead to radical formation (by Oxygen in air). This radical may autopolymerized. Even when the utmost care was taken and stored in glovebox,

4 yielded a tar-like black sticky material, which could not be analyzed since it was not soluble in common organic solvents.



Scheme 2.1: Synthesis of monomer and attempted polymerization

2.2 POLYTHIAZOLE

2.2.1 Introduction:

As describe in Chapter 1, there is a critical need to develop novel n-type OSCs which have good solubility, facile synthesis and air stability. To obtain such OSCs, this project was started.

2.2.2 Design:

Thiazole is five-membered heterocyclic aromatic compound containing nitrogen and sulfur.³⁸ The electron withdrawing nature of the imine (C=N) functional group in this moiety causes the electron density to be low in the aromatic ring.³⁹ Hence, it has been used in various small molecules and polymers as an electron acceptors.⁴⁰ Due to this electron deficiency, thiazole is a promising moiety for the development of n-type CPs. An alkyl chain was added to the core

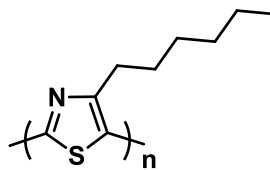


Figure 2.2: Poly(4-alkylthiazole)

moiety to impart solubility. This proposed research was to synthesize n-type CPs “poly(4-alkylthiazoles)” (Figure 2.2).

2.2.3 Attempted reactions to make thiazole derivatives:

In order to synthesize the desired polymer, the monomer 2,5-dibromo-4-hexylthiazole had to be prepared. First we wanted to attach an alkyl chain to the thiazole core. Then a bromination reaction was to be used to get the desired monomer. In the first attempt, no reaction took place

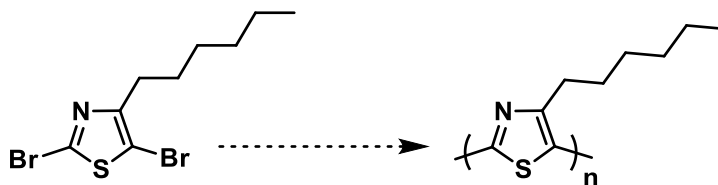


Figure 2.3: Proposed polymerization

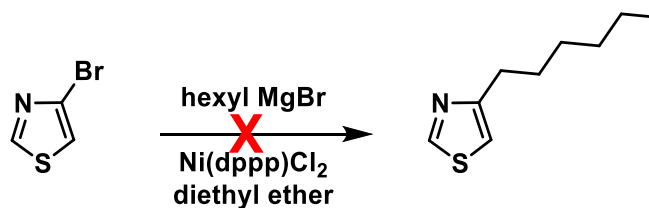


Figure 2.4: Alkylation of 4-Bromothiazole

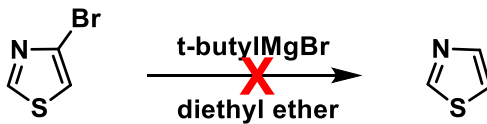


Figure 2.5: Debromination of thiazole

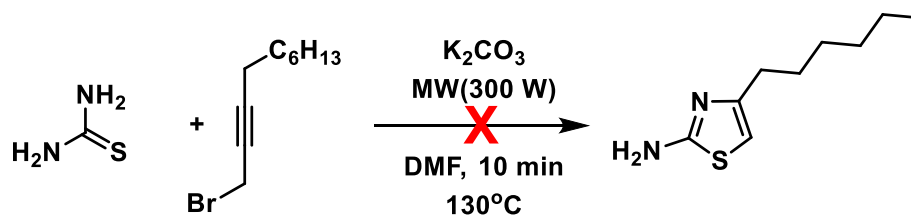


Figure 2.6: Synthesis of 4-hexylthiazole

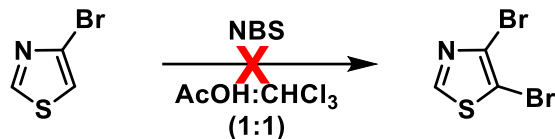


Figure 2.7: Bromination of 4-Bromothiazole



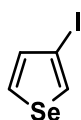
Figure 2.8: Cyanation of 2-Bromothiazole

with Kumada coupling (**Figure 2.4**).²⁰ Only starting material was recovered. Consequently, a reaction was performed to test the reactivity of bromine at the 4-position with the *t*-Butylmagnesiumchloride (**Figure 2.5**). Only starting material was recovered. A microwave synthetic method was carried out in an attempt to make 2-amino-4-hexylthiazole (**Figure 2.6**).⁴¹ But the process failed. Bromination of 4-Bromothiazole was tried with N-Bromosuccinamide (**Figure 2.7**). However, only starting material was recovered. We wanted to attach a cyano group at 2-position of thiazole (**Figure 2.8**), but this reactions was unsuccessful, too. The focus of our research was shifted to other projects, and this project was not pursued further.

2.3 Experimental Section:

All reactions were purged with Ar gas. Chemicals were purchased from Sigma Aldrich, Oakwood Chemicals and Fisher Chemicals and were used as received. Column chromatography was performed with Silica (60 Å, 230 x 400 mesh, Sorbent technology). Solvents used were from Solvent Purification System (Innovative Technology). All the glassware were oven dried. NMR experiments were performed with an I-400 Bruker NMR instrument. CDCl₃ was used as solvent for ¹H NMR samples, and all the spectra were referenced to δ 7.26 (residual Chloroform solvent peak).

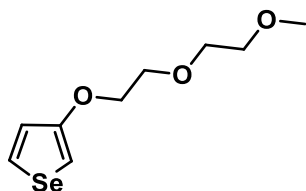
3-Iodoselenophene (**2**):



A solution of selenophene (5 g, 0.038 mol) in acetic acid (200 mL) was added to a 500 mL 3-necked rounded-Bottomed flask, containing mercury(II) acetate (48.76 g, 0.153 mol). The mixture was heated at 95-100 °C. Then, I₂ (38.74 g, 0.153 mol) was added portion wise over 15 min to the flask. Initially, the reaction color was yellow, the addition of two I₂ portions the color turned orange. After addition of all the I₂ portions, the color became purple, but eventually turned to yellow again. The reaction was refluxed for 1 h, then cooled to r.t., and deionized water (300 mL) was added. The reaction mixture was white in color with, an orange solid suspended. After placing in a refrigerator overnight, the mixture was filtered and washed with deionized water. The orange solid was stirred with aqueous KI (35 g in 350 mL of H₂O) solution for 2.5 h and then was filtered and washed with water (3 x 150 mL). The crude product was a pale yellow solid **1** (20.5 g, 85%) The crude was recrystallized with DMF/water. (lit³⁷ 205-210 °C). Tetraiodoselenophene (20 g, 0.031 mol) was placed in a 3-necked round-Bottomed flask with 80% AcOH (250 mL) and the solution was sonicated for 15 min. The flask was transferred to a

preheated bath of aluminum beads (120 °C). After the reaction started to boil, activated Zn (10.8 g, 0.165 mol) was added in four portions over 15 min. The color of the reaction was gray. After 3 h of refluxing, the color of the reaction mixture was dark brown. The reaction mixture was cooled to r.t. and saturated aqueous NaHCO₃ solution (1 L) was added to neutralize the reaction mixture, which was extracted with ethyl acetate (3 x 200 mL). The organic layer was washed with water and brine. The organic layer was dried (MgSO₄) and the solvent was removed with rotatory evaporation. The remaining liquid was purified *via* distillation under reduced pressure to give **2** (5.34 g, 65%) as a pale yellow liquid. ¹H NMR (300 MHz, CDCl₃) δ 8.10 (m, 1H), 7.86 (dd, *J* = 5.6, 2.5 Hz, 1H), 7.32 (d, *J* = 5.5 Hz, 1H).

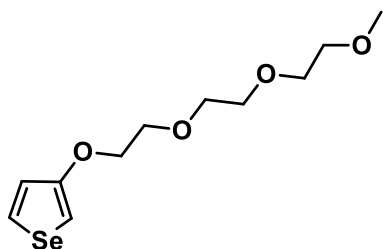
3-[2-(2-Methoxyethoxy)ethoxy]selenophene (**3a**):



A dry, 100-mL 3-necked round-bottomed flask equipped with a condenser and an addition funnel was purged with N₂ and charged with NaH [0.535 g (60% in mineral oil), 15.6 mmol] and anhydrous DMF (15 mL). The reaction flask was cooled to 0 °C, whereupon diethylene glycol monomethyl ether (4.49 g, 37.4 mmol) was added dropwise from the addition funnel over a 30 min period. The solution was allowed to stir for additional 1 h to assure complete consumption of NaH, while the temperature was maintained at 0 °C. To this reaction mixture, 3-iodoselenophene (0.2 g, 7.8 mmol) and CuBr (0.11 g, 0.78 mmol) were added. The reaction color was green. The ice bath was replaced with a heating bath, and the solution was heated to ~ 110 °C. After 60 min at the elevated temperature, an aliquot was (quenched with a 1 M aqueous solution of NH₄Cl, extracted with ethyl acetate and subjected to TLC analysis. If starting material was detected, a small amount of CuBr was added and the reaction was allowed to proceed a further 30 min at 110

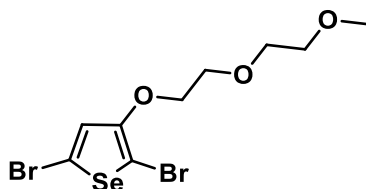
°C. The material was then poured into a 1 M aqueous solution of NH_4Cl (100 mL) and the mixture was stirred for 10 min. The organic phase was extracted with ethyl acetate (3 x 10 mL), and the extracts were dried over magnesium sulfate (MgSO_4). After the product was filtered, the solvent was removed with rotary evaporation. The crude product was purified with column chromatography using hexane/ethyl acetate mixture (from 10% ethyl acetate to 50% ethyl acetate) to yield **3a** (0.16 g, 85%) as a colorless oil. $^1\text{H NMR}$ (400 MHz, CDCl_3) δ 7.80 (dd, $J = 5.7, 2.6$ Hz, 1H), 7.15–7.11 (m, 1H), 6.68 (dd, $J = 2.6, 1.6$ Hz, 1H), 4.15–4.11 (m, 2H), 3.87–3.83 (m, 2H), 3.73–3.70 (m, 2H), 3.59–3.56 (m, 2H), 3.39 (s, 3H).

3-[2-[2-(2-Methoxyethoxy)ethoxy]ethoxy]selenophene (**3b**):



The reaction procedure was that used for **3a**. The crude product was purified with column chromatography with hexane/ethyl acetate (from 15% ethyl acetate to 50% ethyl acetate) to obtain **3b** (4.7 g, 82%) as a yellow oil. $^1\text{H NMR}$ (400 MHz, CDCl_3) δ 7.80 (dd, $J = 5.7, 2.6$ Hz, 1H), 7.13 (dd, $J = 5.7, 1.6$ Hz, 1H), 6.68 (dd, $J = 2.6, 1.6$ Hz, 1H), 4.14–4.10 (m, 2H), 3.87–3.83 (m, 2H), 3.74–3.65 (m, 6H), 3.57–3.53 (m, 2H), 3.38 (s, 3H).

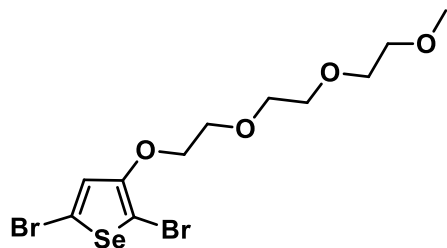
2,5-Dibromo-3-[2-(2-methoxyethoxy)ethoxy]selenophene (**4a**):



A solution of **3a** (1.0 g, 4.0 mmol) in anhydrous THF (20 mL) was added to a 100 mL 3-necked

round-Bottomed flask. The reaction flask was cooled to $-78\text{ }^{\circ}\text{C}$, and dibromohydantoin (1.16 g, 4.04 mmol) was added. The mixture was stirred for 30 min at $-78\text{ }^{\circ}\text{C}$. The dry ice bath was removed and the reaction was allowed to slowly warm to ambient temperature. The reaction was stopped in 2 h, after which the solution became dark green in color. The solvent was removed by rotary evaporation. The resulting residue was washed with hexanes, filtered, and purified using column chromatography on silica gel with hexanes and ethyl acetate (10:0 to 9:1). The product was dried over MgSO_4 , and decolorizing carbon was added to remove any residual radicals that could promote possible auto-polymerization. The solution underwent a distinct color change from green to colorless. After filtration, the solvent was removed by rotary evaporation. Pure **4a** (0.84 g, 50% yield) was obtained as pale yellow liquid. $^1\text{H NMR}$ (300 MHz, CDCl_3) δ 7.13 (s, 1H), 4.16 (m, 2H), 3.83–3.76 (m, 2H), 3.71 (m, 2H), 3.59–3.54 (m, 2H), 3.40 (s, 3H).

2,5-Dibromo-3-[2-[2-(2-methoxyethoxy)ethoxy]ethoxy]selenophene (**4b**):



The reaction procedure was the same as that used to produce **4a**. The crude product was purified by column chromatography with hexane/ethyl acetate (85:15 to 50:50) to obtain **4b** (1.5 g, 52%) as a yellow oil. $^1\text{H NMR}$ (300 MHz, CDCl_3) δ 4.18–4.12 (m, 2H), 3.81–3.76 (m, 2H), 3.75–3.63 (m, 6H), 3.58–3.53 (m, 2H), 3.39 (s, 3H).

2.4 References:

1. Osaka, I.; McCullough, R. D., Advances in molecular design and synthesis of regioregular polythiophenes. *Accounts of Chemical Research* **2008**, *41* (9), 1202-1214.
2. Sheina, E. E.; Khersonsky, S. M.; Jones, E. G.; McCullough, R. D., Highly conductive, regioregular alkoxy-functionalized polythiophenes: a new class of stable, narrow bandgap materials. *Chemistry of Materials* **2005**, *17* (13), 3317-3319.
3. Heeney, M.; Zhang, W.; Crouch, D. J.; Chabynyc, M. L.; Gordeyev, S.; Hamilton, R.; Higgins, S. J.; McCulloch, I.; Skabara, P. J.; Sparrowe, D.; Tierney, S., Regioregular poly(3-hexyl)selenophene: a narrow bandgap organic hole transporting polymer. *Chemical Communications* **2007**, (47), 5061-5063.
4. Hollinger, J.; Gao, D.; Seferos, D. S., Selenophene electronics. *Israel Journal of Chemistry* **2014**, *54* (5-6), 440-453.
5. Ballantyne, A. M.; Ferenczi, T. A. M.; Campoy-Quiles, M.; Clarke, T. M.; Maurano, A.; Wong, K. H.; Zhang, W.; Stingelin-Stutzmann, N.; Kim, J.-S.; Bradley, D. D. C.; Durrant, J. R.; McCulloch, I.; Heeney, M.; Nelson, J.; Tierney, S.; Duffy, W.; Mueller, C.; Smith, P., Understanding the influence of morphology on poly(3-hexylselenothiophene):PCBM solar cells. *Macromolecules* **2010**, *43* (3), 1169-1174.
6. Patra, A.; Wijsboom, Y. H.; Zade, S. S.; Li, M.; Sheynin, Y.; Leitus, G.; Bendikov, M., Poly(3,4-ethylenedioxy-selenophene). *Journal of the American Chemical Society* **2008**, *130* (21), 6734-6736.
7. Zade, S. S.; Zamoshchik, N.; Bendikov, M., Oligo- and polyselenophenes: a theoretical study. *Chemistry – A European Journal* **2009**, *15* (34), 8613-8624.
8. Patra, A.; Bendikov, M., Polyselenophenes. *Journal of Materials Chemistry* **2010**, *20* (3), 422-433.

9. Hollinger, J.; Jahnke, A. A.; Coombs, N.; Seferos, D. S., Controlling phase separation and optical properties in conjugated polymers through selenophene–thiophene copolymerization. *Journal of the American Chemical Society* **2010**, *132* (25), 8546-8547.
10. Franchetti, P.; Cappellacci, L.; Sheikha, G. A.; Jayaram, H. N.; Gurudutt, V. V.; Sint, T.; Schneider, B. P.; Jones, W. D.; Goldstein, B. M.; Perra, G.; De Montis, A.; Loi, A. G.; La Colla, P.; Grifantini, M., Synthesis, structure, and antiproliferative activity of selenophenfurin, an inosine 5'-monophosphate dehydrogenase inhibitor analogue of selenazofurin. *Journal of Medicinal Chemistry* **1997**, *40* (11), 1731-1737.
11. Yamashita, Y., Development of high-performance n-type organic field-effect transistors based on nitrogen heterocycles. *Chemistry Letters* **2009**, *38* (9), 870-875.
12. Eicher, T.; Hauptmann, S.; Speicher, A., *The chemistry of heterocycles: Structures, reactions, synthesis, and applications 3rd, completely revised and enlarged edition*. Wiley: 2013.
13. Lin, Y.; Fan, H.; Li, Y.; Zhan, X., Thiazole-based organic semiconductors for organic electronics. *Advanced Materials* **2012**, *24* (23), 3087-3106.
14. Tamao, K.; Sumitani, K.; Kumada, M., Selective carbon-carbon bond formation by cross-coupling of Grignard reagents with organic halides. Catalysis by nickel-phosphine complexes. *Journal of the American Chemical Society* **1972**, *94* (12), 4374-4376.
15. Castagnolo, D., Mafalda Pagano, Martina Bernardini, and Maurizio Botta, Domino Alkylation-cyclization reaction of propargyl bromides with thioureas/thiopyrimidinones: a new facile synthesis of 2-aminothiazoles and 5h-thiazolo[3,2-a]pyrimidin-5-ones. *Cheminform* **2009**, *40* (52), 2093-2096.

CHAPTER III

POLYTHIOPHENE BASED MATERIAL FOR Li-ION BATTERY ELECTRODE

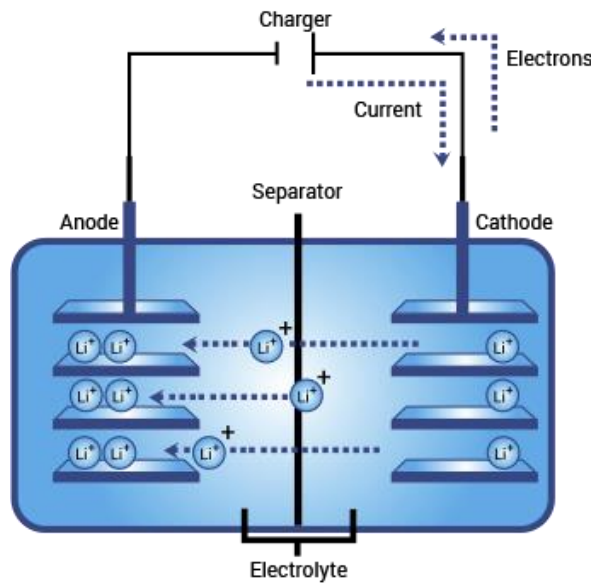
3.1 Introduction:

It is known that Li-ion batteries have many superior characteristics compared to other batteries such as, light weight, high energy density and no memory effect. Such batteries can endure large numbers of charge/discharge cycles. Compared to other batteries, they have less than half self-discharge during storage. Because of these many advantages, Li-ion batteries are prominently used in cell phones, tablets, laptops and electric cars. Work on Li-ion batteries was started in 1912 by G.N. Lewis. In the 1970s, for the first time non rechargeable Li-ion batteries were commercially available. However rechargeable batteries failed due to many safety concerns. In 1991, the Sony Corporation commercialized rechargeable Li-ion batteries, which was a major step forward. Consequently, the market for these batteries has increased exponentially.⁴²⁻⁴⁴

In this chapter, a discussion on the theory for the project will be presented. This will be followed by a discussion about polymer synthesis and polymer salt mixture preparation. Initial results, from our collaborator will be stated.

In **Figure 3.1**, a typical Li-ion battery is shown. Its major components are as follows: the cathode, the anode, the electrolyte and the separator. **Figure 3.1** also shows the charging/discharging process. During the charging process, when the load is applied the Li-ions flow from the cathode to the anode. Electrons flow from the outer circuit to the anode, since electron

Lithium-ion rechargeable battery Charge mechanism



Lithium-ion rechargeable battery Discharge mechanism

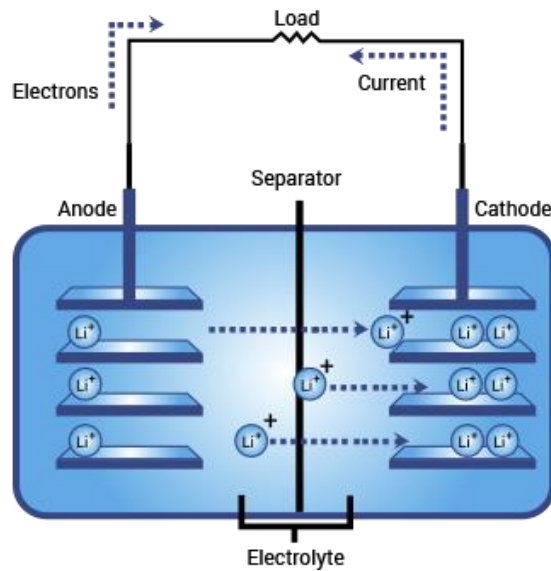


Figure 3.1: Li-ion battery

cannot pass through electrolyte. When a device is attached to a Li-ion battery resulting in a discharge process, the Li ions travel from the anode to the cathode through the electrolyte.

Electrons pass through outer circuit, powering the device. The battery is completely discharge when all of the Li ions reach the cathode.⁴⁵⁻⁴⁶

The current Li-ion batteries are designed using a carbon based anode (Li_xC_6), a cathode (LiCoO_2), a non-aqueous liquid electrolyte, and a separator.^{42, 47} The most practical rechargeable batteries deliver capacities and energy densities far below their theoretical values. To improve efficiency, novel materials for the electrodes need to be developed. LiCoO_2 is the most widely used material for the cathode. Due to degradation of the lithium cobalt oxides over the time, oxygen is generated and the resistance for the Li-ion also increases which generates heat. There is a layer of small molecules, such as ethylene carbonate, dimethyl carbonate, or diethyl carbonate, in the middle part of the battery. These small molecules act as the electrolyte materials. They are flammable and have low boiling points. Heat, oxygen and flammable compounds are a perfect recipe for fire. Thus, a major concern for the Li-ion batteries is fire. To overcome this issue, one needs to develop an alternative material for the cathode.⁴⁸

3.2 Design:

In 2013, Balsara et al. synthesized a block co-polymer as shown in **Figure 3.2**. It showed reasonable electron and Li-ion conductivity.⁴⁹ However, this copolymer has some drawbacks. The copolymer synthesis requires multiple steps. Due to the two separate blocks in this copolymer, it might undergo phase separation. In the different phases Li-ions and electrons may

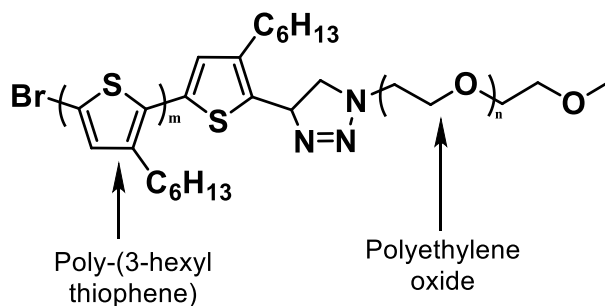


Figure 3.2: Block co-polymer for Li ion and electron conductivity

get trapped, which eventually decreases the efficiency. However this approach is very intriguing. Hence we planned to make a mixture of a CP and a Li-ion salt as an alternative material based on the above approach. We made a homopolymer, poly(3-alkoxythiophene) (PAoT) (**Figure 3.3**). The backbone of the polymer will conduct the electrons, due to extended conjugation.

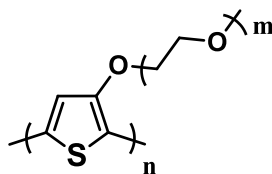
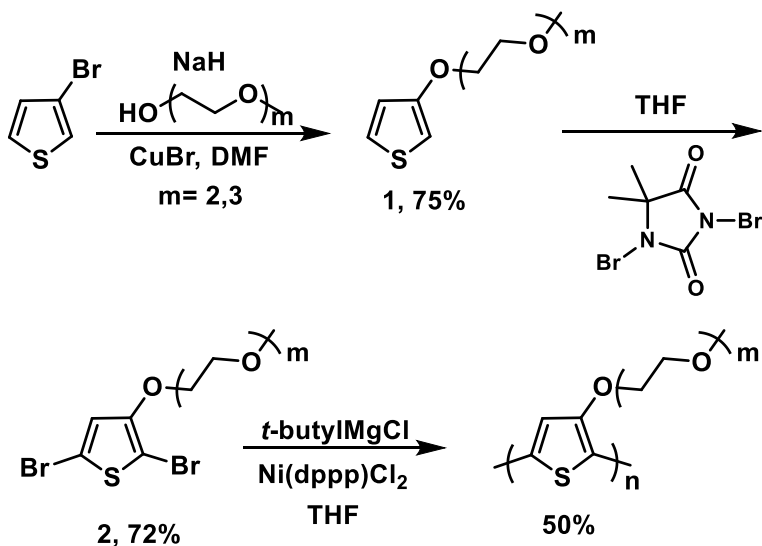


Figure 3.3: Proposed polymer, poly(3-alkoxythiophene)

The side chain will host the Li-ions. The Li-ions are weakly attached to oxygen atoms in the side chain. These side chains are free to move to some extent. Due to the side chains and the electrical field, Li-ions can conduct from one place to another.

3.3 Synthesis of PAoT:

First, an alkoxy group was attached to thiophene at the 3-position to generate **1**. Bromination of **1** with 1,3-Dibromo-5,5-dimethylhydantoin yielded **2**. This monomer was polymerized via the GRIM method.²⁹



Scheme 3.1: Synthesis of PAoT

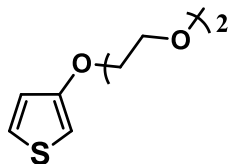
3.4 Polymer/salt mixture preparation and initial testings:

In order to test if PAoTs could serve as cathode material, several PAoT/lithium salt mixtures were prepared. The lithium trifluoromethanesulfonate (LiTFSi) was used as the source of the Li-ion. Due to the low solubility of LiTFSi in chloroform, the polymer/salt mixtures were prepared in a 15% THF/chloroform solution. First, PAoT was reduced with hydrazine hydrate as described here. Then, 100 mg of PAoT was dissolved in 20 mL of chloroform in a 1-necked round-bottomed flask with the system under Ar. Chloroform was removed via simple distillation. Hydrazine hydrate was removed under reduced pressure. The resulting polymer was kept under vacuum overnight. Dry chloroform (5 mL) was added to the flask, and the system was sonicated for 1 h. This flask was transferred to the glovebox. The polymer solution was filtered with a 0.45 μ filter and 3 mL chloroform was added to the solution. Separately, 3 mg of LiTFSi was dissolved in 1.5 mL of THF. This salt solution was added to the polymer solution and the mixture was stirred overnight in the glovebox. Films of this mixture were formed *via* drop cast method.

To measure Li-ion conductivity, the polymer salt mixtures were sent to Dr. Alexander Lopez, department of Chemical Engineering, University of Mississippi. His evaluations, based on the preliminary results obtained for our materials, was that the resistance levels alone made the materials interesting and viable candidates for Li-ion transfer. Further testing is under progress.

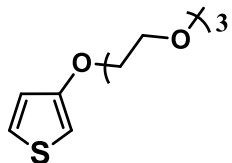
3.5 Experimental section:

3-[2-(2-Methoxyethoxy)ethoxy]thiophene (**1A**):



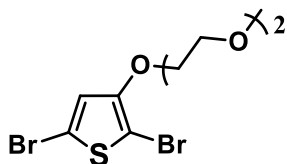
A dry 100-mL three-necked round-bottomed flask, equipped with a condenser and an addition funnel, was purged with N₂ and charged with NaH [0.535 g (60% in mineral oil), 15.6 mmol] and anhydrous DMF (15 mL). The reaction flask was cooled to 0 °C, whereupon diethylene glycol monomethyl ether (4.49 g, 37.4 mmol) was added dropwise from the addition funnel over a 30 min time period. The solution was allowed to stir for an additional 1 h to assure complete consumption of NaH, while the temperature was maintained at 0 °C. To this reaction mixture was added 3-bromothiophene (1.2 g, 7.8 mmol) and CuBr (0.11 g, 0.78 mmol). The color of the reaction mixture was green. The ice bath was replaced with a heating bath, and the solution was heated to 110 °C. After 60 minutes at the elevated temperature, an aliquot was taken and quenched with a 1 M aqueous solution of NH₄Cl. The resulting mixture was extracted with ethyl acetate, and subjected to TLC analysis. If a relative abundance of the starting material was detected, a small amount of CuBr was added and the reaction was allowed to proceed for an additional 30 min at the elevated temperature. The material was then poured into a 1 M aqueous solution of NH₄Cl (100 mL) and stirred for 10 minutes. The organic phase was extracted with hexanes:ethyl acetate (3 x 15 mL) and dried (MgSO₄). After the product was filtered, the solvent was removed by rotary evaporation. The crude product was purified by column chromatography with hexane/ethyl acetate (from 10% ethyl acetate to 50% ethyl acetate) to obtain **1A** (1.6 g, 85%) as a colorless oil. ¹H NMR (400 MHz, CDCl₃) δ 7.17 (dd, *J* = 5.2, 3.1 Hz, 1H), 6.78 (dd, *J* = 5.3, 1.6 Hz, 1H), 6.26 (dd, *J* = 3.1, 1.6 Hz, 1H), 4.16–4.11 (m, 2H), 3.87–3.83 (m, 2H), 3.73–3.69 (m, 2H), 3.60–3.56 (m, 2H), 3.39 (s, 3H).

3-[2-[2-(2-Methoxyethoxy)ethoxy]ethoxy]thiophene (**1B**):



The reaction procedure was the same as that used for **1A**. The crude product was purified by column chromatography with hexane/ethyl acetate (from 15% ethyl acetate to 50% ethyl acetate) to obtain **1B** (4.7g, 82%) as a yellow oil. ¹H NMR (400 MHz, CDCl₃) δ 7.16 (dd, *J* = 5.3, 3.1 Hz, 1H), 6.78 (dd, *J* = 5.2, 1.5 Hz, 1H), 6.26 (dd, *J* = 3.1, 1.5 Hz, 1H), 4.12 (dd, *J* = 5.7, 4.0 Hz, 2H), 3.84 (dd, *J* = 5.7, 3.9 Hz, 2H), 3.77–3.51 (m, 9H), 3.38 (s, 4H).

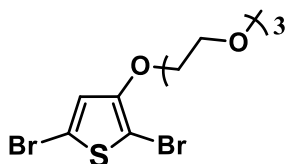
2,5-Dibromo-3-[2-(2-methoxyethoxy)ethoxy]selenophene (**2A**):



A solution of **1A** (0.81 g, 4.0 mmol) in anhydrous THF (20 mL) was added to a 100 mL 3-necked round-bottomed flask. The reaction flask was cooled to -78 °C, and dibromohydantoin (1.16 g, 4.04 mmol) was added. The reaction mixture was stirred for 30 min at -78 °C. The ice bath was removed, and the reaction was allowed to slowly warm to ambient temperature. The reaction was stopped after 2 h. The color of the reaction mixture became dark green. The solvent was removed by rotary evaporation. The resulting residue was washed with hexanes (2 x 15 mL), filtered, and purified using column chromatography on silica gel with hexanes:ethyl acetate (9:1). The solution was dried (MgSO₄), and decolorizing carbon was added to remove any residual radicals that could promote possible autopolymerization. The neat solution underwent a distinct color change from green to colorless. After filtration, the solvent was removed by rotary evaporation. The pure product, **2A** (0.72 g, 50% yield) was as pale yellow liquid. The latter was

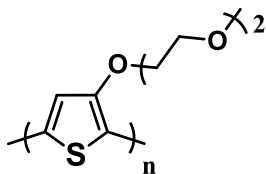
flushed with Ar in an amber vial and stored in a freezer at -20 °C. $^1\text{H NMR}$ (400 MHz, CDCl_3) δ 6.78 (s, 1H), 4.23 (t, $J = 5.1$ Hz, 2H), 3.84 (t, $J = 5.1$ Hz, 2H), 3.75 (m, 2H), 3.59 (m, 2H), 3.41 (s, 3H).

2,5-Dibromo-3-[2-[2-(2-methoxyethoxy)ethoxy]ethoxy]thiophene (**2B**):



The reaction procedure was the same as that used for **2A**. The crude product was purified with column chromatography with hexane/ethyl acetate (85:15 to 50:50) to obtain a yellow oil of 2,5-dibromo-3-[2-[2-(2-methoxyethoxy)ethoxy]ethoxy]thiophene, **2B** (1.5 g, 52%). $^1\text{H NMR}$ (400 MHz, CDCl_3) δ 6.82 (s, 1H), 4.16 (t, $J = 4.8$ Hz, 2H), 3.87–3.52 (m, 12H), 3.38 (s, 3H).

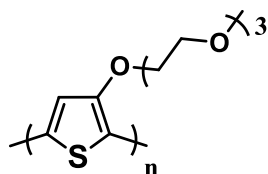
Poly(3-[2-(2-methoxyethoxy)ethoxy]thiophene):



The monomer, **2A** (0.22 g, 0.61 mmol) was added to a dry 100mL 3-necked round-bottomed flask, which was kept under vacuum for 2 h. The system was purged with Ar. Anhydrous THF (6 mL) and cyclohexylmagnesium chloride (0.31 mL, 2 M) were added to the flask. The reaction mixture was allowed to stir for 30 minutes at room temperature followed by addition of $\text{Ni}(\text{dppp})\text{Cl}_2$ (5.5 mg, 0.01 mmol) previously dissolved in anhydrous THF (0.5 mL). The polymerization was allowed to proceed for 12 hours at reflux conditions. The reaction mixture was then allowed to cooled to room temperature, and precipitation was initiated by adding the reaction mixture to pentane (2 mL). The polymers were filtered, purified by Soxhlet extraction in

sequence with hexanes (5 mL), methanol (5 mL) and chloroform (5 mL). The solvent was removed by rotatory evaporation. The dark purple-Blue precipitates were identified as the polymer (65%). The polymer was stored under an inert atmosphere. $^1\text{H NMR}$ (300 MHz, CDCl_3): δ 6.98 (s, 1H), 4.23 (t, 2H), 3.84 (bt, 2H), 3.75 (bm, 2H), 3.59 (m, 2H), 3.41 (s, 3H).

Poly(3-[2--[2-(2-methoxyethoxy)ethoxy]ethoxy]selenophene):



The polymer was synthesized by the above mentioned polymerization method. $^1\text{H NMR}$ (300 MHz, CDCl_3): 6.99 (s, 1H), 4.37 (bm, 2H), 3.97 (bm, 2H) 3.80(m, 2H),), 3.73 (m, 2H), 3.68 (m, 2H), 3.54 (m, 2H), 3.37 (s, 3H).

3.6 References:

1. Skotheim, T. A.; Reynolds, J., *Conjugated Polymers: Processing and Applications*. Taylor & Francis: 2006.
2. Rockett, A., *The Materials Science of Semiconductors*. Springer US: 2007.
3. Capek, I., *ADVANCES IN POLYMER SCIENCE V145.: Radical polymerisation polyelectrolytes*. Springer Berlin Heidelberg: 1999.
4. Sirdeshmukh, D.; Sirdeshmukh, L.; Subhadra, K. G.; Sunandana, C. S., *Electrical, Electronic and Magnetic Properties of Solids*. Springer International Publishing: 2014.
5. Bundgaard, E.; Krebs, F. C., Narrow bandgap polymers for organic photovoltaics. *Solar Energy Materials and Solar Cells* **2007**, 91 (11), 954-985.

6. Dou, L.; Liu, Y.; Hong, Z.; Li, G.; Yang, Y., Low-Bandgap Near-IR Conjugated Polymers/Molecules for Organic Electronics. *Chemical Reviews* **2015**, *115* (23), 12633-12665.
7. Sirringhaus, H., Organic semiconductors: An equal-opportunity conductor. *Nat Mater* **2003**, *2* (10), 641-642.
8. Organic Semiconductors. In *The Materials Science of Semiconductors*, Springer US: Boston, MA, 2008; pp 395-453.
9. Lei, T.; Dou, J.-H.; Cao, X.-Y.; Wang, J.-Y.; Pei, J., Electron-Deficient Poly(p-phenylene vinylene) Provides Electron Mobility over $1 \text{ cm}^2 \text{ V}^{-1} \text{ s}^{-1}$ under Ambient Conditions. *Journal of the American Chemical Society* **2013**, *135* (33), 12168-12171.
10. Anthony, J. E.; Facchetti, A.; Heeney, M.; Marder, S. R.; Zhan, X., n-Type Organic Semiconductors in Organic Electronics. *Advanced Materials* **2010**, *22* (34), 3876-3892.
11. Usta, H.; Risko, C.; Wang, Z.; Huang, H.; Deliomeroğlu, M. K.; Zhukhovitskiy, A.; Facchetti, A.; Marks, T. J., Design, Synthesis, and Characterization of Ladder-Type Molecules and Polymers. Air-Stable, Solution-Processable n-Channel and Ambipolar Semiconductors for Thin-Film Transistors via Experiment and Theory. *Journal of the American Chemical Society* **2009**, *131* (15), 5586-5608.
12. Facchetti, A., π -Conjugated Polymers for Organic Electronics and Photovoltaic Cell Applications†. *Chemistry of Materials* **2010**, *23* (3), 733-758.
13. Osaka, I.; McCullough, R. D., Advances in Molecular Design and Synthesis of Regioregular Polythiophenes. *Accounts of Chemical Research* **2008**, *41* (9), 1202-1214.
14. McCullough, R. D.; Lowe, R. D.; Jayaraman, M.; Anderson, D. L., Design, synthesis, and control of conducting polymer architectures: structurally homogeneous poly(3-alkylthiophenes). *The Journal of Organic Chemistry* **1993**, *58* (4), 904-912.
15. Mei, J.; Bao, Z., Side Chain Engineering in Solution-Processable Conjugated Polymers. *Chemistry of Materials* **2014**, *26* (1), 604-615.

16. Miyaura, N.; Suzuki, A., Palladium-Catalyzed Cross-Coupling Reactions of Organoboron Compounds. *Chemical Reviews* **1995**, *95* (7), 2457-2483.
17. Milstein, D.; Stille, J. K., A general, selective, and facile method for ketone synthesis from acid chlorides and organotin compounds catalyzed by palladium. *Journal of the American Chemical Society* **1978**, *100* (11), 3636-3638.
18. Beletskaya, I. P.; Cheprakov, A. V., The Heck Reaction as a Sharpening Stone of Palladium Catalysis. *Chemical Reviews* **2000**, *100* (8), 3009-3066.
19. King, A. O.; Okukado, N.; Negishi, E.-i., Highly general stereo-, regio-, and chemo-selective synthesis of terminal and internal conjugated enynes by the Pd-catalysed reaction of alkynylzinc reagents with alkenyl halides. *Journal of the Chemical Society, Chemical Communications* **1977**, (19), 683-684.
20. Tamao, K.; Sumitani, K.; Kumada, M., Selective carbon-carbon bond formation by cross-coupling of Grignard reagents with organic halides. Catalysis by nickel-phosphine complexes. *Journal of the American Chemical Society* **1972**, *94* (12), 4374-4376.
21. Sonogashira, K.; Tohda, Y.; Hagihara, N., A convenient synthesis of acetylenes: catalytic substitutions of acetylenic hydrogen with bromoalkenes, iodoarenes and bromopyridines. *Tetrahedron Letters* **1975**, *16* (50), 4467-4470.
22. Bates, R., *Organic Synthesis Using Transition Metals*. Wiley: 2000.
23. Jana, R.; Pathak, T. P.; Sigman, M. S., Advances in Transition Metal (Pd,Ni,Fe)-Catalyzed Cross-Coupling Reactions Using Alkyl-organometallics as Reaction Partners. *Chemical Reviews* **2011**, *111* (3), 1417-1492.
24. Yin; Liebscher, J., Carbon–Carbon Coupling Reactions Catalyzed by Heterogeneous Palladium Catalysts. *Chemical Reviews* **2006**, *107* (1), 133-173.
25. Delord Joanna, G. F., C-H bond activation enables the rapid construction and late-stage diversification of functional molecules. *Nature Chemistry* **2013**, *5* (5), 369-375.
26. Ackermann, L., *Modern Arylation Methods*. Wiley: 2009.

27. Do, H.-Q.; Daugulis, O., Copper-Catalyzed Arylation of Heterocycle C–H Bonds. *Journal of the American Chemical Society* **2007**, *129* (41), 12404-12405.
28. Yu, J.-Q., Lutz. Ackermann, Zhangjie. Shi, *C-H Activation (Topics in Current Chemistry, 292)*. SpringerLink: 2010; Vol. 292.
29. Sheina, E. E.; Khersonsky, S. M.; Jones, E. G.; McCullough, R. D., Highly Conductive, Regioregular Alkoxy-Functionalized Polythiophenes: A New Class of Stable, Narrow bandgap Materials. *Chemistry of Materials* **2005**, *17* (13), 3317-3319.
30. Heeney, M.; Zhang, W.; Crouch, D. J.; Chabinyk, M. L.; Gordeyev, S.; Hamilton, R.; Higgins, S. J.; McCulloch, I.; Skabara, P. J.; Sparrowe, D.; Tierney, S., Regioregular poly(3-hexyl)selenophene: a narrow bandgap organic hole transporting polymer. *Chemical Communications* **2007**, (47), 5061-5063.
31. Hollinger, J.; Gao, D.; Seferos, D. S., Selenophene Electronics. *Israel Journal of Chemistry* **2014**, *54* (5-6), 440-453.
32. Ballantyne, A. M.; Ferenczi, T. A. M.; Campoy-Quiles, M.; Clarke, T. M.; Maurano, A.; Wong, K. H.; Zhang, W.; Stingelin-Stutzmann, N.; Kim, J.-S.; Bradley, D. D. C.; Durrant, J. R.; McCulloch, I.; Heeney, M.; Nelson, J.; Tierney, S.; Duffy, W.; Mueller, C.; Smith, P., Understanding the Influence of Morphology on Poly(3-hexylselenothiophene):PCBM Solar Cells. *Macromolecules* **2010**, *43* (3), 1169-1174.
33. Patra, A.; Wijsboom, Y. H.; Zade, S. S.; Li, M.; Sheynin, Y.; Leitus, G.; Bendikov, M., Poly(3,4-ethylenedioxy-selenophene). *Journal of the American Chemical Society* **2008**, *130* (21), 6734-6736.
34. Zade, S. S.; Zamoshchik, N.; Bendikov, M., Oligo- and Polyselenophenes: A Theoretical Study. *Chemistry – A European Journal* **2009**, *15* (34), 8613-8624.
35. Patra, A.; Bendikov, M., Polyselenophenes. *Journal of Materials Chemistry* **2010**, *20* (3), 422-433.

36. Hollinger, J.; Jahnke, A. A.; Coombs, N.; Seferos, D. S., Controlling Phase Separation and Optical Properties in Conjugated Polymers through Selenophene–Thiophene Copolymerization. *Journal of the American Chemical Society* **2010**, *132* (25), 8546-8547.
37. Franchetti, P.; Cappellacci, L.; Sheikha, G. A.; Jayaram, H. N.; Gurudutt, V. V.; Sint, T.; Schneider, B. P.; Jones, W. D.; Goldstein, B. M.; Perra, G.; De Montis, A.; Loi, A. G.; La Colla, P.; Grifantini, M., Synthesis, Structure, and Antiproliferative Activity of Selenophenfurin, an Inosine 5'-Monophosphate Dehydrogenase Inhibitor Analogue of Selenazofurin. *Journal of Medicinal Chemistry* **1997**, *40* (11), 1731-1737.
38. Yamashita, Y., Development of High-performance n-Type Organic Field-effect Transistors Based on Nitrogen Heterocycles. *Chemistry Letters* **2009**, *38* (9), 870-875.
39. Eicher, T.; Hauptmann, S.; Speicher, A., *The Chemistry of Heterocycles: Structures, Reactions, Synthesis, and Applications 3rd, Completely Revised and Enlarged Edition*. Wiley: 2013.
40. Lin, Y.; Fan, H.; Li, Y.; Zhan, X., Thiazole-Based Organic Semiconductors for Organic Electronics. *Advanced Materials* **2012**, *24* (23), 3087-3106.
41. Castagnolo, D., Mafalda Pagano, Martina Bernardini, and Maurizio Botta, Domino Alkylation-Cyclization Reaction of Propargyl Bromides with Thioureas/Thiopyrimidinones: A New Facile Synthesis of 2-Aminothiazoles and 5H-Thiazolo[3,2-a]pyrimidin-5-ones. *Cheminform* **2009**, *40* (52), 2093-2096.
42. Yoshio, M.; Brodd, R. J.; Kozawa, A., *Lithium-Ion Batteries: Science and Technologies*. Springer New York: 2010.
43. Erickson, E. M.; Ghanty, C.; Aurbach, D., New Horizons for Conventional Lithium Ion Battery Technology. *The Journal of Physical Chemistry Letters* **2014**, *5* (19), 3313-3324.
44. van Schalkwijk, W.; Scrosati, B., *Advances in Lithium-Ion Batteries*. Springer US: 2007.
45. Goodenough, J. B.; Park, K.-S., The Li-Ion Rechargeable Battery: A Perspective. *Journal of the American Chemical Society* **2013**, *135* (4), 1167-1176.

46. Deng, D., Li-ion batteries: basics, progress, and challenges. *Energy Science & Engineering* **2015**, 3 (5), 385-418.
47. Bhatt, M. D.; O'Dwyer, C., Recent progress in theoretical and computational investigations of Li-ion battery materials and electrolytes. *Physical Chemistry Chemical Physics* **2015**, 17 (7), 4799-4844.
48. Periodic graphics: Why Li-ion batteries catch fire.
<http://cen.acs.org/articles/94/i45/Periodic-graphics-Li-ion-Batteries.html>.
49. Javier, A. E.; Patel, S. N.; Hallinan, D. T.; Srinivasan, V.; Balsara, N. P., Simultaneous Electronic and Ionic Conduction in a Block Copolymer: Application in Lithium Battery Electrodes. *Angewandte Chemie International Edition* **2011**, 50 (42), 9848-9851.

CHAPTER IV

SYNTHESIS OF BENZODITHIOPHENE-S,S-TETRAOXIDE (BDTT) BASED SMALL MOLECULES VIA COPPER CATALYZED DIRECT ARYLATION

4.1 Introduction

Heterocycle building blocks are a fundamental part of various organic semiconductor (OSCs). Heteroatoms in these blocks are extremely crucial to impart different electronic properties (such as electron donating/accepting, electrons/holes conduction) to OSCs. Heteroatoms directly affect the bandgap, HOMO and LUMO levels of an OSC. These values dictate the application of an OSC for a particular device. These atoms also affect crystal packing and other characteristics. The main featured heteroatoms are “S, N, O, Se and Si”. Common heterocycles are as follows: thiophene, thiazole, oxazole, selenophene, indole, benzobisthiophene, benobisoxazole, benothiazole, benzobisthiazole, 9-silafluorene, pyridine, carbazole, benzothiadiazole, dialkylnaphthalenedicarboximidodithiophene (NDI), diketopyrrolo [3,4-*c*] pyrrole-1,4-dione (DPP) and thienopyrazine (**Figure 4.1**). As described in Chapter 1, there have been many p-type CPs reported, yet air stable and soluble n-type CPs are very limited.¹ This remains a major obstacle to the advancement of organic electronics. One of the main reasons is that coupling reactions between two electron poor molecules do not proceed very successfully. Electron-deficient monomers are more difficult to controllably polymerize to high molecular weights than

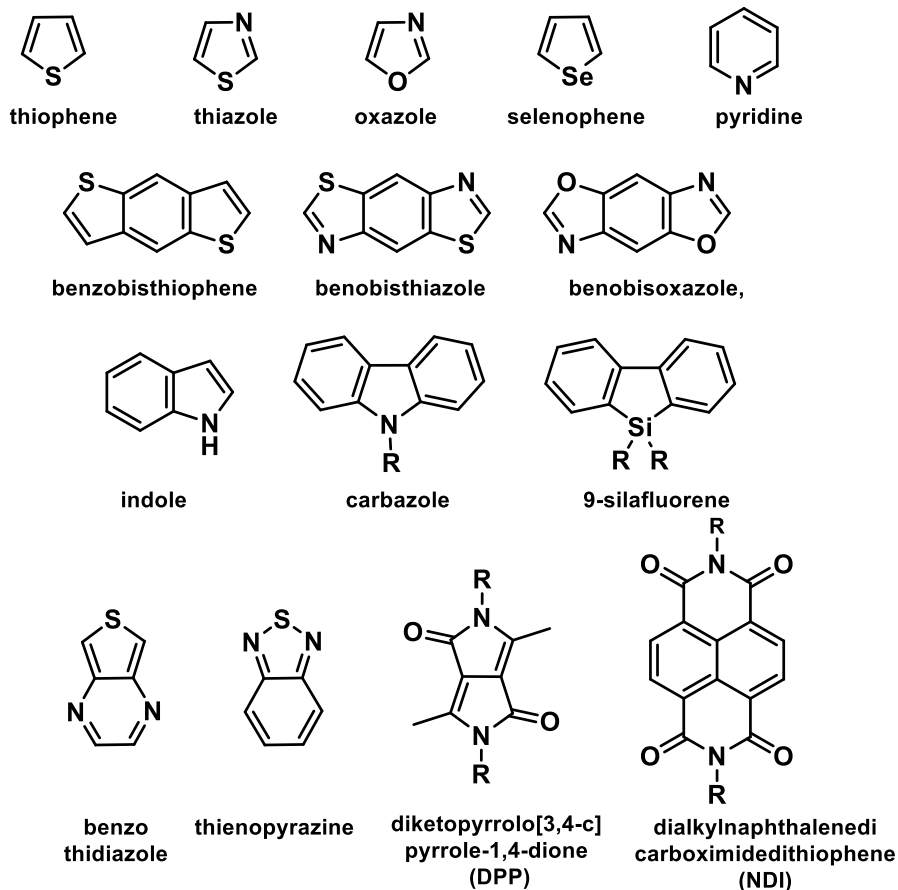


Figure 4.1: Widely used heterocyclic blocks for OSCs

well-studied electron-rich monomers used for p-type polymers.²⁻³ To overcome this problem novel synthetic approaches need to be discovered, such as a direct arylation method.

In this Chapter, the importance of the benzodithiophene-*S,S*-tetraoxide (BDTT) moiety and Cu-catalyzed direct arylation method will be discussed. In addition, various experiment conditions to optimize the yield of the bifunctionalized product will be stated. Additionally the scope of the reaction will be presented. Optical properties of different derivatives of BDTT will be described. Beside Cu-catalyzed direct arylation, other projects, using BDTT moiety, will also be discussed. These latter projects are under progress.

4.2 Design

N-type OSCs tend to be composed of the building blocks with electron-poor/withdrawing groups.

Benzodithiophene (BDT) is inherently an electron rich molecule due to two sulfur atoms.

However, these two sulfurs can be oxidized to sulfone functional groups. This group is a strong electron withdrawing group. Complete oxidation of BDT results in the formation of BDTT (Figure 4.2).

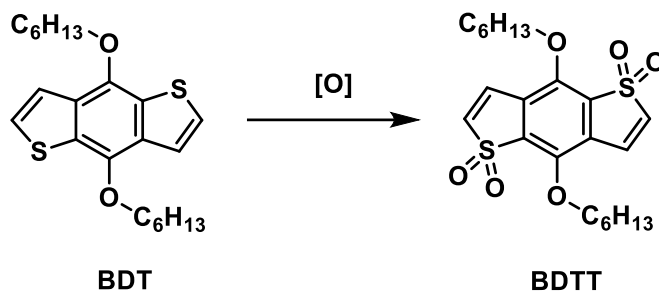


Figure 4.2: Oxidation of BDT

	BDT(V)	BDTT (V)
E_{ox}	0.86, 1.33	--
E_{red}	--	-1.04, -1.47

Table 4.1: Oxidation and reduction potential of BDT and BDTT

Due to two sulfone groups, BDTT is electron poor. This phenomena is also evident from their oxidation and reduction potentials (Table 4.1).⁴ BDT can be oxidized (0.86 V, 1.33 V), but cannot be reduced. While, BDTT can be reduced (-1.04 V, -1.47 V), but cannot be oxidized. The electron poor nature makes BDTT a promising block for an n-type material.⁵⁻¹³ From our best knowledge, BDTT has seen very limited utility as a building block for the synthesis of OSCs despite it being an electron poor heterocycle with promise for development of electron acceptor materials.^{4, 14-15} These oxidized oligomeric thiophene units are also potential materials for OLEDs.^{4, 16-19} This lack of effort is probably due to the difficulties of precursor syntheses

(conventional C-C cross coupling reactions) that result in low yields.⁴

4.3 Cu-catalyzed direct arylation:

To circumvent this synthesis challenge, we decided to use a direct arylation method. This approach does not require prefunctionalized compounds. There are many examples of such reactions in the literature^{4, 14-15} during the last 15 years. This is a facile approach for an aryl C-C bond formation. This route is also atom economical, which makes it even more attractive with respect to green chemistry. The direct arylation approach enables previously unachievable C-C disconnections. Glorious et al. have suggested that this approach could be used for the late stage diversification of compounds to have large library of derivatives.²⁰ A direct comparison between direct arylation and the conventional cross coupling method is given (**Figure 4.3**).

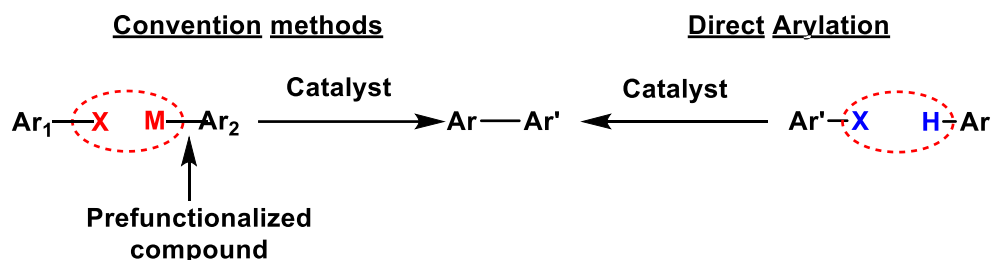


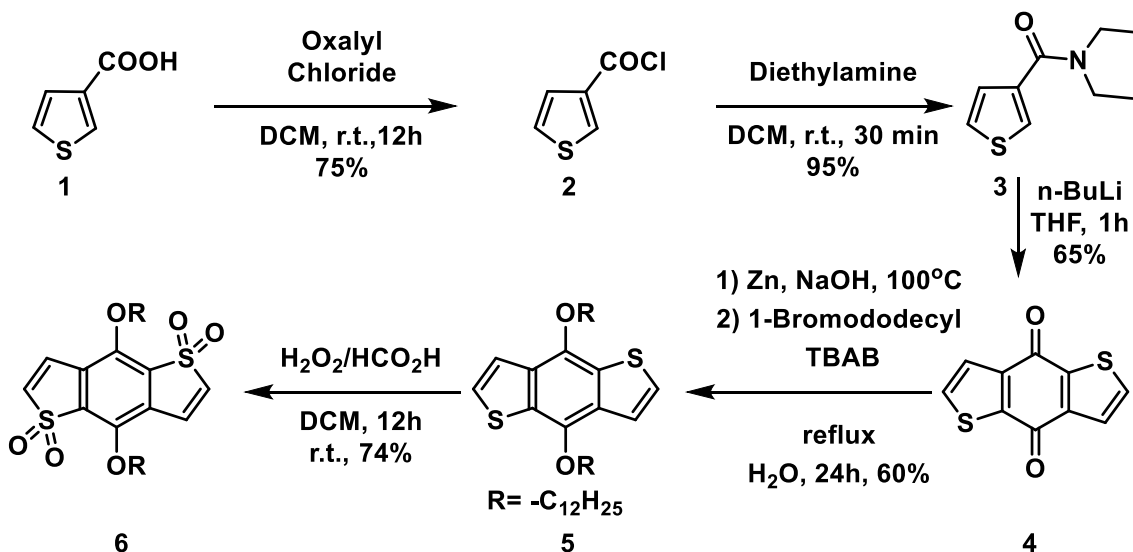
Figure 4.3: Conventional coupling reaction and direct arylation

Generally Pd, Ru and Rh based catalysts are used for direct arylation. These catalysts can be expensive and toxic. Lately, Cu catalysts have been used for direct arylation.²¹⁻²⁴ Cu catalysts are inexpensive as well as environmentally friendly. Therefore, reactions with the Cu catalyst, CuI, were initiated.

4.4 Synthesis of BDTT

BDTT, the precursor for direct arylation was synthesized as described **Scheme 4.1**. Reaction of thiophene-3-carboxylic acid with oxalyl chloride yielded the acid chloride compound, **2** (yield 75%). By reacting **2** with diethylamine, the acid chloride was converted to the amide **3** (yield 95%). Reaction of **3** with *n*BuLi yielded 4,8-dihydrobenzo[1,2-B:4,5-B']dithiophen-4,8-dione (**4**)

(yield 65%). Reduction of **4** with activated Zn, followed by reaction with 1-Bromododecane afforded 2,6-dibromo-4,8-didodecyloxybenzo[1,2-B;3,4-B]dithiophene (**5**) (yield 60%).¹³ The desired molecule, **6** was obtained by oxidation of **5** with hydrogen peroxide and formic acid.¹⁵ The yield of the reaction was 74%.



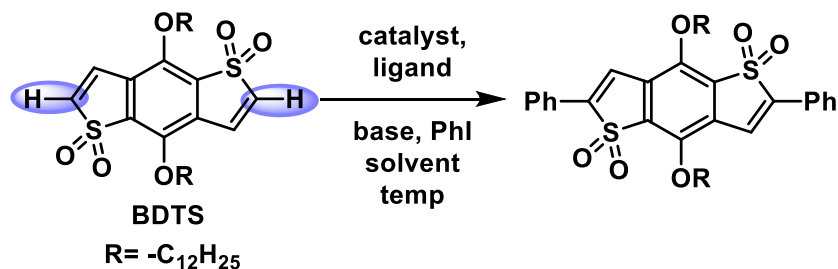
Scheme 4.1: Synthesis of BDTT

4.5 Results and discussion of direct arylation of BDTT is illustrated:

4.5.1 Reaction optimization:

Attempt 1 (**Table 4.2**): All these conditions were chosen initially, since similar kinds of electron deficient compounds have undergone direct arylation reactions using these conditions.^{21, 23-26}

Reactions 1-4 were worked up by adding deionized water and extracting the resulting mixtures with ethyl acetate. The organic layers were dried. All crude products were yellow in color. For all reactions, the TLC analysis had multiple spots and the ¹H NMR spectra were inconclusive.

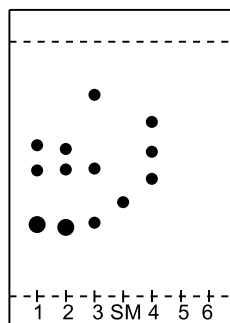


	Ph-I (eq)	CuI (% mol)	Ligand (% mol)	Base (eq)	Solvent	Temp °C	Result
1	2.5	100	Phen. (100)	K ₃ PO ₄ (1.33)	DMF	130	#
2	2.5	100	Phen. (100)	K ₃ PO ₄ (1.33)	DMF + Xylene	130	#
3	2.5	100	Phen. (100)	<i>t</i> -BuOLi (2)	DMF	130	#
4	6	100	-	<i>t</i> -BuOLi (2)	DMF	140	#
5	6	100	PPh ₃ (20)	Na ₂ CO ₃ (2)	DMF + DCB*	140	#
6	2.5	100	PPh ₃ (20 eq)	K ₃ PO ₄ (2)	DMF	160	#

Table 4.2: Various parameters for reaction optimization

(*DCB = 1,4-dichlorobenzene)

(# = complicated mixture which could not be analyzed)



9:1 Hex: E.A
under 365 nm

Figure 4.4: Thin layer chromatography for the reactions in **Table 4.2**

Attempt 2: Ph-I (6 eq), and *t*-BuOLi (4 eq) were kept constant and other parameters were varied as shown in the **Table 4.3**. In these experiments neither the starting material nor the product was obtained. On TLC analysis, there were multiple spots. ¹H NMR spectra were also inconclusive.

	Pd(OAc) ₂ (% mol)	Ligand (% mol)	Temp (°C)	Result
7	10	-	140	#
8	10	-	100	#
9	10	PPh ₃ (20)	140	#
10	10	(<i>o</i> -tol) ₃ (20)	140	#

Table 4.3: Various parameters for reaction optimization

(# = complicated mixture which could not be analyzed)

Attempt 3: PhI (6 eq), DMF (0.033 M), and 140 °C were kept constant and other parameters were varied as shown in **Table 4.4**. The reactions were worked up as mentioned earlier. ¹H NMR analysis of the crude products were performed. For reactions 11 and 12, there were phenyl iodide, the desired product and some other compound but no BDTT. For the reactions 13 and 14, only phenyl iodide and some unknown compounds were detected. But neither the starting material nor the desired product was present. Thus, it was decided to proceed with conditions 11 and 12.

	CuI (% mol)	Base (eq)	Result
11	100	K ₃ PO ₄ (2)	+
12	100	Na ₂ CO ₃ (2)	+
13	100	<i>t</i> -BuOLi (2)	#
14	20	<i>t</i> -BuOLi (2)	#

Table 4.4: Various parameters for reaction optimization

(# = complicated mixture which could not be analyzed)
(+ = desired product was observed)

Attempt 4: Temperature (140 °C), and DMF (0.033 M) were kept constant and other parameters were changed as shown in **Table 4.5**. Here, this study was undertaken to determine whether starting material could tolerate harsh reaction conditions. TLC analysis were done at 1 h, 2 h, 4 h, 8 h. In all TLC analysis only starting material was present in the reactions 15 and 16. No starting

#	CuI (% mol)	<i>t</i> -BuOLi	Result
15	-	-	NR
16	100	-	NR
17	-	2 eq	-
18	100	2 eq	-

Table 4.5: Various parameters for reaction optimization

(- = BDTT was decomposed)

material was present in the reactions 17 and 18. Thus, it could be inferred that, strong base tBuOLi was decomposing the starting material. Consequently, for reactions 11-18, only weak bases were used.

Attempt 5: PhI (6 eq), and DMF (0.033 M) were kept constant and other parameters were changed as shown in **Table 4.6**. From TLC analysis after 12 h, all reaction mixtures had monoarylated product and starting material. So, all the reactions were heated for an additional 12 h. After 24 h, the results are summarized in **Table 4.6**. The reaction was worked up and purified, which yielded 22% isolated desired product. From here on the reactions were performed with ligand and additives.

#	Base (eq)	Temp °C	Starting material	Monoarylated product	Diarylation product
19	K ₃ PO ₄ (4)	70	+	+	-
20		95	-	+	+
21		115	-	+	++
22	Na ₂ CO ₃ (4)	70	+	+	-
23		95	-	++	+
24		115	-	++	+

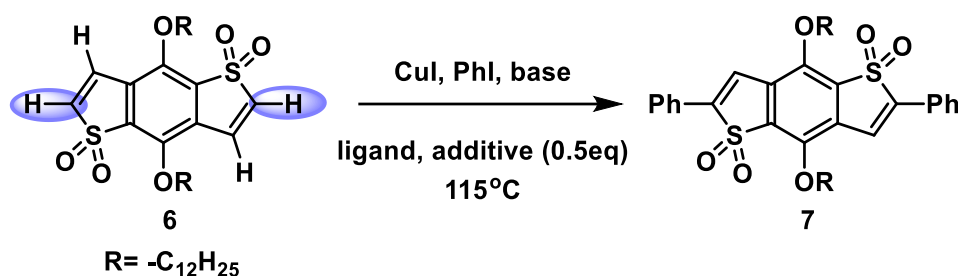
Table 4.6: Various parameters for reaction optimization

(++ = major product, + = minor product, - = absent)

Final optimization:

Initially, literature conditions were applied for the Cu-catalyzed direct arylation of electron deficient molecules^{13, 21-24} to BDTT **6**. As a base, K₃PO₄, was used (**Table 4.7**, entry 1), which gave a 10% isolated yield. It has been reported that higher yields can be achieved when 1,10-phenanthroline (Phen) is used as a ligand in Cu-catalyzed C-H activation reactions.²⁷⁻²⁸ This outcome was also observed with the addition of Phen to our reaction (**Table 4.7**, entry 2). We noted that increasing the amount of aryl iodide from 3 equiv to 5 equiv induced an increase in isolated yield from 22 % to 30 % (**Table 4.7**, entry 3). According to the literature, when aryl

iodides are used, the addition of the silver salt, Ag_2CO_3 is necessary to achieve higher yields. Otherwise liberated iodide ions hinder the direct arylation reaction.²⁹⁻³¹ An addition of 0.5 eq. of Ag_2CO_3 further increased the isolated yield from 30 % to 57 % (**Table 4.7**, entry 5). We opted to use silver carbonate because of its increased ease of handling and lower cost. The amount of K_3PO_4 was optimized at 1 equiv. (**Table 4.7**, entry 7) with an isolated yield of 60 %. Using these optimized conditions, we examined the role of CuI as the functioning catalyst by decreasing both CuI and Phen loadings from 100 mol% to 15 mol% (**Table 4.7**, entry 8). Other mild bases (Na_2CO_3 , K_2CO_3 and Cs_2CO_3) were employed, but resulted in much lower yields (**Table 4.7**, entries 9-11). The best overall result was realized with CuI (15 mol%), Phen (30 mol%), K_3PO_4



Scheme 4.2: Cu-catalyzed direct arylation of BDDT

Entry	Base (eq)	CuI mol%	Phen mol%	PhI (eq)	Additive	Yield*
2	K_3PO_4 (2)	100	-	3	-	10%
3	K_3PO_4 (2)	100	100	3	-	22%
4	K_3PO_4 (2)	100	100	5	-	30%
5	K_3PO_4 (2)	100	100	5	Ag_2CO_3	57%
6	K_3PO_4 (2)	100	100	5	AgOTf	9%
7	K_3PO_4 (1)	100	100	5	Ag_2CO_3	60%
8	K_3PO_4 (1)	15	15	5	Ag_2CO_3	60%
9	Na_2CO_3 (1)	15	15	5	Ag_2CO_3	22%
10	K_2CO_3 (1)	15	15	5	Ag_2CO_3	27%
11	Cs_2CO_3 (1)	15	15	5	Ag_2CO_3	<10%
12	K_3PO_4 (1)	15	30	5	Ag_2CO_3	69%

Table 4.7: Optimization of BDDT cross-coupling reaction with iodobenzene

(1 eq), and Ag_2CO_3 (0.5 eq) in dry DMF at 115 °C for 20 h which afforded only the bifunctional product **2** in an isolated yield of 69 % (Table 4.7, entry 12), which was the highest yield so far.

4.5.2 Study of the reaction scope:

Electron-neutral aryl iodides, iodobenzene and 4-iodotoluene (Figure 4.5, compounds **8,9**) afforded the desired bifunctionalized products in good isolated yields at 69% and 72%, respectively. Electron-rich aryl iodides 4-iodoanisole, 4-Bromo-1-iodobenzene and 4-iodobiphenyl (Figure 4.5, compounds **10-12**) gave the desired products in good to excellent yields at 65 %, 81 % and 72 %, respectively. Aryl iodides with electron withdrawing groups, 4-iodobenzotrifluoride, 4-fluoroiodobenzene, 1-iodo-4-nitrobenzene and methyl 4-iodobenzoate, 4-iodobenzotrifluoride, 4-fluoroiodobenzene, 1-iodo-4-nitrobenzene and methyl 4-iodobenzoate, 4-iodobenzotrifluoride, 4-fluoroiodobenzene, 1-iodo-4-nitrobenzene and methyl 4-iodobenzoate,

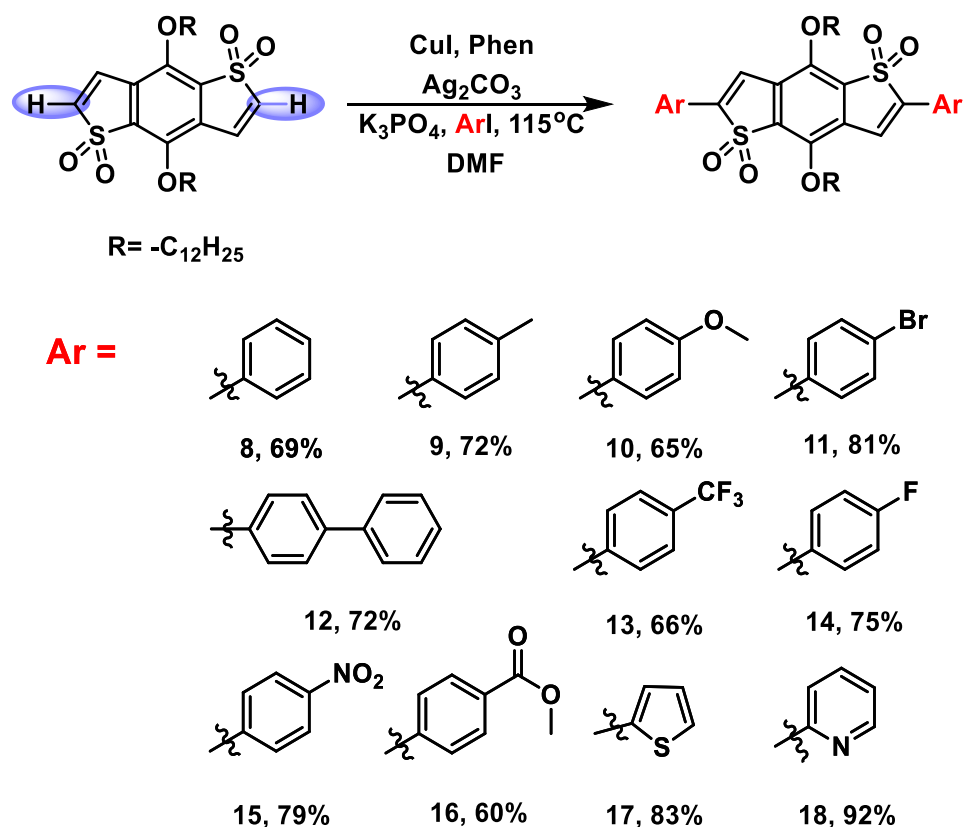
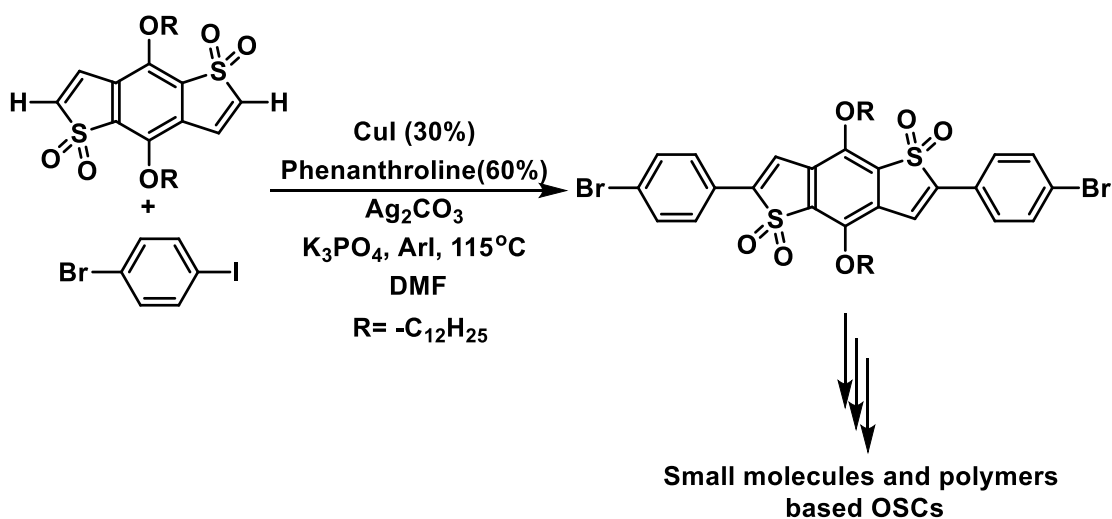


Figure 4.5: Substrate scope of Cu-catalyzed cross-coupling of aryl iodides with BDDT provided the bifunctionalized products in moderate to high isolated yields (Figure 4.5, compounds **13-16**) at 66 %, 75 %, 79 % and 60 %, respectively. These data suggest that this

approach could be used as a robust methodology for the synthesis of electron donor-acceptor-donor and electron acceptor compounds with the potential applications as narrow bandgap OSCs and electron transport materials, respectively. In the case of heterocyclic aromatic compounds, electron rich 2-iodothiophene gave the desired product in excellent isolated yield of 83% (**Figure 4.5**, compound **17**). Surprisingly, 2-iodopyridine was well tolerated in the reaction conditions and afforded the bifunctionalized product in high isolated yield of 92 % (**Figure 4.5**, compound **18**). These coupling partners can be problematic due to the possibility of coordinative binding to the metal centers.

The reaction's specificity of aryl iodides over the bromides opens new avenues for the synthesis of new BDTT based small molecules and polymers (**Scheme 4.3**).



Scheme 4.3: Utilization of the Cu-catalyzed direct arylation

4.6 Plausible mechanism:

There are many possible mechanism for Cu-catalyzed direct arylation, such as oxidative addition, single electron transfer and σ -bond metathesis. Out of these, oxidative addition is most widely accepted (**Figure 4.6**). First, the acidic proton on of this Cu^{I} complex to the aryl halide leads to the formation of a Cu^{III} intermediate. Reductive elimination of this intermediates yielded the

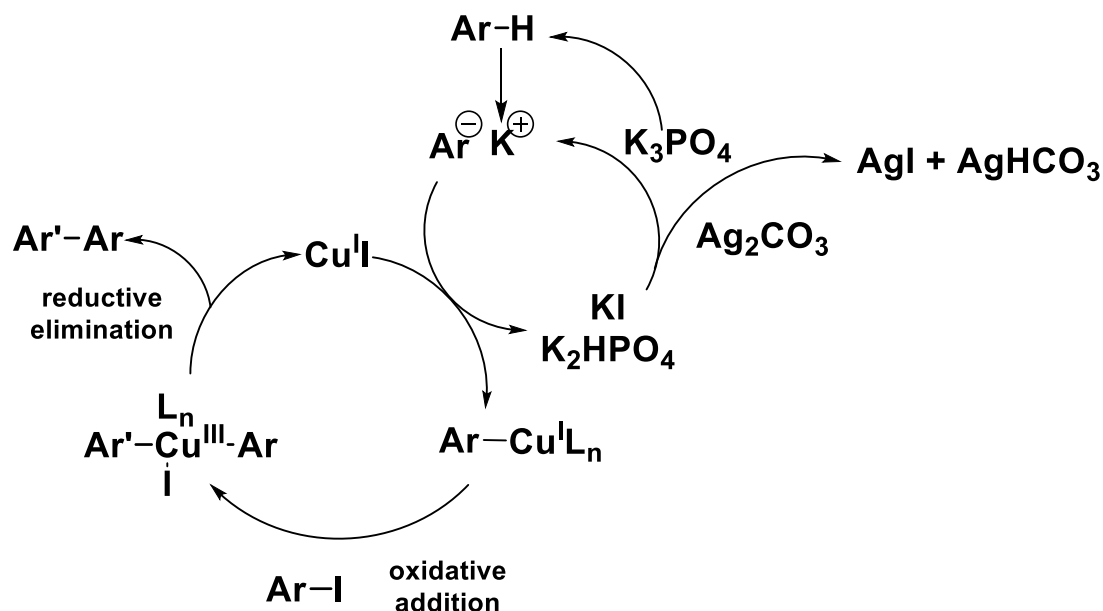


Figure 4.6: Plausible mechanism for Cu-catalyzed direct arylation

coupling product and regenerates the Cu^{I} species.³² When aryl iodides are used, iodide ions generated during the reaction may poison the catalyst, which would suppress the reaction. To remove this iodide ion, silver carbonate is used.²⁹⁻³¹

4.7 Other projects in progress using BDTT:

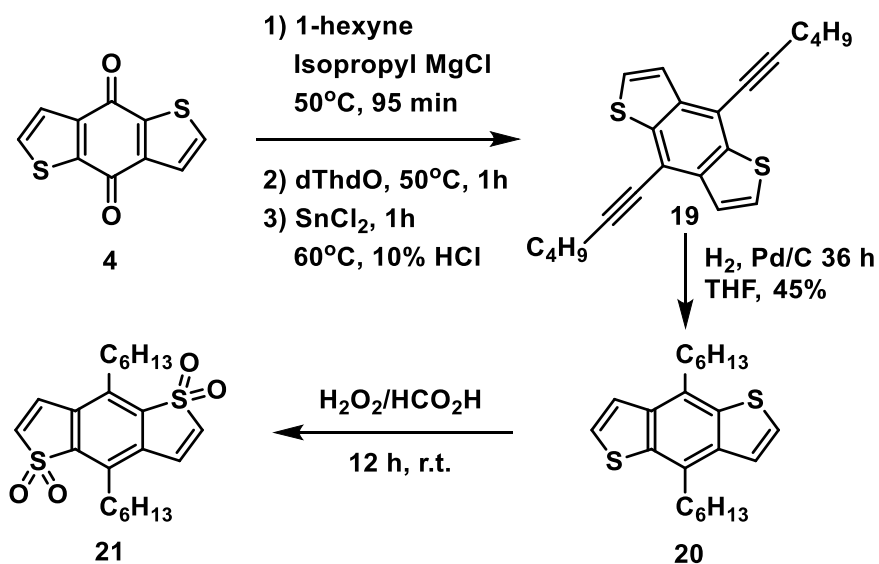
The following projects were started to make various OSCs based BDTT moieties.

4.7.1 Synthesis of 4,8-Dihexynbenzo[1,2-*b*:4,5-*b'*]dithiophene-*S,S*-tetroxide:

Reaction of 1-hexyne with isopropylmagnesium chloride, followed by addition of benzo[1,2-*b*:4,5-*b'*]dithiophene-4,8-dione (dThdO) and further reduction with SnCl_2 yielded 4,8-dihexynylbenzo[1,2-*b*:4,5-*b'*]dithiophene. This compound was reduced with H_2 , using Pd/C as catalyst. 4,8-Dihexynylbenzo[1,2-*b*:4,5-*b'*]dithiophene was oxidized with $\text{H}_2\text{O}_2/\text{HCO}_2\text{H}$ to give 4,8-Dihexynylbenzo[1,2-*b*:4,5-*b'*]dithiophene-*S,S*-tetroxide (**Scheme 4.4**).

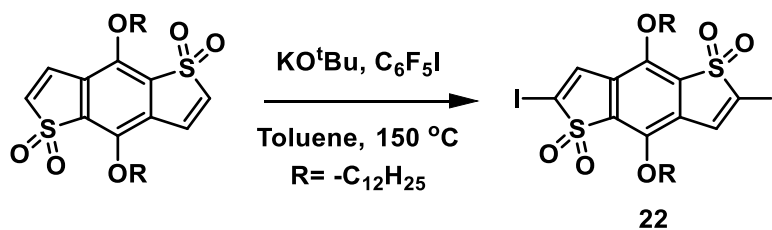
4.7.2 Synthesis of 2,6-diiodo-4,8-didodecyloxybenzo[1,2-*b*:3,4-*b'*]dithiophene-*S,S*-tetraoxide (DIBDTT):

This molecule could be used in various coupling reactions to make different OSCs. This reactions were performed according to Marder et al. (Scheme 4.5).³³ The product was



Scheme 4.4: Synthesis of BDTT with alkyl chain

confirmed with Low resolution mass spectroscopy (LRMS). However, it was not possible to purify the desired product.

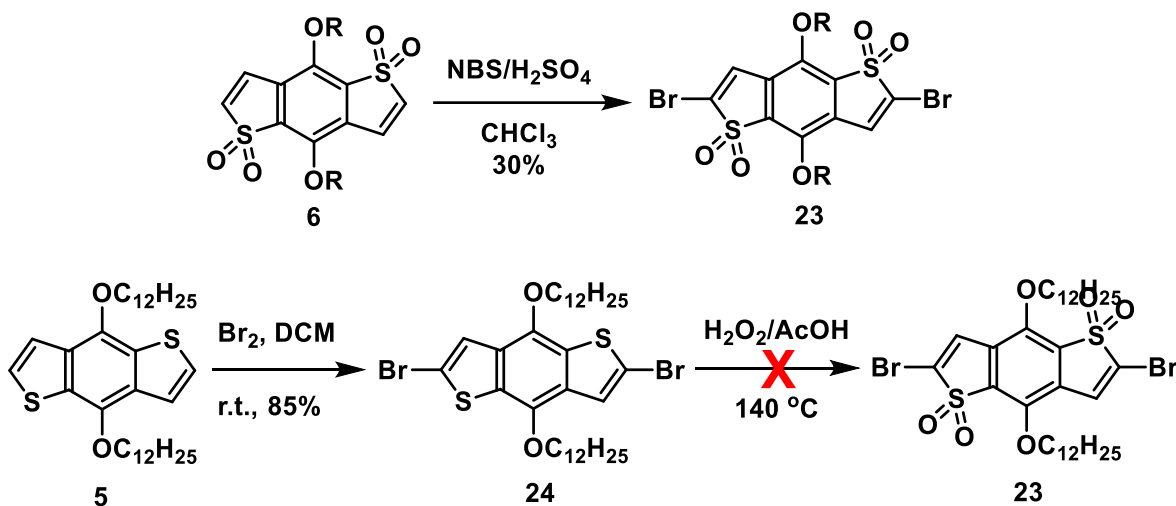


Scheme 4.5: Synthetic routes for DIBDTT

4.7.3 Synthesis of 2,6-dibromo-4,8-didodecyloxybenzo[1,2-*b*;3,4-*b'*]dithiophene-*S,S*-tetroxide (DBBDTT):

This molecule can be used in various coupling reactions to make different OSCs. There are two approaches to synthesize the target from BDT. First oxidize BDT, followed by bromination to obtain DBBDTT. In the second route, BDT can be brominated and further oxidize to yield the

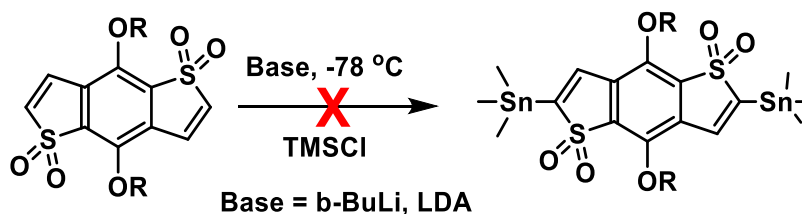
desired product (**Scheme 4.6**). The first approach gave a 32% isolated yield of the compounds which could not be separated.



Scheme 4.6: Synthetic routes for DBBDTT

4.7.4 4,8-Bis(dodecyloxy)-2,6-Bis(trimethylstannyl)benzo[1,2-*b*:4,5-*b'*]dithiophene-*S,S*-tetraoxide:

It was planned to synthesize the tin coupling reagent of BDTT in order to make many OSCs via Stille coupling (**Scheme 4.7**). However, even after several of attempts, the product was not obtained. This approach was abandoned.

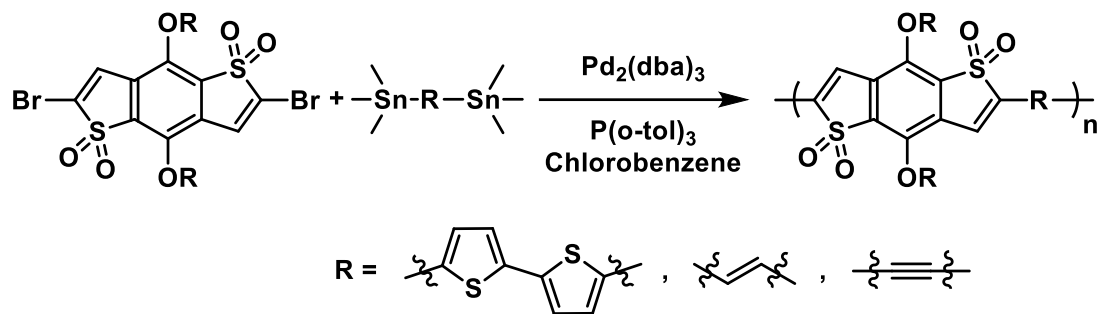


Scheme 4.7: proposed synthetic routes for BDTT tin reagent

4.7.5 Synthesis of BDTT containing CPs via Stille coupling reactions:

The following CPs were attempted via Stille coupling (**Scheme 4.8**). The purification was done with soxhlet extraction using hexane and, methanol. Black or brown solid particles were

obtained, which were not soluble. Hence, the decision was made to synthesize BDTT with a branched chain instead of a linear chain, to increase solubility. This work is in progress.



Scheme 4.8: Proposed synthetic route to make BDTT containing CPs

4.8 Optical properties:

Absorption and emission spectra are shown in **Figure 4.7 and 4.8**, respectively. $\lambda_{\text{ab}}(\text{nm})$, $\lambda_{\text{em}}(\text{nm})$ and $E_{\text{opt}}(\text{eV})$ are summarized in **Table 4.8**. From this data, it was observed that electron rich substituents, Ph-CH₃, Ph-OMe, Th and Ph-Ph have red shifted maxima at 451 nm, 465 nm, 471 nm, and 480 nm, respectively. There is also a pattern where, comparatively more electron rich compounds have higher absorption maxima than substituents with weak electron donating groups. Ph group has an absorption maximum was at 442 nm. Electron poor substituents have lower absorption maxima. Ph-CF₃, 2-pyridyl, Ph-F, Ph-NO₂, Ph-Br, Ph-CO₂CH₃ have absorption maxima at 437 nm, 440 nm, 443 nm, 449 nm, 450 nm and 450 nm, respectively.

Electron-rich substituents make donor-acceptor-donor compounds. In such compounds, the donor increases the HOMO and the acceptor decreases the LUMO, which leads to a narrow bandgap. Electron-poor substituents make acceptor-acceptor-acceptor compounds. The acceptor decrease the LUMO level but does not affect the HOMO level significantly. Therefore, these compounds have a higher bandgap compared to donor-acceptor-donor compounds.

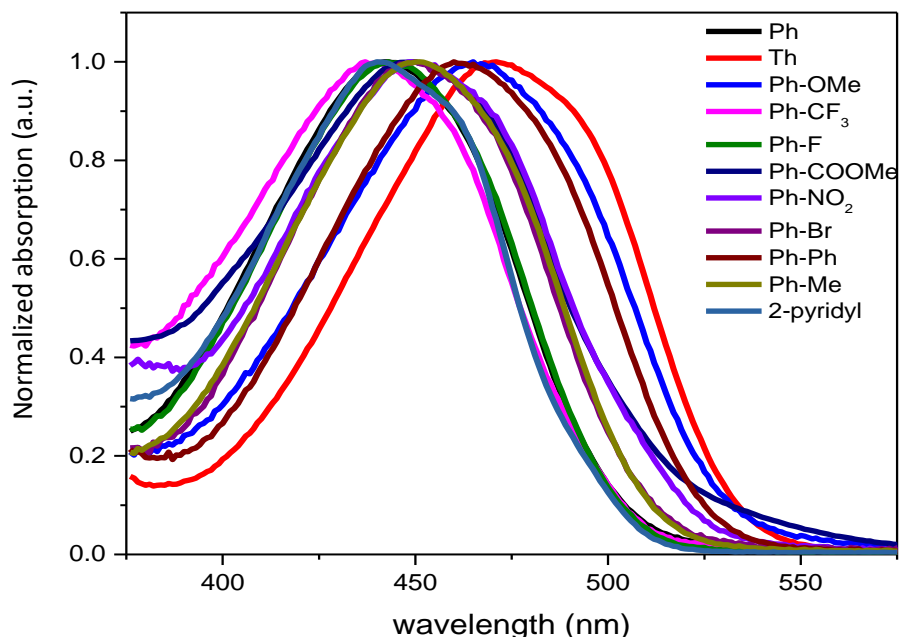


Figure 4.7: Absorption spectra of BDTT derivatives (in chloroform solution)

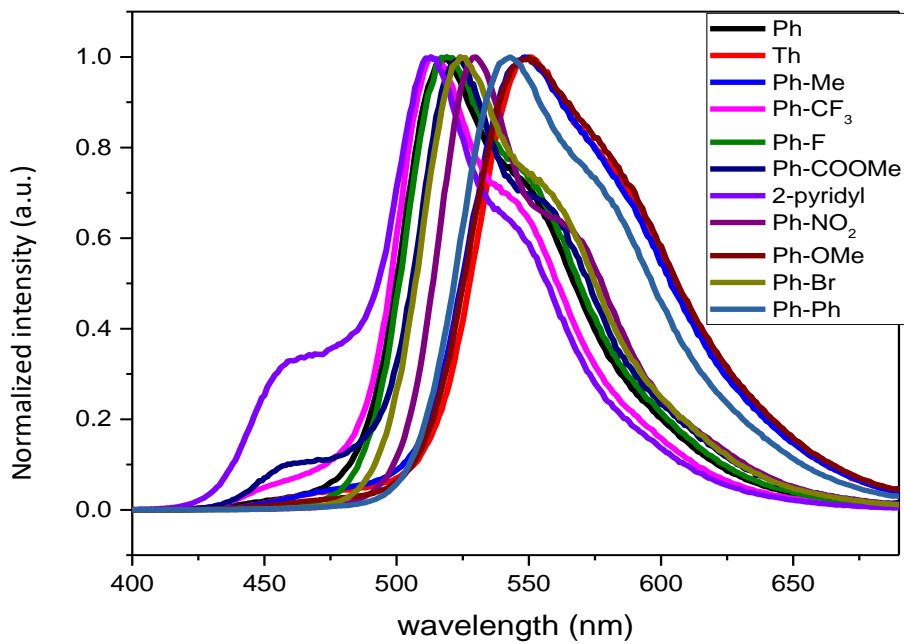


Figure 4.8: Emission spectra BDTT derivatives (in chloroform solution)

	Ph-CF ₃	2-pyridyl	Ph	Ph-F	Ph-NO ₂
$\lambda_{ab}(nm)$	437	440	442	443	449
$\lambda_{em}(nm)$	513	513	518	519	530
$E_{opt}(eV)$	2.4	2.5	2.4	2.4	2.3

	Ph-Br	Ph-CO ₂ Me	Ph-CH ₃	Ph-OMe	Th	Ph-Ph
$\lambda_{ab}(nm)$	450	450	451	465	471	480
$\lambda_{em}(nm)$	524	524	549	548	551	542
$E_{opt}(eV)$	2.4	2.4	2.4	2.3	2.3	2.3

Table 4.8: Optical properties of BDTT derivatives (in chloroform solution)

4.9: Crystal structure:

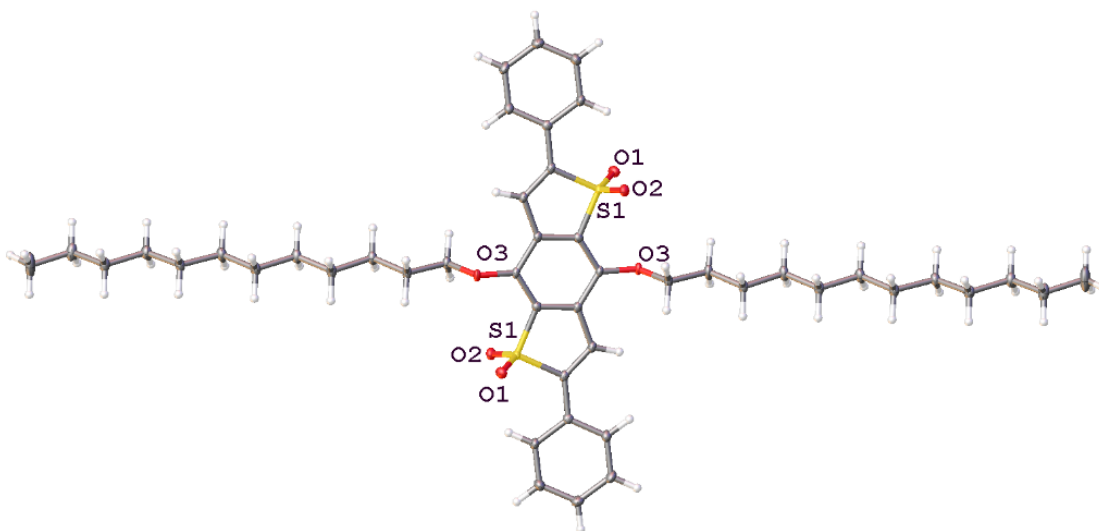


Figure 4.9: Crystal structure of Ph-BDTP-Ph

Crystal structure of Ph-BDTP-Ph confirms that direct arylation reaction is taking place at C next to the sulfone group.

4.10 Experimental section:

General methods:

All the reactions were performed under an Ar atmosphere. Tetrabutylammonium bromide (TBAB), *n*-BuLi (2.5 M in hexanes), CuI, K₃PO₄, Cs₂CO₃ and Ag₂CO₃ were purchased from Sigma-Aldrich. Thiophene-3-carboxylic acid, oxalyl chloride, formic acid and aryl iodides were purchased from Oakwood Chemicals. Diethylamine was purchased from Alfa-Aesar. Zinc powder was purchased from Acros Organics. Na₂CO₃ was purchased from Fischer Scientific. All the chemicals were used as purchased. Column chromatography was performed with Silica (60 Å, 230 x 400 mesh, Sorbent Technology). Solvents used were from a Solvent Purification System (Innovative Technology) for all the reactions. All glassware were oven dried. Melting points were uncorrected. A MBraun UNILab pro glove box workstation was used for the reactions.

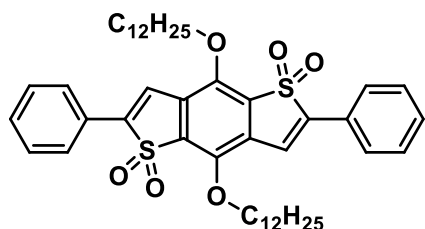
NMR experiments were performed with an I-400 Bruker NMR instrument. CDCl₃ was used as the solvent for NMR samples. All the spectra were referenced to the δ 7.26 residual chloroform solvent peak. HRMS analysis was performed at the Biochemistry and Molecular Biology Recombinant DNA and Protein Core Facility. 4,8-Didodecyloxybenzo[1,2-*b*;3,4-*b'*]dithiophene-*S,S*-dioxide (BDTT) was synthesized according to the literature.^{13, 15}

C-H activation/Direct arylation, General procedure:

In the glovebox, 4,8-didodecyloxybenzo[1,2-*b*;3,4-*b'*]dithiophene-*S,S*-dioxide (50 mg, 0.080 mmol) was added to a 10 mL reaction test tube, followed by the aryl iodide (0.800 mmol), CuI (4.6 mg, 0.024 mmol), 1,10-phenanthroline (8.7 mg, 0.048 mmol), Ag₂CO₃ (22.1 mg, 0.080 mmol), K₃PO₄ (34.9 mg, 0.161 mmol), and dry DMF (2 mL). The reaction color was dark brown green. The thick-walled reaction vials were sealed, taken out of the glovebox, and stirred at 115-120 °C for 20 h. The color of the reaction turned a darker brown. The reaction mixture was allowed to cool to room temperature, poured into water and extracted with 1:1 diethyl ether and

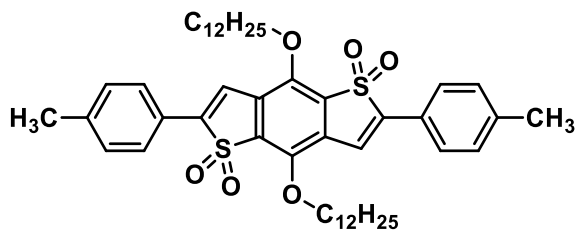
hexanes (2 x 5mL). The resulting solution was washed with deionized water (5 x 15 mL), brine (2 x 15 mL) and dried (over MgSO₄). The organic layer was passed through a silica and celite plug to remove the solid impurities. Solvents were removed with rotatory evaporation. Further purification was obtained by dissolving the crude in dichloromethane/ethanol (1:1) and subsequent rotary evaporation to precipitate the product. The suspension was then filtered and washed with cold ethanol to obtain the pure product.

4,8-Didodecyloxy-2,6-diphenylbenzo[1,2-*b*:4,5-*b'*]dithiophene-*S,S*-tetraoxide (**8**):



Orange color solid, yield 69%, mp 163-167 °C; ¹H NMR (400 MHz, CDCl₃) δ 7.87–7.80 (m, 4H), 7.49 (dd, *J* = 5.2, 2.0 Hz, 6H), 7.45 (s, 2H), 4.51 (t, *J* = 6.5 Hz, 4H), 1.93 (p, *J* = 6.5 Hz, 4H), 1.57–1.52 (m, 4H), 1.43–1.22 (m, 32H), 0.88 (t, *J* = 6.7 Hz, 6H). ¹³C NMR (101 MHz, CDCl₃) δ 145.10, 142.74, 131.76, 130.80, 129.35, 127.59, 126.83, 126.76, 118.35, 31.93, 30.01, 29.69, 29.66, 29.62, 29.58, 29.37, 29.35, 25.82, 22.70, 14.13. HRMS (*m/z*): calcd. 797.3877; found, 797.3825

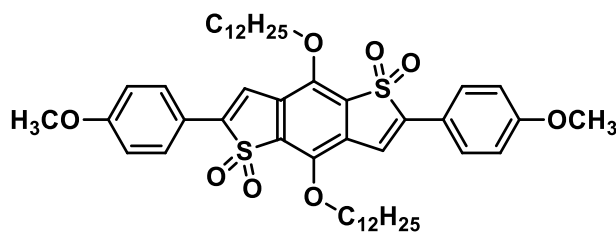
4,8-Bis(dodecyloxy)-2,6-di-*p*-tolylbenzo[1,2-*b*:4,5-*b'*]dithiophene-*S,S*-tetraoxide (**9**):



Orange color solid, yield 72%, mp 185-189 °C; ¹H NMR (400 MHz, CDCl₃) δ 7.72 (d, *J* = 7.8 Hz, 4H), 7.38 (s, 2H), 7.30 (d, *J* = 7.9 Hz, 4H), 4.49 (t, *J* = 6.6 Hz, 4H), 2.42 (s, 6H), 1.92 (p, *J* = 6.8

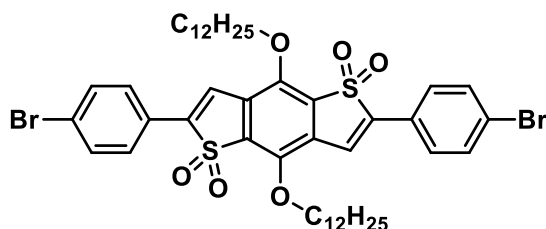
Hz, 4H), 1.53 (m, 4H), 1.46–1.17 (m, 32H), 0.88 (t, $J = 6.7$ Hz, 6H). ^{13}C NMR (101 MHz, CDCl_3) δ 145.02, 142.74, 141.35, 131.74, 130.05, 127.58, 126.63, 124.01, 117.27, 31.94, 30.02, 29.70, 29.67, 29.63, 29.59, 29.38, 29.36, 25.82, 22.71, 21.61, 14.14. HRMS (m/z): calcd. 825.4193; found, 825.4165

4,8-Bis(dodecyloxy)-2,6-Bis(4-methoxyphenyl)benzo[1,2-B:4,5-B']dithiophene-*S,S*-tetraoxide
(10):



Orange color solid, yield 65%, mp 174–178 °C. ^1H NMR (400 MHz, CDCl_3) δ 7.77 (d, $J = 8.4$ Hz, 4H), 7.28 (s, 2H), 6.99 (d, $J = 8.4$ Hz, 4H), 4.47 (t, $J = 6.7$ Hz, 4H), 3.87 (s, 6H), 1.92 (p, $J = 6.7$ Hz, 4H), 1.55 (m, 4H), 1.42–1.25 (m, 32H), 0.88 (t, $J = 6.7$ Hz, 6H). ^{13}C NMR (101 MHz, CDCl_3) δ 161.59, 144.94, 142.37, 131.60, 128.36, 127.54, 119.35, 115.90, 114.87, 55.50, 31.94, 30.03, 29.70, 29.67, 29.64, 29.60, 29.38, 25.83, 22.71, 14.14. HRMS (m/z): calcd. 857.4092; found, 857.4026.

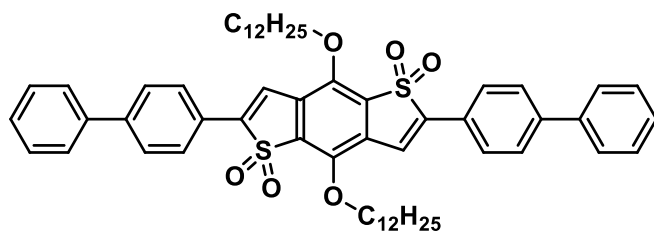
2,6-Bis(4-Bromophenyl)-4,8-Bis(dodecyloxy)benzo[1,2-*b*:4,5-*b'*]dithiophene-*S,S*-tetraoxide (11):



Bright orange color solid, yield 69%, mp 157–160 °C; ^1H NMR (400 MHz, CDCl_3) δ 7.72–7.65 (m, 4H), 7.65–7.58 (m, 4H), 7.44 (s, 2H), 4.50 (t, $J = 6.5$ Hz, 4H), 1.97–1.86 (p, $J = 6.7$ Hz, 4H), 1.55–1.49 (m, 4H), 1.44–1.16 (m, 32H), 0.88 (t, $J = 6.7$ Hz, 6H). ^{13}C NMR (101 MHz, CDCl_3) δ

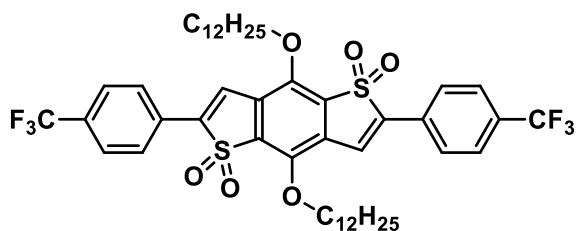
145.07, 141.53, 132.59, 131.42, 128.05, 127.45, 125.63, 125.40, 118.87, 31.94, 29.99, 29.71, 29.68, 29.64, 29.59, 29.39, 29.35, 25.79, 22.71, 14.15. HRMS (m/z): calcd. 955.207; found, 955.2041

2,6-Di([1,1'-Biphenyl]-4-yl)-4,8-Bis(dodecyloxy)benzo[1,2-*b*:4,5-*b'*]dithiophene-*S,S*-tetraoxide
(12):



Orange color solid, yield 72%, mp 207-209 °C; ^1H NMR (400 MHz, CDCl_3) δ 7.95–7.87 (m, 4H), 7.76–7.69 (m, 4H), 7.63 (dt, $J = 6.4, 1.3$ Hz, 4H), 7.52–7.45 (m, 6H), 7.43–7.38 (m, 2H), 4.54 (t, $J = 6.5$ Hz, 4H), 1.99–1.91 (m, 4H), 1.58 (d, $J = 7.5$ Hz, 4H), 1.47–1.21 (m, 34H), 0.86 (t, $J = 6.6$ Hz, 6H). ^{13}C NMR (101 MHz, CDCl_3) δ 144.10, 142.52, 141.38, 138.78, 130.68, 127.97, 127.12, 126.92, 126.63, 126.12, 126.08, 124.62, 116.93, 30.91, 29.01, 28.69, 28.65, 28.62, 28.58, 28.36, 28.34, 24.81, 21.67, 13.10. HRMS (m/z): calcd. 949.4506; found, 949.4489.

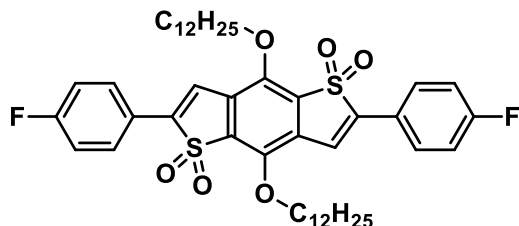
4,8-Bis(dodecyloxy)-2,6-Bis(4-(trifluoromethyl)phenyl)benzo[1,2-*b*:4,5-*b'*]dithiophene-*S,S*-tetraoxide (13):



Yellow-orange color solid, yield 69%, mp 177-181 °C. ^1H NMR (400 MHz, CDCl_3) δ 7.92 (d, $J = 8.2$ Hz, 4H), 7.72 (d, $J = 8.1$ Hz, 4H), 7.54 (s, 2H), 4.51 (t, $J = 6.5$ Hz, 4H), 1.92 (t, $J = 7.5$ Hz, 4H), 1.52 (m, 4H), 1.38–1.25 (m, 32H), 0.88 (t, $J = 6.6$ Hz, 6H). ^{13}C NMR (101 MHz, CDCl_3) δ

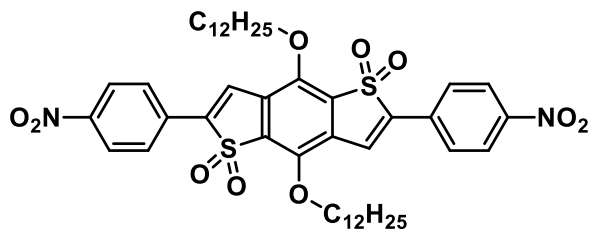
145.27, 141.39, 131.48, 130.13, 127.56, 127.10, 127.10, 126.33, 126.30, 31.92, 29.98, 29.71, 29.69, 29.67, 29.62, 29.57, 29.37, 29.32, 25.79, 22.69, 14.11. HRMS (m/z): calcd. 933.3628; found, 933.3607

4,8-Bis(dodecyloxy)-2,6-Bis(4-fluorophenyl)benzo[1,2-*b*:4,5-*b'*]dithiophene-*S,S*-tetraoxide (**14**):



Orange color solid, yield 75%, mp 157-160 °C; ^1H NMR (400 MHz, CDCl_3) δ 7.87–7.80 (m, 4H), 7.38 (s, 2H), 7.23–7.16 (m, 4H), 4.50 (t, $J = 6.5$ Hz, 4H), 1.96–1.88 (m, 4H), 1.53 (q, $J = 7.5$ Hz, 6H), 1.42–1.25 (m, 34H), 0.88 (t, $J = 6.7$ Hz, 6H). ^{13}C NMR (101 MHz, CDCl_3) δ 164.10 (d, $J = 253.0$ Hz), 145.06, 141.64, 131.43, 128.93(d, $J = 8.6$ Hz), 127.47, 123.04 (d, $J = 3.4$ Hz), 118.17(d, $J = 1.6$ Hz), 116.70 (d, $J = 22.2$ Hz), 31.93, 30.00, 29.72, 29.69, 29.67, 29.63, 29.58, 29.38, 29.34, 25.80, 22.71, 14.14. HRMS (m/z): calcd. 833.3692; found, 833.3659

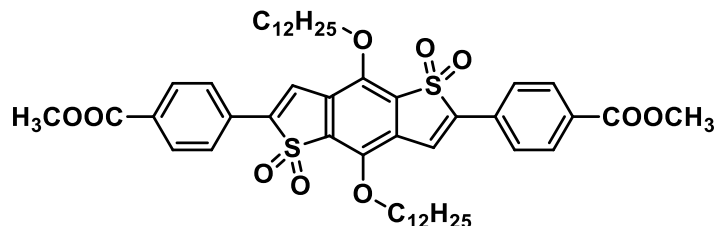
4,8-Bis(dodecyloxy)-2,6-Bis(4-nitrophenyl)benzo[1,2-*b*:4,5-*b'*]dithiophene-*S,S*-tetraoxide (**15**):



Dark red color solid, yield 77%, mp 175-178 °C; ^1H NMR (400 MHz, CDCl_3) δ 8.38–8.34 (m, 4H), 8.03–7.99 (m, 4H), 7.65 (s, 2H), 4.56 (t, $J = 6.5$ Hz, 4H), 1.98–1.91 (m, 4H), 1.57 (d, $J = 2.5$ Hz, 4H), 1.33–1.25 (m, 32H), 0.88 (d, $J = 1.6$ Hz, 6H). ^{13}C NMR (101 MHz, CDCl_3) δ 148.59, 145.37, 140.55, 132.60, 131.22, 127.59, 124.54, 121.87, 31.94, 29.98, 29.72, 29.72,

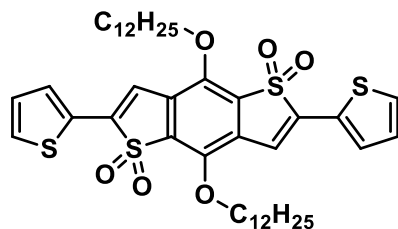
29.70, 29.63, 29.58, 29.39, 29.33, 25.78, 22.71, 14.15. HRMS (m/z): calcd. 887.3582; found, 887.3566

Dimethyl-4,4'-(4,8-Bis(dodecyloxy)-*S,S*-tetraoxidobenzo[1,2-*b*:4,5-*b'*]-dithiophene-2,6-diyl)dibenzoate (**16**):



Dark green color solid, yield 60%, mp 186-190 °C; ^1H NMR (400 MHz, CDCl_3) δ 7.72–7.65 (m, 4H), 7.65–7.58 (m, 4H), 7.44 (s, 2H), 4.50 (t, $J = 6.5$ Hz, 4H), 1.97–1.86 (p, $J = 6.5$ Hz, 4H), 1.55–1.49 (m, 4H), 1.44–1.16 (m, 32H), 0.88 (t, $J = 6.7$ Hz, 6H). ^{13}C NMR (101 MHz, CDCl_3) δ 145.11, 141.63, 132.63, 131.45, 128.09, 127.49, 125.65, 125.43, 118.81, 31.95, 29.99, 29.71, 29.68, 29.64, 29.59, 29.39, 29.35, 25.80, 22.72, 14.16. HRMS (m/z): calcd. 913.3990; found, 913.3963

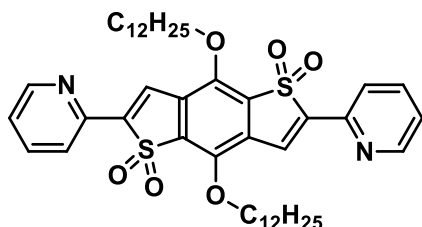
4,8-Bis(dodecyloxy)-2,6-di(thiophen-2-yl)benzo[1,2-*b*:4,5-*b'*]dithiophene-*S,S*-tetraoxide (**17**):



Bright red color solid, yield 83%, mp 167-169 °C. ^1H NMR (400 MHz, CDCl_3) δ 7.71 (dd, $J = 3.7, 1.0$ Hz, 2H), 7.51 (dd, $J = 5.1, 1.1$ Hz, 2H), 7.22–7.15 (m, 4H), 4.48 (t, $J = 6.5$ Hz, 4H), 1.93 (p, $J = 6.7$ Hz, 4H), 1.58–1.52 (m, 4H), 1.43–1.24 (m, 32H), 0.88 (t, $J = 6.7$ Hz, 6H). ^{13}C NMR (101 MHz, CDCl_3) δ 145.22, 137.85, 131.26, 129.09, 129.02, 128.80, 128.80, 127.66, 115.76,

31.94, 29.99, 29.69, 29.67, 29.61, 29.58, 29.38, 29.34, 25.82, 22.71, 14.14. HRMS (m/z): calcd. 809.3008; found, 809.2949

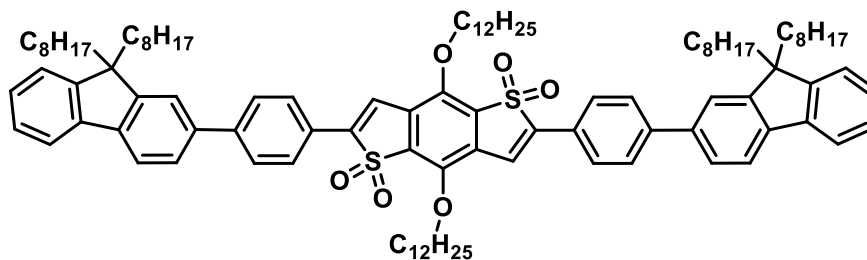
4,8-Bis(dodecyloxy)-2,6-di(pyridin-2-yl)benzo[1,2-*b*:4,5-*b'*]dithiophene-*S,S*-tetraoxide (**18**):



Bright green color solid, yield 92%, mp 178-181 °C; ^1H NMR (400 MHz, CDCl_3) δ 8.70 (d, $J =$ Hz, 4H), 1.88 (p, $J = 6.8$ Hz, 4H), 1.53–1.44 (m, 4H), 1.39–1.10 (m, 36H), 0.81 (t, $J = 6.8$ Hz, 6H). ^{13}C NMR (101 MHz, CDCl_3) δ 149.74, 144.95, 144.70, 141.25, 136.02, 131.40, 126.72, 123.58, 121.11, 49.85, 30.90, 29.00, 28.66, 28.63, 28.59, 28.54, 28.34, 24.71, 21.67, 13.11.

HRMS (m/z): calcd. 799.3785; found, 799.3716

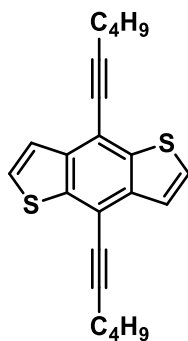
2,6-Bis(4-(9,9-dioctyl-9H-fluoren-2-yl)phenyl)-4,8-Bis(dodecyloxy)benzo[1,2-*B*:4,5-*B'*]dithiophene 1,1,5,5-tetraoxide:



In a 10 mL Schlenk flask (inside the glove box) following compounds were added: 2,6-Bis(4-Bromophenyl)-4,8-Bis(dodecyloxy)benzo[1,2-*B*:4,5-*B'*]dithiophene 1,1,5,5-tetraoxide (50.0 mg, 0.054 mmol), 9,9-dioctylfluorene-2-Boronic acid pinacol ester (56.7 mg, 0.109 mmol), $\text{Pd}(\text{PPh}_3)_4$ (1.8 mg, 3 mol %) and potassium carbonate (123.3 mg, 0.894 mmol). A condenser with a septum on was connected at the top of the flask. Vacuum was applied to the reaction for 15 min and then

the system was filled with Ar. Dry THF (1.5 mL) and degassed distilled water (1.5 mL) was added into the reaction. The reaction flask was heated to 110 °C for 20 h. After 20 h, distilled water (10 mL) was added to the reaction flask and the crude product was extracted in to ethyl acetate (3 x 15 mL). The organic layer was washed with saturated sodium chloride (2 x 15 mL) and dried using sodium sulfate. Then the solvent was evaporated. The resulting residue was purified by column chromatography using dichloromethane/hexane (2:3) followed by recrystallization with dichloromethane and methanol to afford an orange colored solid (43.0 mg, 52%). mp 102-104 °C. ¹H NMR (400 MHz, CDCl₃) δ 7.93 (s, 4H), 7.84–7.56 (m, 12H), 7.49 (s, 2H), 7.36 (s, 6H), 4.55 (s, 4H), 1.99 (s, 12H), 1.57 (s, 9H), 1.17 (d, *J* = 85.6 Hz, 76H), 0.84 (d, *J* = 23.8 Hz, 19H), 0.68 (s, 8H). ¹³C NMR (101 MHz, CDCl₃) δ 151.84, 151.30, 145.33, 144.25, 142.68, 141.56, 140.65, 138.70, 131.94, 128.15, 127.89, 127.57, 127.35, 127.08, 126.20, 125.62, 123.16, 121.60, 120.34, 120.13, 117.98, 55.42, 40.55, 32.15, 31.99, 30.26, 30.22, 29.92, 29.89, 29.86, 29.83, 29.60, 29.43, 29.41, 26.07, 24.01, 22.92, 22.82, 14.36, 14.30. HRMS (*m/z*): calcd. 1574.0140; found, 1575.0169

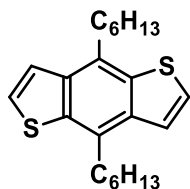
4,8-Dihexynylbenzo[1,2-*b*:4,5-*b'*]dithiophene:



1-Hexyne (1.39 g, 16.9 mmol) in THF (3.36 mL) was taken in a 100-mL 3-necked round-Bottomed flask, equipped with a condenser. At 0-5 °C, a solution of isopropylmagnesium chloride (6 mL, 12.03 mmol, 2 M) was added dropwise to the 3-necked round-Bottomed flask. After addition, the reaction mixture was heated at 50 °C for 95 min and then cooled to room

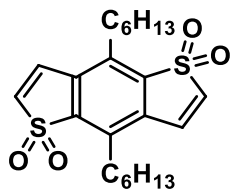
temperature. The reaction mixture color was gray-black. Benzo[1,2-*b*:4,5-*b'*]dithiophene-4,8-dione (0.5 g, 2.27 mmol) was added and the reaction mixture color became green. If the reaction mixture solidified, THF (3 mL) was added. The mixture was heated at 50 °C for 1 h before cooling to room temperature. Subsequently, a solution of 3.33 g of SnCl₂ in 8.32 mL in 10% aq. HCl was added dropwise to keep the temperature between 15 °C-25 °C. As SnCl₂ solution was added, the reaction mixture became yellow orange and the solid in reaction dissolved. This was followed by further heating at 60 °C for 1 h. As temperature was increasing, the reaction mixture color became orange red. The organic chemistry layer was passed through a silica plug. Solvent was removed. Recrystallization of crude product from 2-propanol gave a pure compound (0.33 g, 0.93 mmol, 41 % yield) as yellow-red crystals. ¹H NMR (400 MHz, CDCl₃) δ 7.59 (d, *J* = 5.5 Hz, 2H), 7.51 (d, *J* = 5.5 Hz, 2H), 2.66 (t, 4H), 1.74 (m, 4H), 1.64 (m, 4H), 1.03 (t, 6H).

4,8-Dihexylbenzo[1,2-*b*:4,5-*b'*]dithiophene:



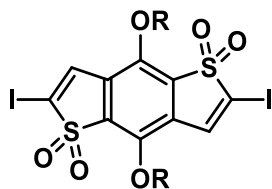
To a solution of 4,8-dihexynylbenzo[1,2-*b*:4,5-*b'*]dithiophene (175 mg, 0.5 mmol) in THF (4.8 mL) in a 25 ml Schleck flask was added 10% Pd/C (53 mg, 0.05 mmol). The mixture was stirred under a hydrogen atmosphere at room temperature for 24 h. After solvent removal and the residue was purified by column chromatography on silica gel (eluent: hexane/dichloromethane, 2/1, v/v). Recrystallization with isopropanol afforded the pure product (75.2 mg, 42% yield) as needle crystals. ¹H NMR (400MHz, CDCl₃) δ 7.49 (d, *J* = 5.8 Hz, 2H), 7.47 (d, *J* = 5.8 Hz, 2H), 3.20 (t, 4H), 1.82 (m, 4H), 1.48 (m, 8H), 1.35 (bs, 36H), 0.91 (t, 6H).

4,8-Dihexylbenzo[1,2-*b*:4,5-*b'*] dithiophene-*S,S*-dioxide:



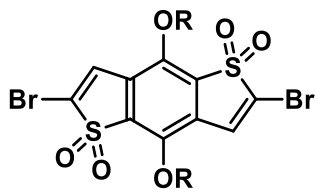
The procedure was that used for 4,8-Bis(dodecyloxy)benzo[1,2-*b*:4,5-*b'*] dithiophene-*S,S*-dioxide. ¹H NMR (400 MHz, CHCl₃) δ 7.33 (d, *J* = 7.1 Hz, 2H), 6.81 (d, *J* = 7.1 Hz, 2H), 3.04–2.89 (m, 4H), 1.75–1.61 (m, 4H), 1.51–1.42(m, 4H), 1.38–1.28 (m, 8H), 0.95–0.82 (m, 6H).

2,6-Diiodo-4,8-didodecyloxybenzo[1,2-*b*:3,4-*b'*]dithiophene-*S,S*-dioxide:



4,8-didodecyloxybenzo[1,2-*b*:3,4-*b'*]dithiophene-*S,S*-dioxide (70 mg, 0.11 mmol) in toluene (6.3 mL) was added to a 1-necked round-Bottomed flask. Iodopentafluorobenzene (291 mg, 0.99 mmol) and K₂OtBu (111 mg, 0.99 mmol) was added to the flask. The reaction mixture was stirred at room temperature for 15 h. The reaction mixture was added to water and extracted with chloroform (5 mL). ¹H NMR analysis of the crude product showed the product, which was also confirmed with LRMS. Column chromatography (on neutral alumina) using hexane:ethyl acetate (98:2 to 50:50), gave very low yield of product. It was not possible to separate the product.

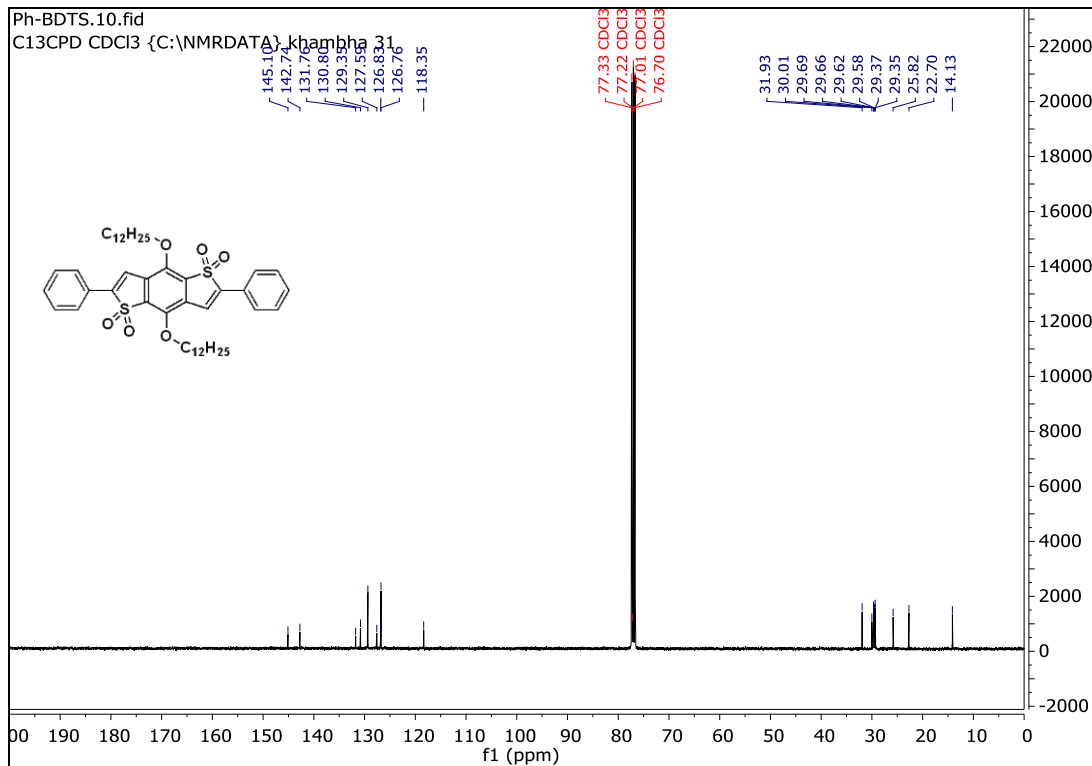
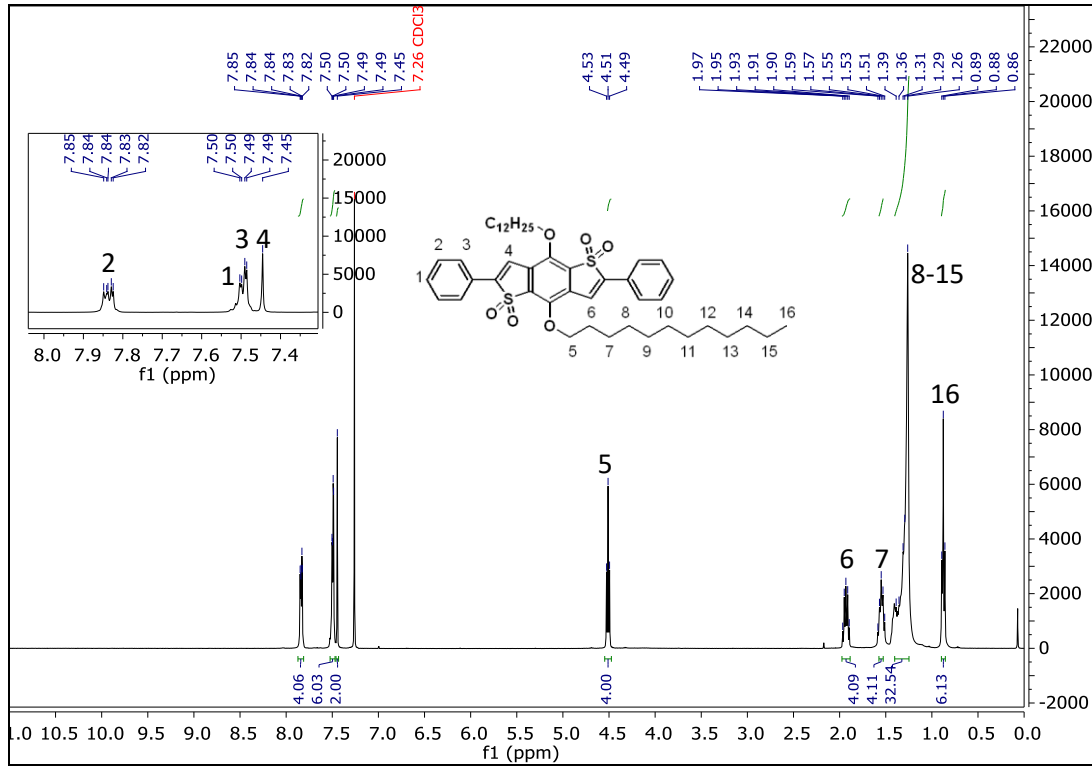
2,6-Dibromo-4,8-didodecyloxybenzo[1,2-*b*:3,4-*b'*]dithiophene-*S,S*-tetroxide:



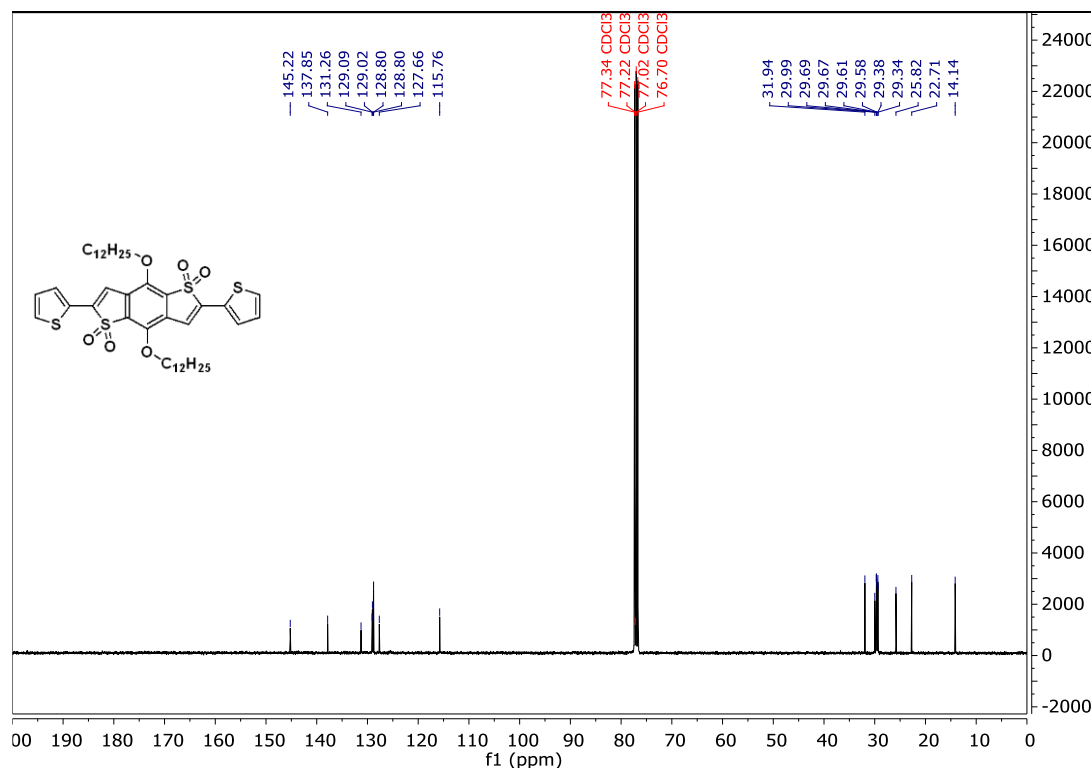
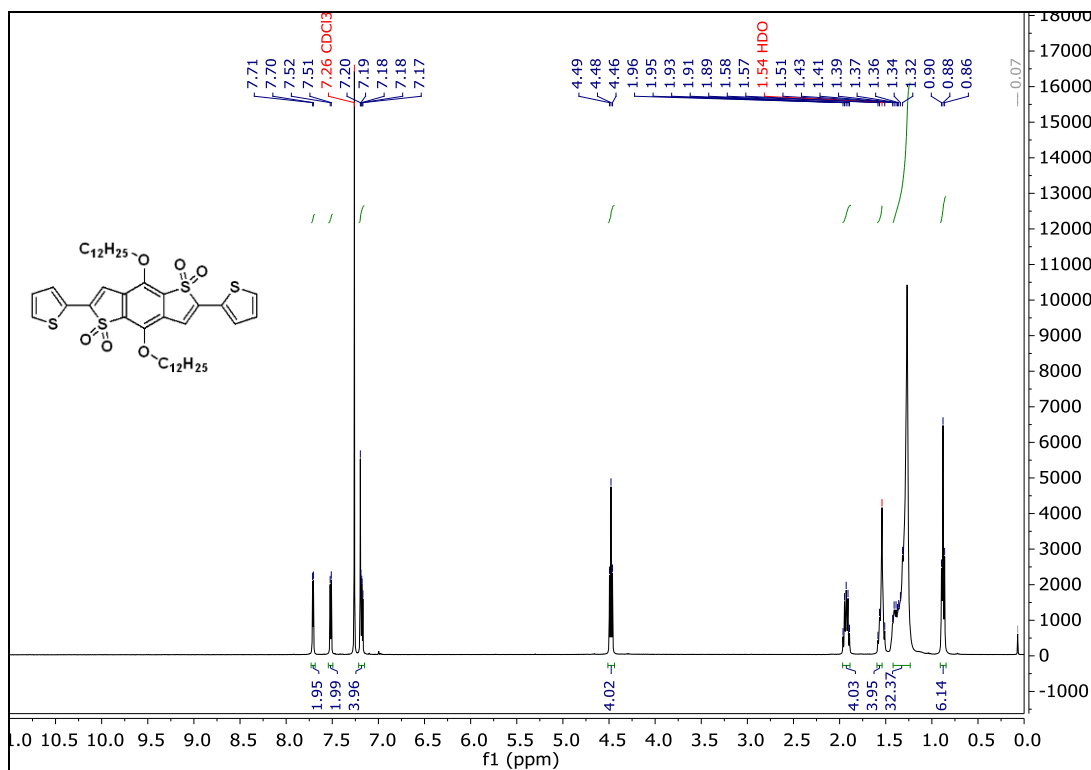
First method: BDTT (300 mg, 0.48 mmol) was added to a 1-necked round-Bottomed flask, followed by addition of CHCl_3 (8 mL) and conc. H_2SO_4 (0.24 mL). NBS (0.19 g, 1.11 mmol) was added in three portions over 15 min. The reaction mixture was heated at 60 °C for 12 h. The reaction mixture was added to water (10 mL) and extracted with dichloromethane (3 x 5 mL). The organic layer was washed with water (3x 10 mL) and brine (3 x 10 mL) and dried over MgSO_4 . The crude product was purified by column chromatography (hexane:dichloromethane-65:35 to 40:60). The product was further purified by recrystallization dichloromethane/ethanol to obtain bright yellow color crystals (120 mg, 32%). ^1H NMR (400 MHz, CDCl_3) δ 7.40 (s, 2H), 4.42 (t, J = 6.5 Hz, 4H), 1.93–1.81 (m, 4H), 1.57–1.43 (m, 8H), 1.43–1.19 (m, 28H), 0.88 (t, J = 6.7 Hz, 6H).

Second method: 2,6-Dibromo-4,8-didodecyloxybenzo[1,2-*b*;3,4-*b'*]dithiophene was added to H_2O_2 (0.04 mL) and acetic acid (0.21 mL) in a 10 mL 1-necked round-Bottomed flask. An Ar balloon was attached. Reaction was stirred at 130 °C–140 °C (of aluminum bead bath) temperature. The reaction mixture was extracted with chloroform. The organic layer was neutralized with saturated NaHCO_3 solution. The organic layer was washed with water, brine and dried (MgSO_4). The crude product was mixture of many compounds. It was not possible to purify the material.

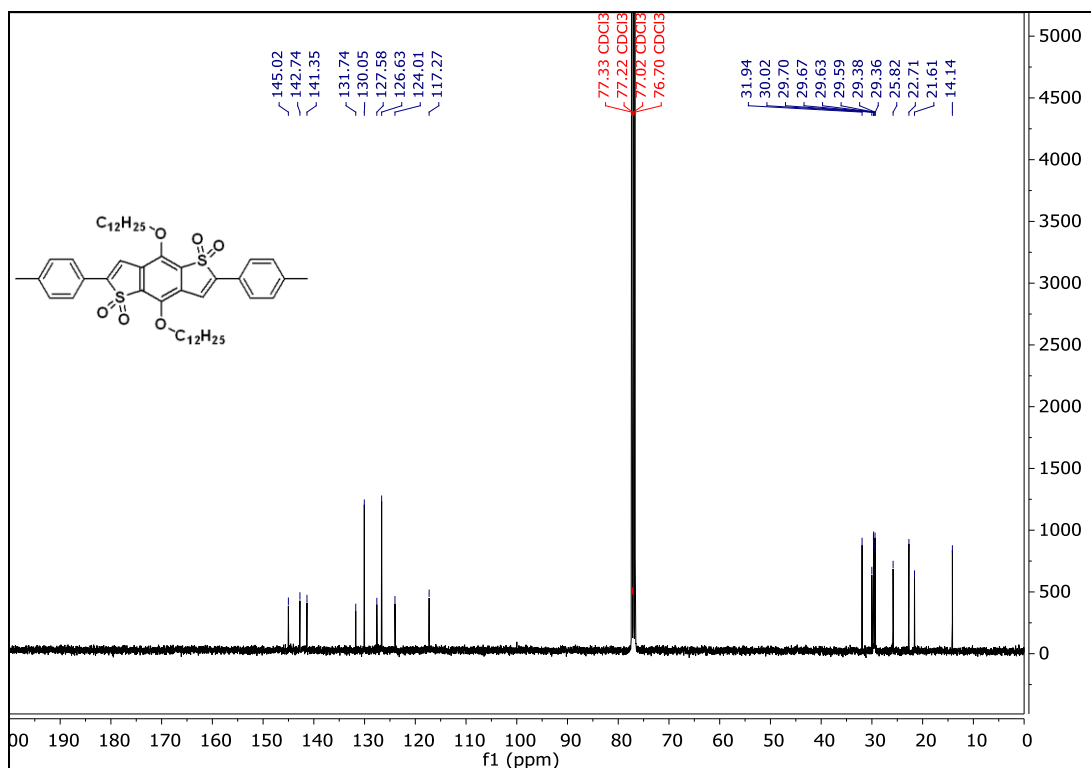
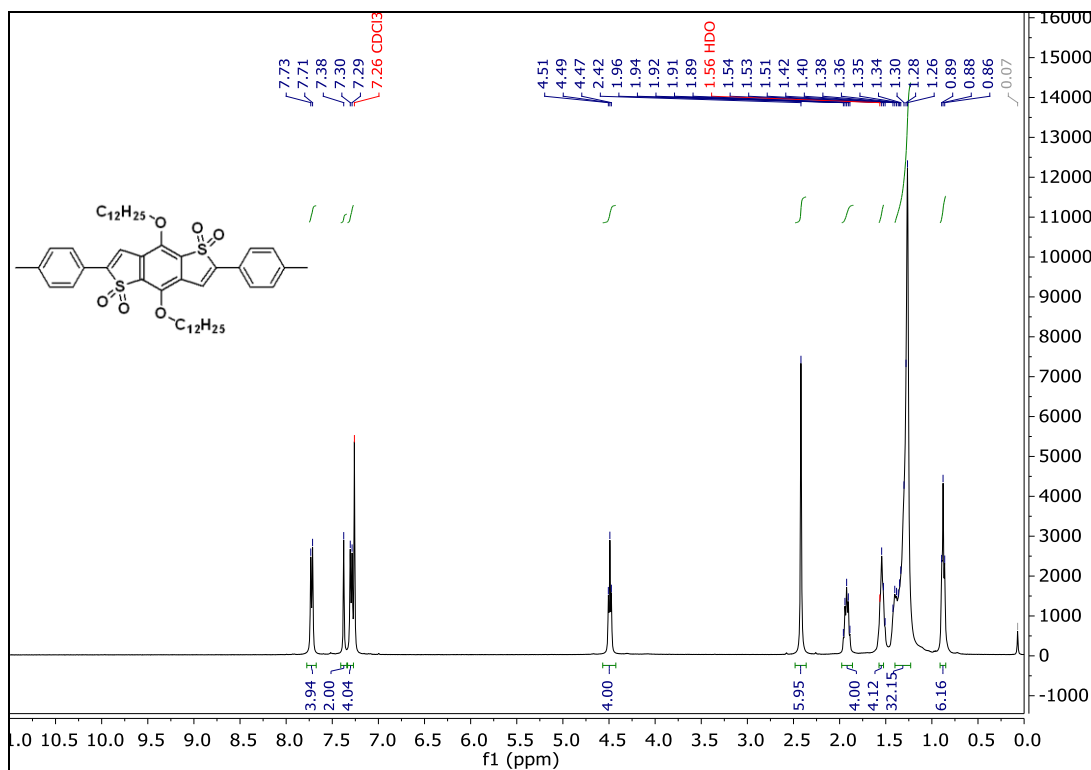
NMR spectra:



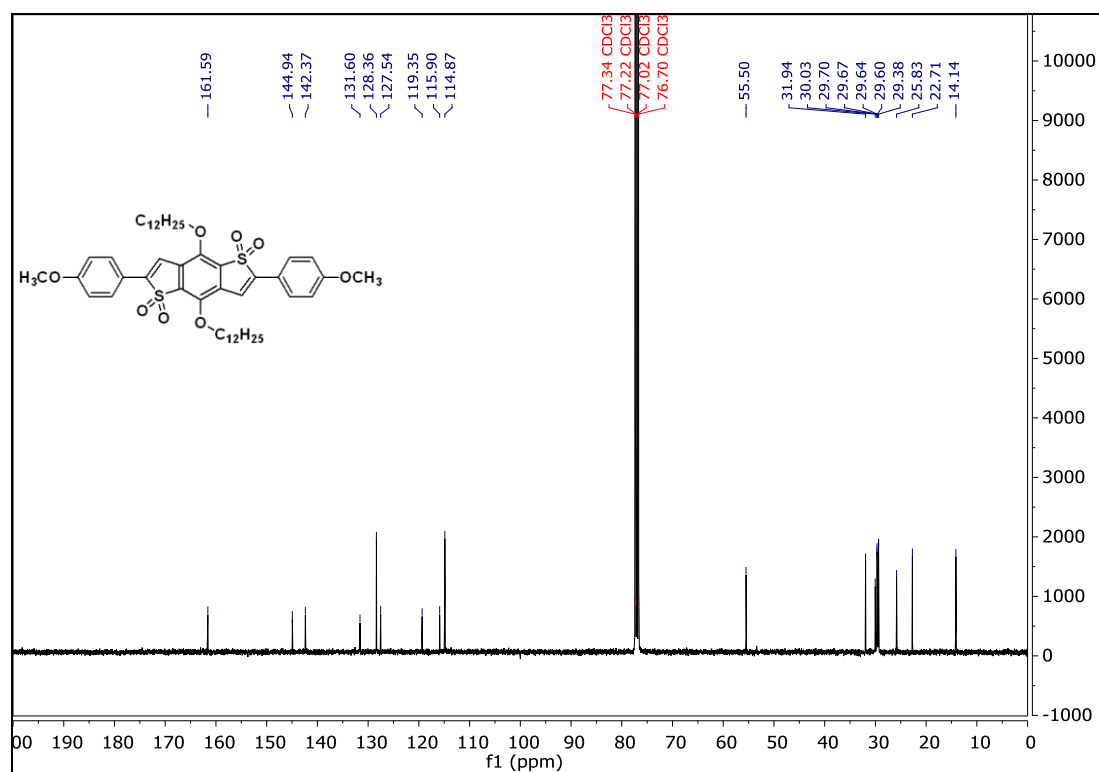
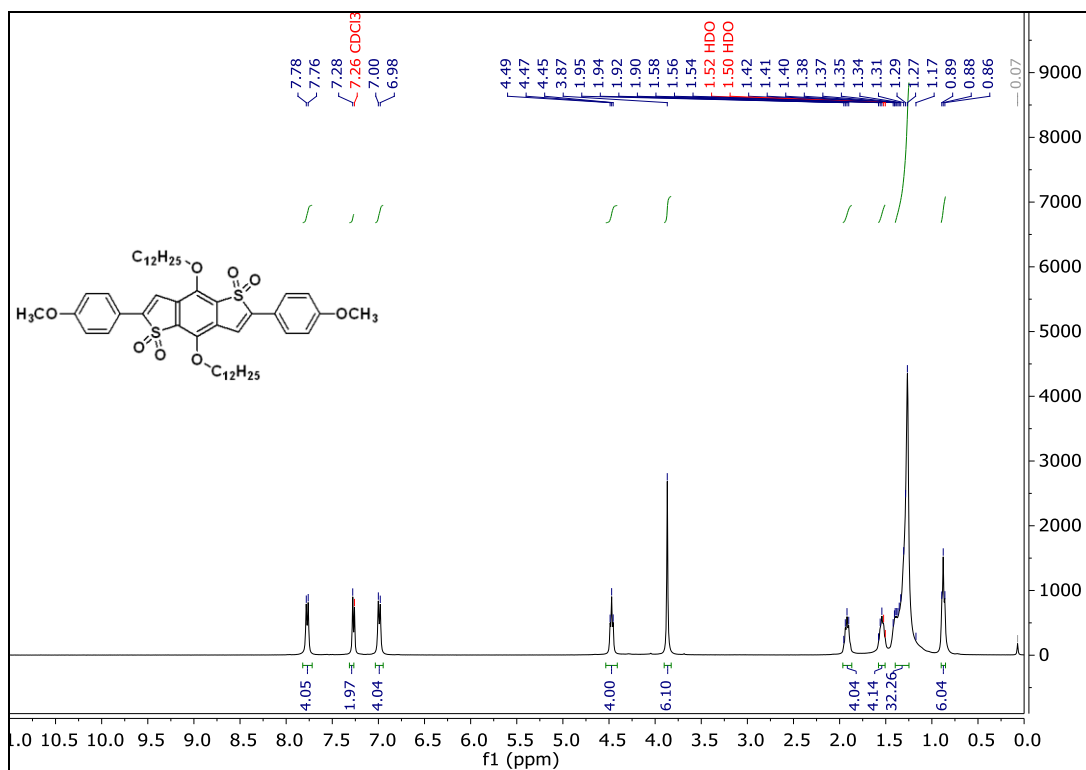
Ph-BDTS-Ph: ¹H NMR (above) and ¹³C NMR (below)



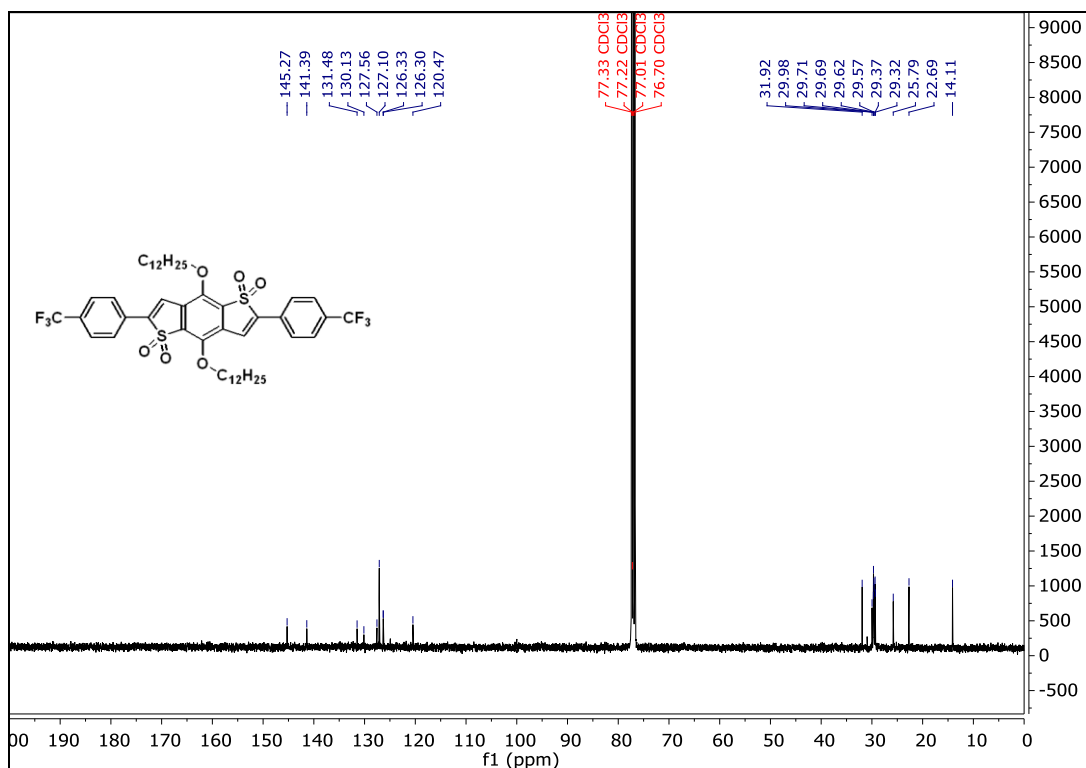
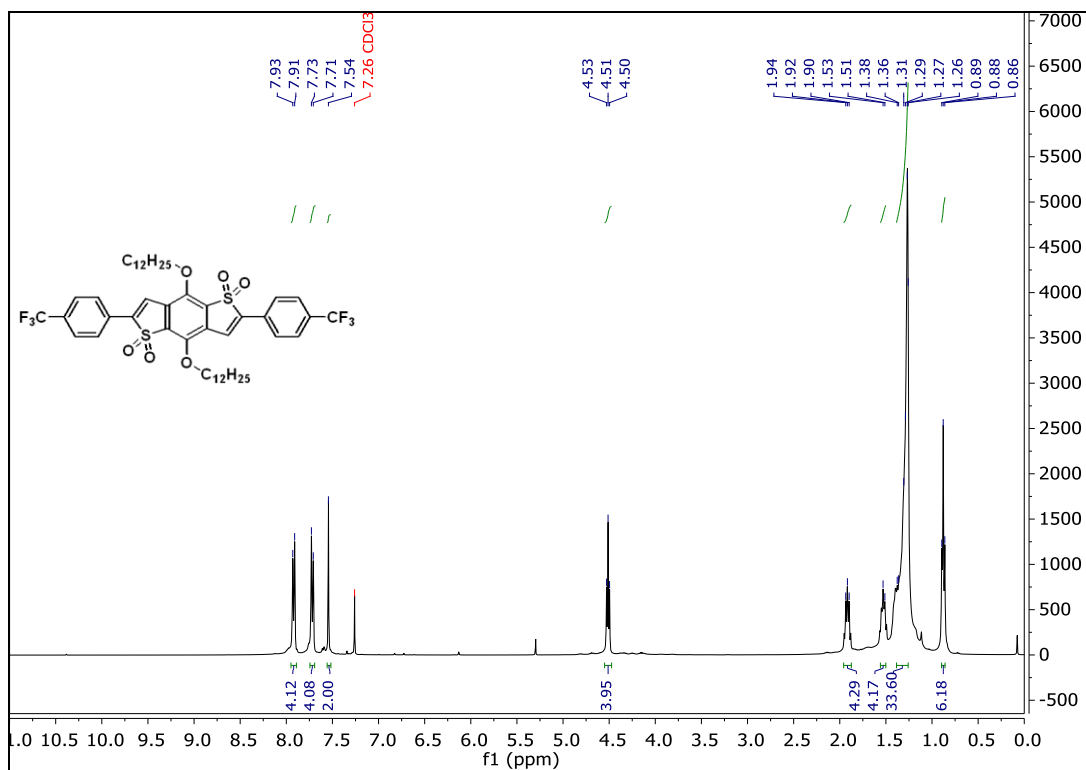
Th-BDTh-Th: ¹H NMR (above) and ¹³C NMR (below)



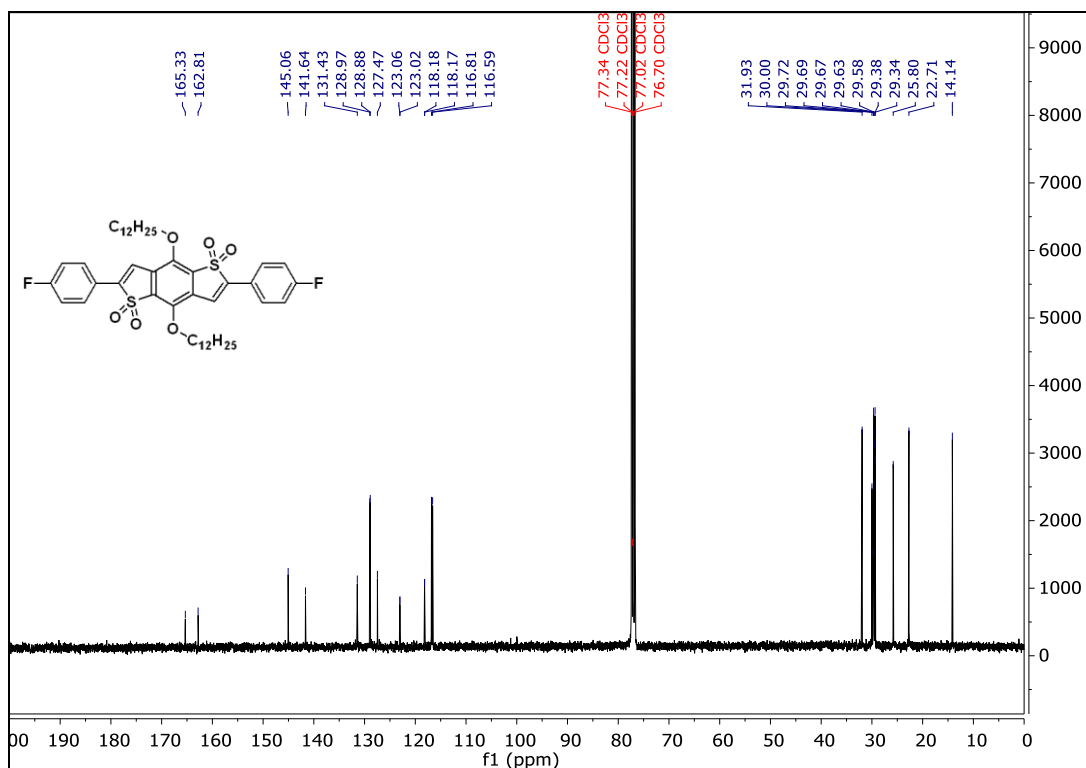
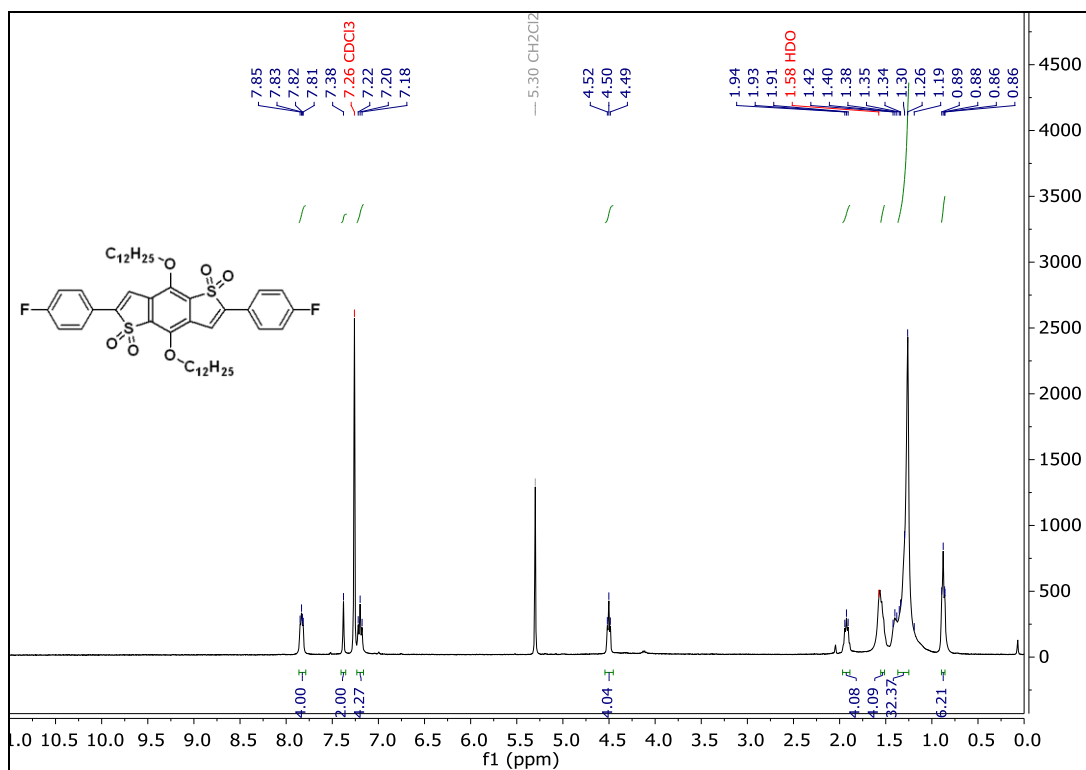
Me-Ph-BDTP-Ph-Me: ¹H NMR (above) and ¹³C NMR (below)



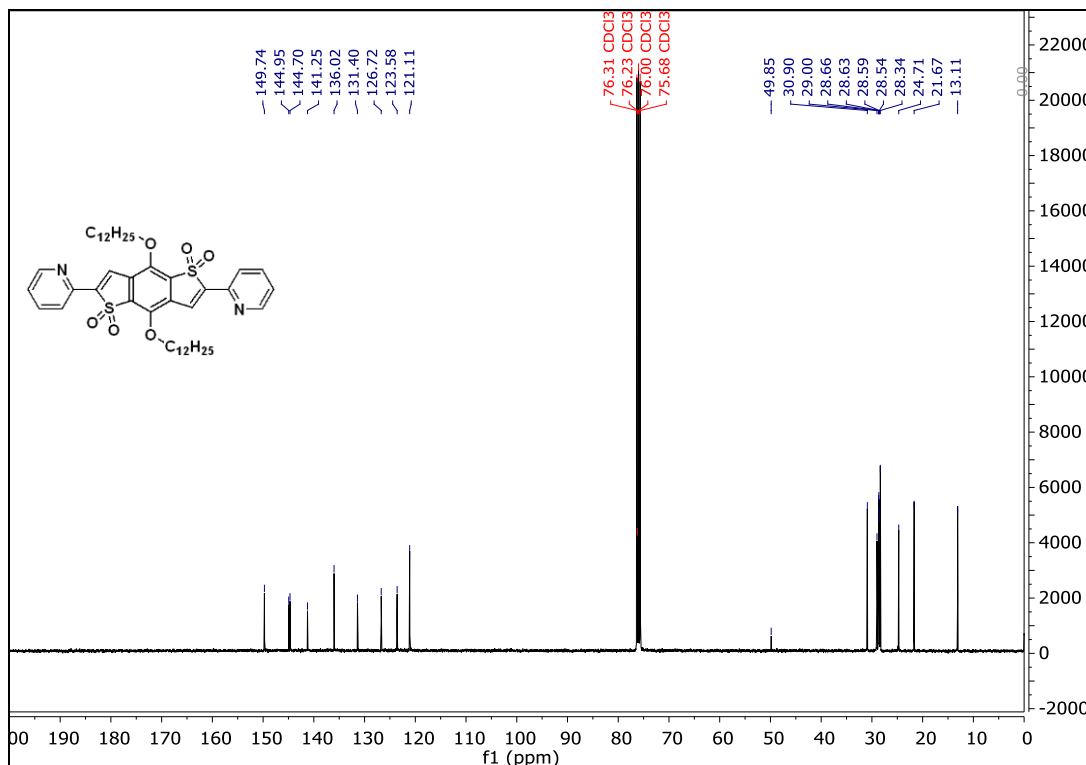
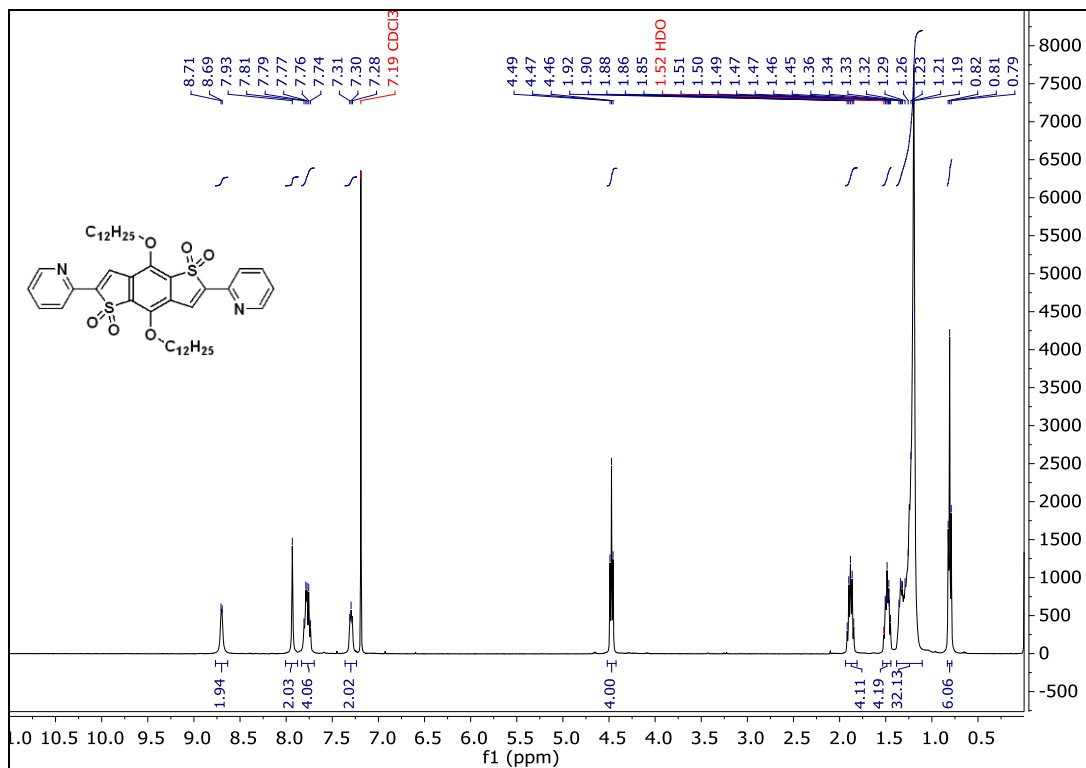
MeO-Ph-BDTP-Ph-OMe: ¹H NMR (above) and ¹³C NMR (below)



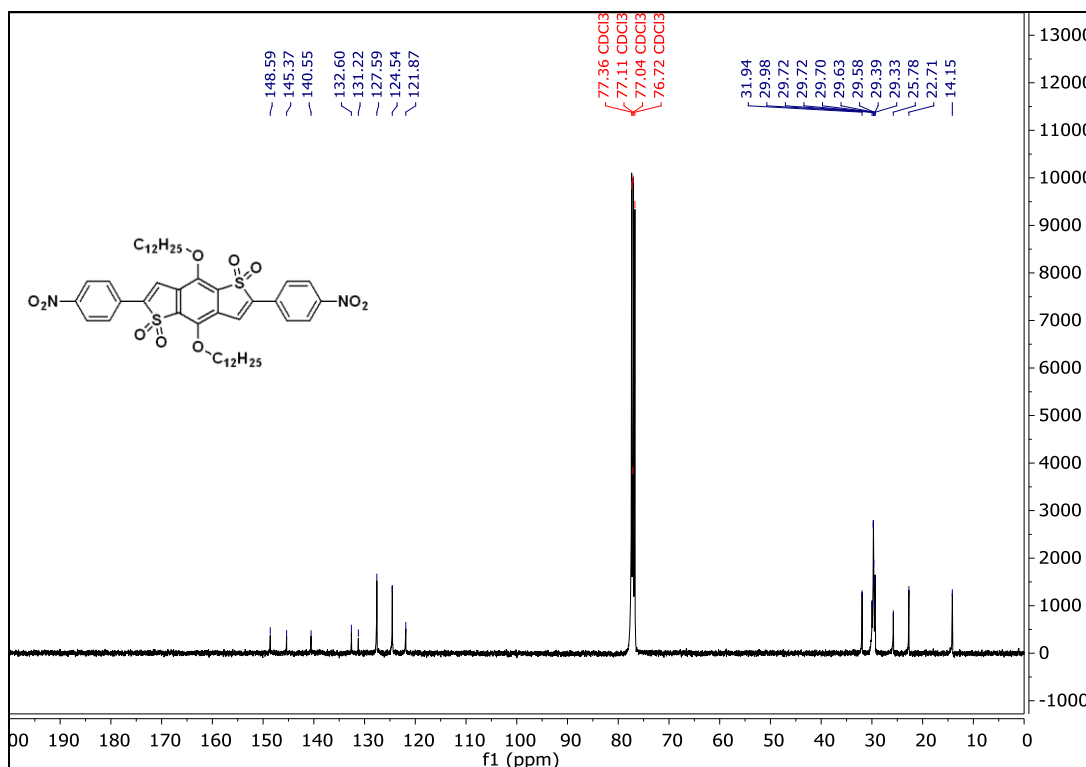
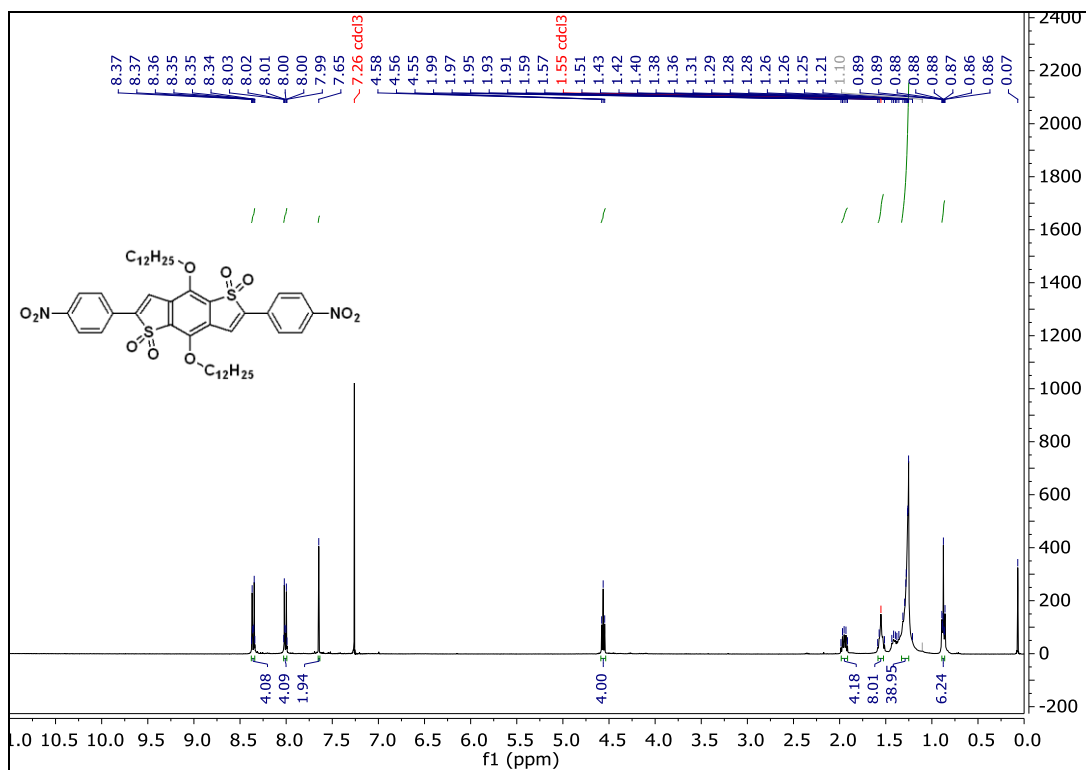
CF₃-Ph-BDTT-Ph-CF₃: ¹H NMR (above) and ¹³C NMR (below)



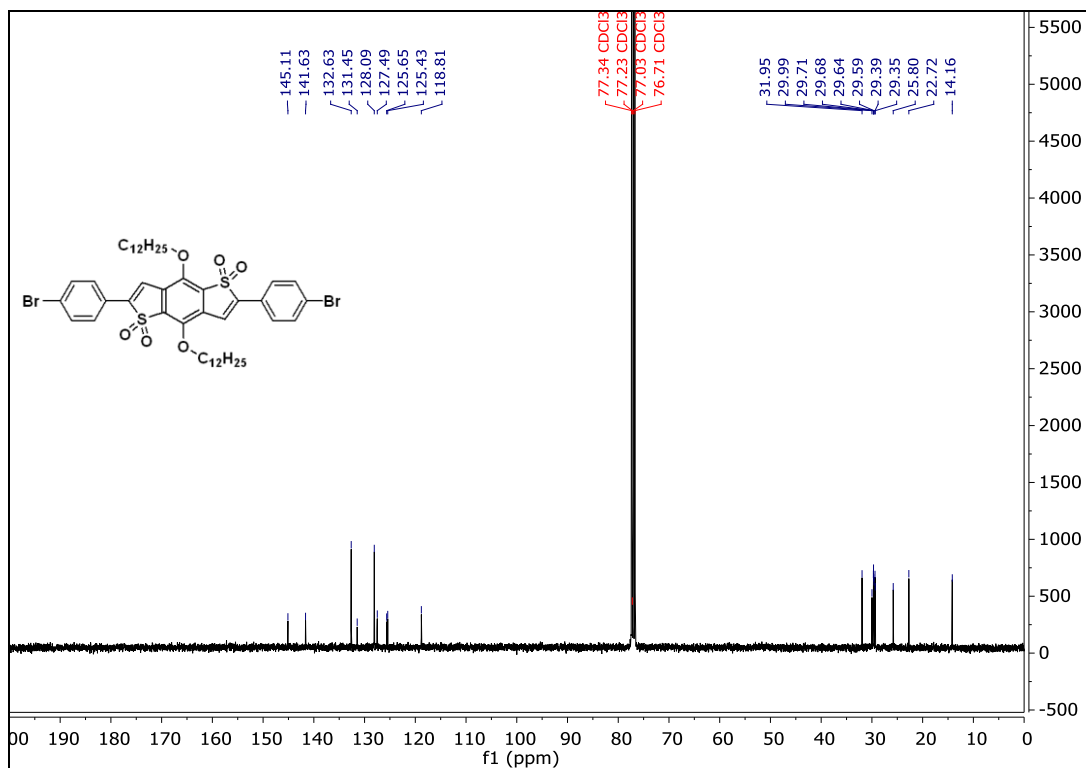
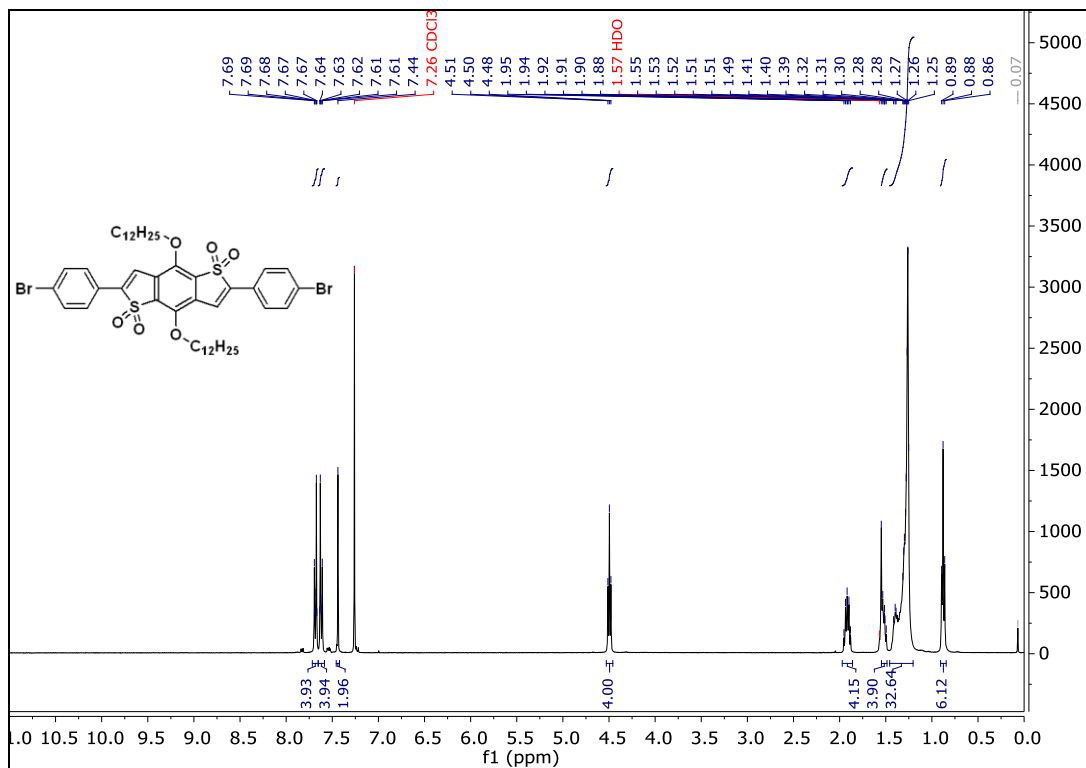
F-Ph-BDTP-Ph-F: ¹H NMR (above) and ¹³C NMR (bel)



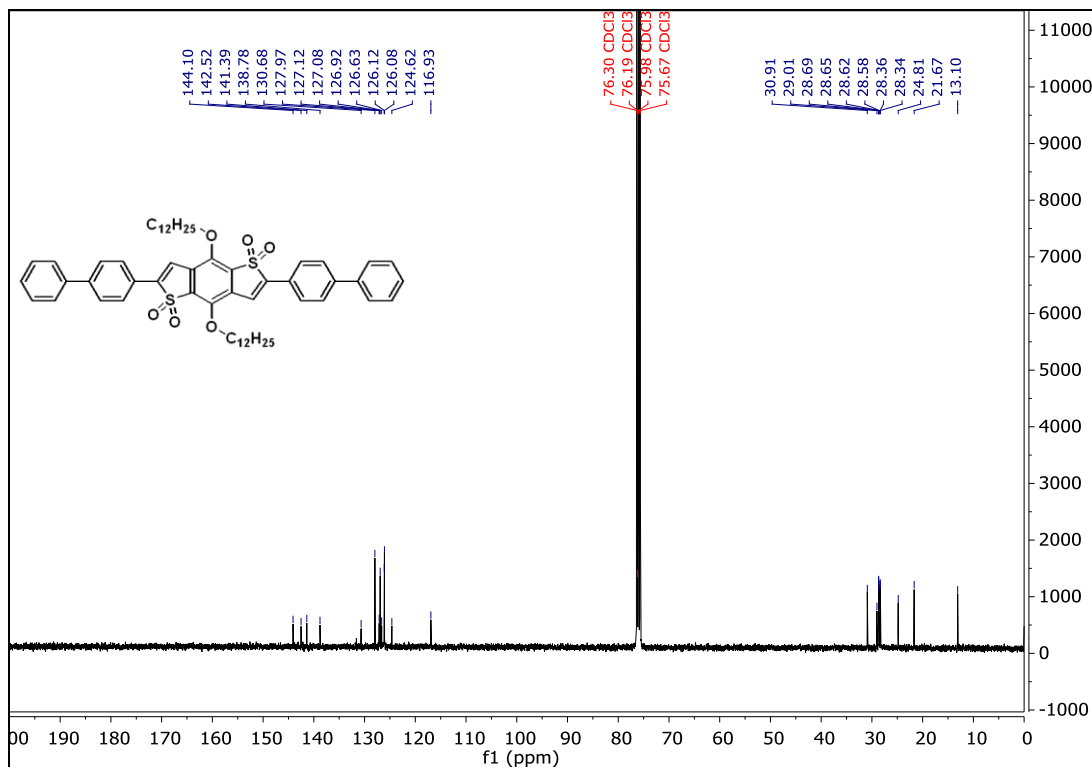
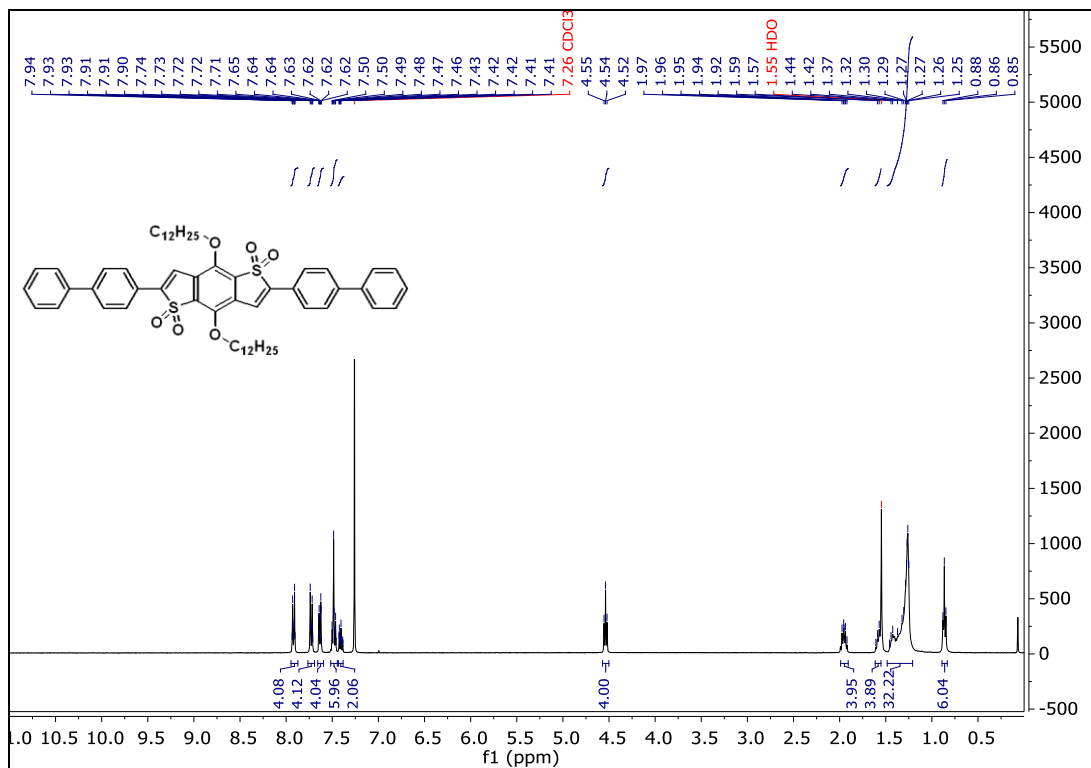
2-pyridyl-BDTP-2-pyridyl: ¹H NMR (above) and ¹³C NMR (below)



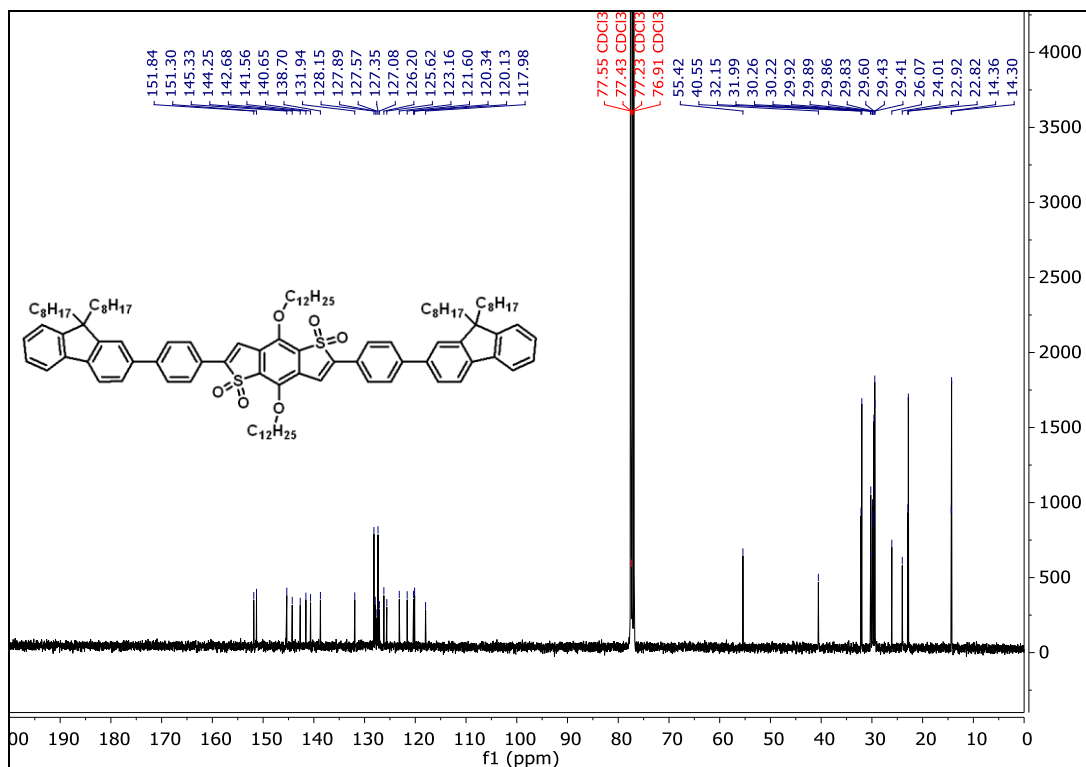
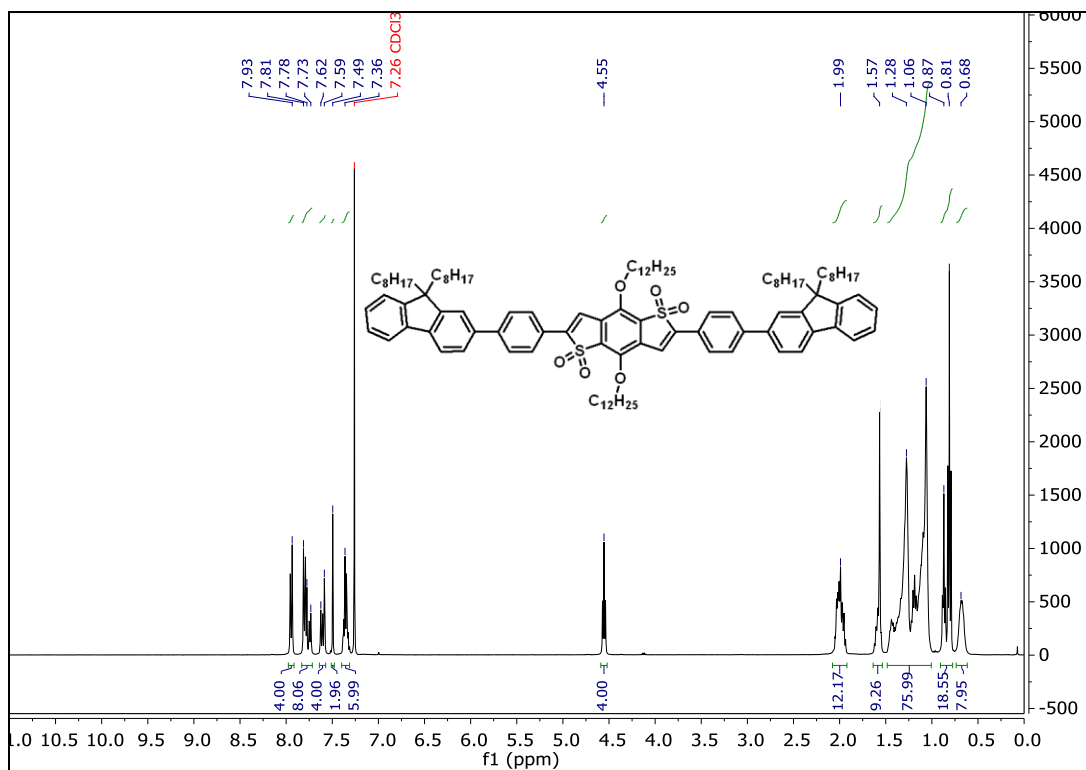
NO₂-Ph-BDTP-Ph-NO₂: ¹H NMR (above) and ¹³C NMR (below)



Br-Ph-BDTP-Ph-Br: ¹H NMR (above) and ¹³C NMR (below)



Ph-Ph-BDTP-Ph-Ph: ¹H NMR (above) and ¹³C NMR (below)



Flu-BDTT-Flu: ¹H NMR (above) and ¹³C NMR (below)

(Flu: fluorine)

Crystallographic data for Ph-BDTT-Ph:

Table 4.9. Crystal data and structure refinement for Ph-BDTT-Ph

Identification code	nelson12_0m_a	
Empirical formula	C ₄₆ H ₆ O ₆ S ₂	
Formula weight	775.07	
Temperature	100.0 K	
Wavelength	1.54178 Å	
Crystal system	Monoclinic	
Space group	P 21/c	
Unit cell dimensions	a = 14.9364(3) Å b = 7.6637(2) Å c = 18.4671(4) Å	α = 90°. β = 97.5930(10)°. γ = 90°.
Volume	2095.36(8) Å ³	
Z	2	
Density (calculated)	1.228 Mg/m ³	
Absorption coefficient	1.521 mm ⁻¹	
F(000)	836	
Crystal size	0.3 x 0.3 x 0.08 mm ³	
Theta range for data collection	2.985 to 68.609°.	
Index ranges	-15<=h<=18, -8<=k<=7, -22<=l<=19	
Reflections collected	17378	
Independent reflections	3784 [R(int) = 0.0545]	
Completeness to theta = 67.679°	98.1 %	
Absorption correction	Semi-empirical from equivalents	
Max. and min. transmission	0.7531 and 0.6039	
Refinement method	Full-matrix least-squares on F ²	
Data / restraints / parameters	3784 / 0 / 245	
Goodness-of-fit on F ²	1.068	
Final R indices [I>2sigma(I)]	R1 = 0.0392, wR2 = 0.0943	
R indices (all data)	R1 = 0.0452, wR2 = 0.0975	
Extinction coefficient	n/a	
Largest diff. peak and hole	0.449 and -0.342 e.Å ⁻³	

Table 4.10. Atomic coordinates ($\times 10^4$) and equivalent isotropic displacement parameters ($\text{\AA}^2 \times 10^3$)

for nelson12_0m_a. $U(\text{eq})$ is defined as one third of the trace of the orthogonalized U_{ij} tensor.

	x	y	z	$U(\text{eq})$
S(1)	5121(1)	1974(1)	1128(1)	12(1)
O(3)	6504(1)	5063(2)	1075(1)	14(1)
O(2)	4893(1)	2628(2)	1811(1)	17(1)
O(1)	5895(1)	860(2)	1147(1)	18(1)
C(13)	5753(1)	5102(2)	568(1)	12(1)
C(14)	5142(1)	3732(2)	506(1)	13(1)
C(16)	3866(1)	2017(2)	33(1)	14(1)
C(15)	4403(1)	3584(2)	-40(1)	13(1)
C(18)	3820(1)	-702(2)	820(1)	14(1)
C(17)	4150(1)	990(2)	607(1)	13(1)
C(19)	3171(1)	-1592(2)	340(1)	16(1)
C(11)	7338(1)	5716(2)	2225(1)	17(1)
C(12)	6484(1)	6130(2)	1723(1)	15(1)
C(8)	8392(1)	7502(2)	4133(1)	17(1)
C(10)	7459(1)	6877(2)	2902(1)	16(1)
C(23)	4151(1)	-1486(2)	1488(1)	16(1)
C(21)	3213(1)	-3994(2)	1177(1)	20(1)
C(6)	9270(1)	8174(2)	5373(1)	19(1)
C(7)	9197(1)	7020(2)	4695(1)	19(1)
C(5)	10093(1)	7772(2)	5930(1)	18(1)
C(20)	2867(1)	-3220(2)	518(1)	20(1)
C(9)	8267(1)	6350(2)	3453(1)	19(1)
C(4)	10139(1)	8863(2)	6626(1)	19(1)
C(22)	3846(1)	-3126(2)	1663(1)	21(1)
C(3)	10932(1)	8402(2)	7202(1)	20(1)
C(2)	10960(1)	9504(3)	7891(1)	26(1)
C(1)	11724(2)	9030(4)	8484(1)	45(1)

Bond lengths [Å] and angles [°] for Ph-BDTP-Ph

S(1)-O(2)	1.4391(12)
S(1)-O(1)	1.4345(12)
S(1)-C(14)	1.7741(16)
S(1)-C(17)	1.7962(16)
O(3)-C(13)	1.3642(19)
O(3)-C(12)	1.4525(19)
C(13)-C(14)	1.385(2)
C(13)-C(15)#1	1.400(2)
C(14)-C(15)	1.398(2)
C(16)-H(16)	0.9500
C(16)-C(15)	1.461(2)
C(16)-C(17)	1.344(2)
C(15)-C(13)#1	1.400(2)
C(18)-C(17)	1.460(2)
C(18)-C(19)	1.401(2)
C(18)-C(23)	1.402(2)
C(19)-H(19)	0.9500
C(19)-C(20)	1.383(2)
C(11)-H(11A)	0.9900
C(11)-H(11B)	0.9900
C(11)-C(12)	1.508(2)
C(11)-C(10)	1.526(2)
C(12)-H(12A)	0.9900
C(12)-H(12B)	0.9900
C(8)-H(8A)	0.9900
C(8)-H(8B)	0.9900
C(8)-C(7)	1.526(2)
C(8)-C(9)	1.526(2)
C(10)-H(10A)	0.9900
C(10)-H(10B)	0.9900
C(10)-C(9)	1.527(2)
C(23)-H(23)	0.9500
C(23)-C(22)	1.390(2)
C(21)-H(21)	0.9500

C(21)-C(20)	1.390(3)
C(21)-C(22)	1.384(3)
C(6)-H(6A)	0.9900
C(6)-H(6B)	0.9900
C(6)-C(7)	1.525(2)
C(6)-C(5)	1.526(2)
C(7)-H(7A)	0.9900
C(7)-H(7B)	0.9900
C(5)-H(5A)	0.9900
C(5)-H(5B)	0.9900
C(5)-C(4)	1.526(2)
C(20)-H(20)	0.9500
C(9)-H(9A)	0.9900
C(9)-H(9B)	0.9900
C(4)-H(4A)	0.9900
C(4)-H(4B)	0.9900
C(4)-C(3)	1.525(2)
C(22)-H(22)	0.9500
C(3)-H(3A)	0.9900
C(3)-H(3B)	0.9900
C(3)-C(2)	1.523(2)
C(2)-H(2A)	0.9900
C(2)-H(2B)	0.9900
C(2)-C(1)	1.518(3)
C(1)-H(1A)	0.9800
C(1)-H(1B)	0.9800
C(1)-H(1C)	0.9800
O(2)-S(1)-C(14)	109.26(7)
O(2)-S(1)-C(17)	110.40(7)
O(1)-S(1)-O(2)	117.98(7)
O(1)-S(1)-C(14)	112.57(7)
O(1)-S(1)-C(17)	110.75(7)
C(14)-S(1)-C(17)	93.12(8)
C(13)-O(3)-C(12)	116.61(12)
O(3)-C(13)-C(14)	120.91(14)

O(3)-C(13)-C(15)#1	122.68(14)
C(14)-C(13)-C(15)#1	116.11(15)
C(13)-C(14)-S(1)	126.16(13)
C(13)-C(14)-C(15)	124.74(15)
C(15)-C(14)-S(1)	108.97(12)
C(15)-C(16)-H(16)	122.1
C(17)-C(16)-H(16)	122.1
C(17)-C(16)-C(15)	115.70(14)
C(13)#1-C(15)-C(16)	127.79(15)
C(14)-C(15)-C(13)#1	119.14(15)
C(14)-C(15)-C(16)	113.05(14)
C(19)-C(18)-C(17)	119.52(15)
C(19)-C(18)-C(23)	118.83(15)
C(23)-C(18)-C(17)	121.63(15)
C(16)-C(17)-S(1)	109.01(12)
C(16)-C(17)-C(18)	130.49(15)
C(18)-C(17)-S(1)	120.44(12)
C(18)-C(19)-H(19)	119.7
C(20)-C(19)-C(18)	120.66(16)
C(20)-C(19)-H(19)	119.7
H(11A)-C(11)-H(11B)	107.9
C(12)-C(11)-H(11A)	109.1
C(12)-C(11)-H(11B)	109.1
C(12)-C(11)-C(10)	112.35(14)
C(10)-C(11)-H(11A)	109.1
C(10)-C(11)-H(11B)	109.1
O(3)-C(12)-C(11)	106.24(13)
O(3)-C(12)-H(12A)	110.5
O(3)-C(12)-H(12B)	110.5
C(11)-C(12)-H(12A)	110.5
C(11)-C(12)-H(12B)	110.5
H(12A)-C(12)-H(12B)	108.7
H(8A)-C(8)-H(8B)	107.6
C(7)-C(8)-H(8A)	108.6
C(7)-C(8)-H(8B)	108.6
C(7)-C(8)-C(9)	114.77(14)

C(9)-C(8)-H(8A)	108.6
C(9)-C(8)-H(8B)	108.6
C(11)-C(10)-H(10A)	109.0
C(11)-C(10)-H(10B)	109.0
C(11)-C(10)-C(9)	112.91(14)
H(10A)-C(10)-H(10B)	107.8
C(9)-C(10)-H(10A)	109.0
C(9)-C(10)-H(10B)	109.0
C(18)-C(23)-H(23)	119.9
C(22)-C(23)-C(18)	120.30(16)
C(22)-C(23)-H(23)	119.9
C(20)-C(21)-H(21)	119.8
C(22)-C(21)-H(21)	119.8
C(22)-C(21)-C(20)	120.39(16)
H(6A)-C(6)-H(6B)	107.7
C(7)-C(6)-H(6A)	108.8
C(7)-C(6)-H(6B)	108.8
C(7)-C(6)-C(5)	113.64(14)
C(5)-C(6)-H(6A)	108.8
C(5)-C(6)-H(6B)	108.8
C(8)-C(7)-H(7A)	109.1
C(8)-C(7)-H(7B)	109.1
C(6)-C(7)-C(8)	112.51(14)
C(6)-C(7)-H(7A)	109.1
C(6)-C(7)-H(7B)	109.1
H(7A)-C(7)-H(7B)	107.8
C(6)-C(5)-H(5A)	108.9
C(6)-C(5)-H(5B)	108.9
C(6)-C(5)-C(4)	113.57(14)
H(5A)-C(5)-H(5B)	107.7
C(4)-C(5)-H(5A)	108.9
C(4)-C(5)-H(5B)	108.9
C(19)-C(20)-C(21)	119.84(16)
C(19)-C(20)-H(20)	120.1
C(21)-C(20)-H(20)	120.1
C(8)-C(9)-C(10)	113.24(14)

C(8)-C(9)-H(9A)	108.9
C(8)-C(9)-H(9B)	108.9
C(10)-C(9)-H(9A)	108.9
C(10)-C(9)-H(9B)	108.9
H(9A)-C(9)-H(9B)	107.7
C(5)-C(4)-H(4A)	108.8
C(5)-C(4)-H(4B)	108.8
H(4A)-C(4)-H(4B)	107.7
C(3)-C(4)-C(5)	113.85(14)
C(3)-C(4)-H(4A)	108.8
C(3)-C(4)-H(4B)	108.8
C(23)-C(22)-H(22)	120.0
C(21)-C(22)-C(23)	119.97(16)
C(21)-C(22)-H(22)	120.0
C(4)-C(3)-H(3A)	109.0
C(4)-C(3)-H(3B)	109.0
H(3A)-C(3)-H(3B)	107.8
C(2)-C(3)-C(4)	112.79(15)
C(2)-C(3)-H(3A)	109.0
C(2)-C(3)-H(3B)	109.0
C(3)-C(2)-H(2A)	108.8
C(3)-C(2)-H(2B)	108.8
H(2A)-C(2)-H(2B)	107.7
C(1)-C(2)-C(3)	113.96(16)
C(1)-C(2)-H(2A)	108.8
C(1)-C(2)-H(2B)	108.8
C(2)-C(1)-H(1A)	109.5
C(2)-C(1)-H(1B)	109.5
C(2)-C(1)-H(1C)	109.5
H(1A)-C(1)-H(1B)	109.5
H(1A)-C(1)-H(1C)	109.5
H(1B)-C(1)-H(1C)	109.5

Symmetry transformations used to generate equivalent atoms:

#1 -x+1,-y+1,-z

Table 4. Anisotropic displacement parameters ($\text{\AA}^2 \times 10^3$) for nelson12_0m_a. The anisotropic

displacement factor exponent takes the form: $-2\pi^2 [h^2 a^{*2} U^{11} + \dots + 2hk a^* b^* U^{12}]$

	U11	U22	U33	U23	U13	U12
S(1)	11(1)	13(1)	10(1)	1(1)	-2(1)	-2(1)
O(3)	13(1)	17(1)	12(1)	-3(1)	-4(1)	2(1)
O(2)	19(1)	20(1)	12(1)	-1(1)	-1(1)	-1(1)
O(1)	15(1)	17(1)	20(1)	3(1)	-1(1)	1(1)
C(13)	10(1)	15(1)	11(1)	-3(1)	-1(1)	0(1)
C(14)	14(1)	13(1)	12(1)	0(1)	2(1)	1(1)
C(16)	12(1)	16(1)	13(1)	-2(1)	0(1)	-1(1)
C(15)	12(1)	14(1)	12(1)	-3(1)	1(1)	0(1)
C(18)	13(1)	14(1)	14(1)	-1(1)	3(1)	0(1)
C(17)	12(1)	15(1)	13(1)	-3(1)	1(1)	-1(1)
C(19)	16(1)	19(1)	13(1)	1(1)	0(1)	-3(1)
C(11)	14(1)	21(1)	14(1)	-4(1)	-3(1)	3(1)
C(12)	15(1)	18(1)	12(1)	-3(1)	-2(1)	1(1)
C(8)	13(1)	22(1)	16(1)	-2(1)	-1(1)	2(1)
C(10)	14(1)	20(1)	14(1)	-2(1)	-1(1)	2(1)
C(23)	16(1)	16(1)	15(1)	0(1)	-3(1)	-3(1)
C(21)	22(1)	17(1)	22(1)	2(1)	2(1)	-5(1)
C(6)	18(1)	22(1)	16(1)	-1(1)	-2(1)	2(1)
C(7)	18(1)	22(1)	16(1)	-2(1)	-2(1)	5(1)
C(5)	18(1)	22(1)	14(1)	0(1)	-2(1)	2(1)
C(20)	18(1)	23(1)	18(1)	-1(1)	0(1)	-8(1)
C(9)	16(1)	25(1)	15(1)	-4(1)	-2(1)	5(1)
C(4)	16(1)	21(1)	18(1)	-2(1)	-1(1)	1(1)
C(22)	23(1)	20(1)	17(1)	5(1)	-2(1)	-2(1)
C(3)	17(1)	25(1)	16(1)	-4(1)	-2(1)	2(1)
C(2)	19(1)	37(1)	20(1)	-9(1)	-2(1)	2(1)
C(1)	37(1)	67(2)	27(1)	-18(1)	-15(1)	14(1)

Table 5. Hydrogen coordinates ($\times 10^4$) and isotropic displacement parameters ($\text{\AA}^2 \times 10^3$) for nelson12_0m_a.

	x	y	z	U(eq)
H(16)	3348	1741	-304	16
H(19)	2938	-1072	-113	19
H(11A)	7863	5870	1955	20
H(11B)	7323	4480	2378	20
H(12A)	5946	5846	1962	18
H(12B)	6463	7384	1593	18
H(8A)	8464	8726	3979	21
H(8B)	7836	7441	4371	21
H(10A)	6904	6821	3142	19
H(10B)	7538	8100	2751	19
H(23)	4585	-893	1822	20
H(21)	3015	-5124	1295	24
H(6A)	8718	8026	5610	23
H(6B)	9299	9409	5221	23
H(7A)	9138	5788	4842	23
H(7B)	9759	7128	4468	23
H(5A)	10646	7981	5702	22
H(5B)	10081	6521	6063	22
H(20)	2423	-3809	192	24
H(9A)	8188	5125	3603	23
H(9B)	8821	6406	3213	23
H(4A)	10183	10111	6496	22
H(4B)	9570	8705	6839	22
H(22)	4072	-3652	2117	25
H(3A)	10891	7155	7333	24
H(3B)	11503	8569	6991	24
H(2A)	11022	10747	7760	31
H(2B)	10379	9371	8088	31

H(1A)	12303	9153	8294	68
H(1B)	11650	7821	8639	68
H(1C)	11712	9811	8903	68

4.11 References:

1. Lei, T.; Dou, J.-H.; Cao, X.-Y.; Wang, J.-Y.; Pei, J., Electron-deficient poly(p-phenylene vinylene) provides electron mobility over $1 \text{ cm}^2 \text{ v}^{-1} \text{ s}^{-1}$ under ambient conditions. *Journal of the American Chemical Society* **2013**, *135* (33), 12168-12171.
2. Li, H.; Kim, F. S.; Ren, G.; Jenekhe, S. A., *J. Am. Chem. Soc.* **2013**, *135*, 14920.
3. Zhou, K.; Dong, H.; Zhang, H.-l.; Hu, W., High performance n-type and ambipolar small organic semiconductors for organic thin film transistors. *Physical Chemistry Chemical Physics* **2014**, *16* (41), 22448-22457.
4. Pappenfus, T. M.; Seidenkranz, D. T.; Lovander, M. D.; Beck, T. L.; Karels, B. J.; Ogawa, K.; Janzen, D. E., Synthesis and electronic properties of oxidized benzo[1,2-B:4,5-B']dithiophenes. *The Journal of Organic Chemistry* **2014**, *79* (19), 9408-9412.
5. Ahmed, E.; Subramanian, S.; Kim, F. S.; Xin, H.; Jenekhe, S. A., Benzobisthiazole-Based donor-acceptor copolymer semiconductors for photovoltaic cells and highly stable field-effect transistors. *Macromolecules* **2011**, *44* (18), 7207-7219.
6. Bhuwalka, A.; Mike, J. F.; He, M.; Intemann, J. J.; Nelson, T.; Ewan, M. D.; Roggers, R. A.; Lin, Z.; Jeffries-El, M., Quaterthiophene-benzobisazole copolymers for photovoltaic cells: effect of heteroatom placement and substitution on the optical and electronic properties. *Macromolecules* **2011**, *44* (24), 9611-9617.
7. Laquindanum, J. G.; Katz, H. E.; Lovinger, A. J.; Dodabalapur, A., Benzodithiophene rings as semiconductor building blocks. *Advanced Materials* **1997**, *9* (1), 36-39.

8. Zhou, J.; Zuo, Y.; Wan, X.; Long, G.; Zhang, Q.; Ni, W.; Liu, Y.; Li, Z.; He, G.; Li, C.; Kan, B.; Li, M.; Chen, Y., Solution-processed and high-performance organic solar cells using small molecules with a benzodithiophene unit. *Journal of the American Chemical Society* **2013**, *135* (23), 8484-8487.
9. Intemann, J. J.; Hellerich, E. S.; Tlach, B. C.; Ewan, M. D.; Barnes, C. A.; Bhuwalka, A.; Cai, M.; Shinar, J.; Shinar, R.; Jeffries-El, M., Altering the conjugation pathway for improved performance of benzobisoxazole-Based polymer guest emitters in polymer light-emitting diodes. *Macromolecules* **2012**, *45* (17), 6888-6897.
10. Chavez Iii, R.; Cai, M.; Tlach, B.; Wheeler, D. L.; Kaudal, R.; Tsyrenova, A.; Tomlinson, A. L.; Shinar, R.; Shinar, J.; Jeffries-El, M., Benzobisoxazole cruciforms: a tunable, cross-conjugated platform for the generation of deep blue OLED materials. *Journal of Materials Chemistry C* **2016**, *4* (17), 3765-3773.
11. Bhuwalka, A.; Ewan, M. D.; Elshobaki, M.; Mike, J. F.; Tlach, B.; Chaudhary, S.; Jeffries-El, M., Synthesis and photovoltaic properties of 2,6-Bis(2-thienyl) benzobisazole and 4,8-Bis(thienyl)-Benzo[1,2-B:4,5-B']dithiophene copolymers. *Journal of Polymer Science Part A: Polymer Chemistry* **2016**, *54* (3), 316-324.
12. Hao, X.; Zhu, J.; Jiang, X.; Wu, H.; Qiao, J.; Sun, W.; Wang, Z.; Sun, K., Ultrastrong polyoxazole nanofiber membranes for dendrite-proof and heat-resistant battery separators. *Nano Letters* **2016**, *16* (5), 2981-2987.
13. Hou, J.; Park, M.-H.; Zhang, S.; Yao, Y.; Chen, L.-M.; Li, J.-H.; Yang, Y., Bandgap and molecular energy level control of conjugated polymer photovoltaic materials based on benzo[1,2-B:4,5-B']dithiophene. *Macromolecules* **2008**, *41* (16), 6012-6018.
14. Jung, I. H.; Lo, W.-Y.; Jang, J.; Chen, W.; Zhao, D.; Landry, E. S.; Lu, L.; Talapin, D. V.; Yu, L., Synthesis and search for design principles of new electron accepting polymers for all-polymer solar cells. *Chemistry of Materials* **2014**, *26* (11), 3450-3459.

15. Nandakumar, M.; Karunakaran, J.; Mohanakrishnan, A. K., Diels–alder reaction of 1,3-diarylbenzo[c]furans with thiophene s,s-dioxide/indenone derivatives: a facile preparation of substituted dibenzothiophene s,s-dioxides and fluorenones. *Organic Letters* **2014**, *16* (11), 3068-3071.
16. Mariano, F.; Mazzeo, M.; Duan, Y.; Barbarella, G.; Favaretto, L.; Carallo, S.; Cingolani, R.; Gigli, G., Very low voltage and stable p-i-n organic light-emitting diodes using a linear S,S-dioxide oligothiophene as emitting layer. *Applied Physics Letters* **2009**, *94* (6), 063510.
17. Yamamoto, Y.; Sakai, H.; Yuasa, J.; Araki, Y.; Wada, T.; Sakanoue, T.; Takenobu, T.; Kawai, T.; Hasobe, T., Controlled excited-state dynamics and enhanced fluorescence property of tetrasulfone[9]helicene by a simple synthetic process. *The Journal of Physical Chemistry C* **2016**, *120* (13), 7421-7427.
18. Geng, Y.; Li, H.; Wu, S.; Duan, Y.; Su, Z.; Liao, Y., The influence of thienyl-S,S-dioxidation on the photoluminescence and charge transport properties of dithienothiophenes: a theoretical study. *Theoretical Chemistry Accounts* **2011**, *129* (2), 247-255.
19. Oliva, M. M.; Casado, J.; Navarrete, J. T. L.; Patchkovskii, S.; Goodson, T.; Harpham, M. R.; Seixas de Melo, J. S.; Amir, E.; Rozen, S., Do [all]-S,S'-dioxide oligothiophenes show electronic and optical properties of oligoenes and/or of oligothiophenes? *Journal of the American Chemical Society* **2010**, *132* (17), 6231-6242.
20. Delord Joanna, G. F., C-H bond activation enables the rapid construction and late-stage diversification of functional molecules. *Nature Chemistry* **2013**, *5* (5), 369-375.
21. Do, H.-Q.; Daugulis, O., Copper-catalyzed arylation and alkenylation of polyfluoroarene C–H bonds. *Journal of the American Chemical Society* **2008**, *130* (4), 1128-1129.

22. Do, H.-Q.; Khan, R. M. K.; Daugulis, O., A general method for copper-catalyzed arylation of arene C–H bonds. *Journal of the American Chemical Society* **2008**, *130* (45), 15185-15192.
23. Yoshizumi, T.; Tsurugi, H.; Satoh, T.; Miura, M., Copper-mediated direct arylation of benzoazoles with aryl iodides. *Tetrahedron Letters* **2008**, *49* (10), 1598-1600.
24. Do, H.-Q.; Daugulis, O., Copper-catalyzed arylation of heterocycle C–H bonds. *Journal of the American Chemical Society* **2007**, *129* (41), 12404-12405.
25. Yu, J.-Q.; Shi, Z., *Topics in current chemistry: C-H activation*. Springer: 2010.
26. Thomas, A. W.; Ley, S. V., Copper-catalyzed arylations of amines and alcohols with boron-Based arylating reagents. In *Modern Arylation Methods*, Wiley-VCH Verlag GmbH & Co. KGaA: 2009; pp 121-154.
27. Gujadhur, R. K.; Bates, C. G.; Venkataraman, D., Formation of aryl–nitrogen, aryl–oxygen, and aryl–carbon bonds using well-defined copper(i)-Based catalysts. *Organic Letters* **2001**, *3* (26), 4315-4317.
28. Kiyomori, A.; Marcoux, J.-F.; Buchwald, S. L., An efficient copper-catalyzed coupling of aryl halides with imidazoles. *Tetrahedron Letters* **1999**, *40* (14), 2657-2660.
29. Lafrance, M.; Shore, D.; Fagnou, K., Mild and General Conditions for the Cross-Coupling of Aryl Halides with Pentafluorobenzene and Other Perfluoroaromatics. *Organic Letters* **2006**, *8* (22), 5097-5100.
30. Lafrance, M.; Rowley, C. N.; Woo, T. K.; Fagnou, K., Catalytic intermolecular direct arylation of perfluorobenzenes. *Journal of the American Chemical Society* **2006**, *128* (27), 8754-8756.
31. Campeau, L.-C.; Parisien, M.; Jean, A.; Fagnou, K., Catalytic Direct arylation with aryl chlorides, bromides, and iodides: intramolecular studies leading to new intermolecular Reactions. *Journal of the American Chemical Society* **2006**, *128* (2), 581-590.

32. Jones, G. O.; Liu, P.; Houk, K. N.; Buchwald, S. L., Computational explorations of mechanisms and ligand-directed selectivities of copper-catalyzed ullmann-type reactions. *Journal of the American Chemical Society* **2010**, *132* (17), 6205-6213.
33. Shi, Q.; Zhang, S.; Zhang, J.; Oswald, V. F.; Amassian, A.; Marder, S. R.; Blakey, S. B., KOtBu-initiated aryl C–H iodination: a powerful tool for the synthesis of high electron affinity compounds. *Journal of the American Chemical Society* **2016**, *138* (12), 3946-3949.

CHAPTER V

CONCLUSIONS AND FUTURE OUTLOOK

5.1 Introduction:

In this Chapter, I have described conclusions from data in the Chapters 2, 3 and 4. Future outlooks, regarding the research topics of these Chapters are also outlined.

5.2 Conclusions:

In Chapter 2, poly(3-alkoxyselenophene) could not be synthesized due to the unstable monomer. Polythiazole has been synthesized via a conventional coupling reaction reported by others.¹ Other thiazole-containing CPs have also been synthesized using conventional coupling reactions.¹⁻³ For an alternative material for the Li-ion cathode (Chapter 3), a conjugated polymer was synthesized. The polymer was mixed with a Li salt, which was the material intended to be used for the cathode. To test this material, we collaborated with Dr. Alexander Lopez at the University of Mississippi. Initial results have shown promising Li ion conductivity.

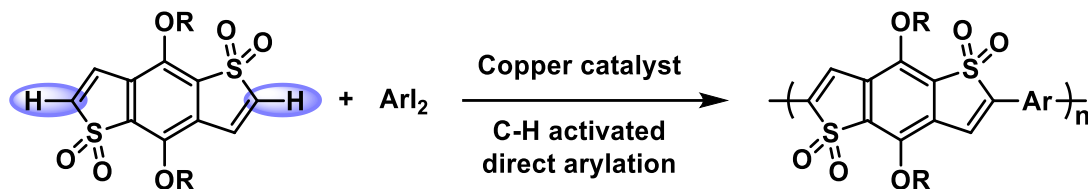
As shown in Chapter 4, Cu catalyzed direct arylation of BDTT was optimized with different parameters. These optimized parameters were used to synthesize BDTT-Based small molecules. Products were obtained in good yields with several aryl iodides having different electronic natures.

5.3 Future outlook:

In future work regarding Chapter 2, one would like to explore simple direct arylation synthesis of polythiazoles and thiazole-containing other CPs.

For a Li-ion battery, we want to fabricate a battery from our material. Various tests will be performed on this battery to determine its properties. Depending on these results, a commercial use of this material will be explored.

In Cu catalyzed direct arylation of BDTT, it is planned that these BDTT-Based small molecules may be used as n-type materials for OPVs, OFTs and OLEDs. Our main future target is to develop a direct arylation method is to synthesize BDTT-containing conjugated polymers (Scheme 5.1).



Scheme 5.1: Extension of Cu catalyzed direct arylation to BDTT containing synthesis polymers

In other work regarding BDTT, we have synthesized BDTT with an alkyl chain instead of an alkoxy chain. The objective is to determine whether, this BDTT derivative will react under the direct arylation reaction. Such a study will provide an assessment as to whether the oxygen atom in the alkoxy side chains is playing a role in mechanism of direct arylation. BDTT with an alkyl chain will be used to synthesize more small molecule and polymer OSCs. Such an investigation will aid in the determination of the structure activity relationship of BDTT.

2,6-dibromoobenzothiazole[1,2-b:4,5-b']dithiophene-S,S-tetraoxide (DiBrBDTT) will be used to synthesize CPs with conventional coupling reactions until Cu catalyzed direct arylation methods are discovered to synthesize these CPs.

5.4 References:

1. Pammer, F.; Jäger, J.; Rudolf, B.; Sun, Y., Soluble head-to-tail regioregular polythiazoles: preparation, properties, and evidence for chain-growth behavior in the synthesis via kumada-coupling polycondensation. *Macromolecules* **2014**, *47* (17), 5904-5912.
2. Guo, X.; Fan, H.; Zhang, M.; Huang, Y.; Tan, S.; Li, Y., Synthesis and characterizations of poly(4-alkylthiazole vinylene). *Journal of Applied Polymer Science* **2012**, *124* (1), 847-854.
3. Bronstein, H.; Hurhangee, M.; Fregoso, E. C.; Beatrup, D.; Soon, Y. W.; Huang, Z.; Hadipour, A.; Tuladhar, P. S.; Rossbauer, S.; Sohn, E.-H.; Shoaee, S.; Dimitrov, S. D.; Frost, J. M.; Ashraf, R. S.; Kirchartz, T.; Watkins, S. E.; Song, K.; Anthopoulos, T.; Nelson, J.; Rand, B. P.; Durrant, J. R.; McCulloch, I., Isostructural, deeper highest occupied molecular orbital analogues of poly(3-hexylthiophene) for high-open circuit voltage organic solar cells. *Chemistry of Materials* **2013**, *25* (21), 4239-4249.

VITA

Devang Khambhati

Candidate for the Degree of

Doctor of Philosophy

Thesis: SYNTHESIS OF THIOPHENE, SELENOPHENE AND THIOPHENE-S-DIOXIDE
BASED ORGANIC SEMICONDUCTORS FOR ORGANIC ELECTRONICS

Major Field: Organic Chemistry

Biographical:

Education:

Completed the requirements for the Doctor of Philosophy in Polymer Chemistry at Oklahoma State University, Stillwater, Oklahoma in May, 2017.

Completed the requirements for the Master of Science in Organic Chemistry at Veer Narmad South Gujarat University, Surat, India in 2007.

Completed the requirements for the Bachelor of Science in Bachelor of Chemistry at B. K. M. Science College, Valsad, India in 2005.

Experience:

Teaching and research assistant, Department of Chemistry, Oklahoma State University, USA, 2011-2017.

Quality Control Chemist, Shri Shantinath Chemical Industries, Valsad, India 2007-2010

Professional Memberships:

American Chemical Society (Organic division, Polymeric Materials: Science and Engineering Division)

Graduate and Professional Student Government Association (GPSGA)